Real-Time Online *in situ* Monitoring and Statistical Design Strategies for Haematopoietic Stem Cell Bioprocessing

THESIS BY

MAYASARI LIM

Submitted in partial fulfilment of the requirement for the degree of

Doctor of Philosophy in Chemical Engineering

Department of Chemical Engineering and Chemical Technology

Imperial College London, London, SW7 2AZ

October 2008

Abstract

In vitro erythropoiesis of cord blood haematopoietic stem cells (HSCs) to produce fully enucleated red blood cells could provide an alternate resource for the erythrocyte. However, haematopoietic processes are highly complex and dynamic; defining process requirements to produce reproducible cells of high purity and yield is not an easy task. One major obstacle is the lack of knowledge in process characteristics. Design of experiments (DOE) is proposed as a tool to unveil process complexities that exists in HSC cultures. Characterisation and optimisation of *in vitro* erythropoiesis as a single-step culture is first performed via a simple DOE experimental strategy. The optimised DOE culture produced significantly better results (higher growth and faster maturation) than other single-step cultures. Subsequently, use of DOE to reveal *in vitro* process dynamics was attempted. This study was much more challenging and the repeatability of DOE process models was compromised in some cases. Process control of HSC culture bioprocesses is required for the delivery of reliable cell culture products suited for clinical applications. The availability of a convenient and economical online real-time process monitoring system can provide the means to translate stem cell culture bioprocesses from the bench-side into manufacturing production. The design and integration of such a system capable of simultaneous process monitoring of multiple analytes (ammonia, pH and oxygen) is presented. Operational and functional stability of this unique online real-time *in situ* monitoring platform was achieved. Stability of oxygen and ammonia sensors was achieved for up to three and six days respectively but biocompatibilities of both sensors require some improvements. Sensors of pH were biocompatible but their stability in cell culture is required.

Acknowledgements

First, I would like to thank my research advisor, Dr. Athanasios Mantalaris, for his constant encouragement, inspiration, generosity and support throughout my PhD pursuit. I have learned many skills and lessons from him, of which I know, will carry me very far into my career. I would also like to thank Dr. Nicki Panoskaltsis for her insight and knowledge in the area of haematology, and support toward my research. A very special thank you goes to Dr. George Papasouliotis, my previous boss and mentor, who has truly inspired me to embark in one of the most extraordinary journeys of my life. To all three individuals, I am forever in debt to their efforts and inspiration.

To my truest friend and love of my life, Robert A. Bowman, I am deeply grateful for his love and unwavering support in pursuing my dreams. He has taught me so much in life and made me a stronger person each day. He has stood by me throughout the difficult times and has always been my cheer leader. I cannot begin to express how much I appreciate him and thank him for his love, patience, and wisdom.

A special thank you goes to Dr. Hua Ye whom I have learned many skills and techniques from. I have enjoyed our many engaging discussions, brainstorming sessions, and performing interesting experiments jointly with her. She has not only been a great work partner but also a wonderful friend who will always be dear to my heart.

I would also like to thank my collaborators in the intelligent stem cell bioprocess project, particularly to Dr. Anna Radomska and Dr. Xicai Yue whose hard work and continuous effort have contributed significantly toward the last part of this thesis.

A special thank you goes to Dr. Taby Ahsan who has been a fountain of knowledge and source of inspiration. I thank her for her generosity in sharing her time and knowledge with us, and for giving me advice when I need it.

To all of my current and ex lab-mates, I cannot begin to express how much I have enjoyed our time together, both inside and outside the lab. They have made my time at Imperial and in London go by so much quicker and each of them has been special to me. I would like to thank them for their friendships and for the laughter we shared together.

I also like to thank my dear friends, Hye Yoon Jo and Ron Muriel, for their friendship, their kindness, and love for me. I enjoyed the many conversations and time we shared together. It has been wonderful knowing them.

To all of the supporting staff in the Department of Chemical Engineering, in particular a big thank you goes to Sarah Payne, Keith Walker and Tawanda Nyabango who have helped us on a day-to-day basis in processing, collecting, and managing our laboratory purchases amongst the many other things that they have done for us.

To my sisters, Juliafie, Megasary, and Permanasari, I cannot imagine life without them and I would like to thank them for their constant support, love, time and effort they have given to me. I will always love them and keep them close to my heart.

Finally, my deepest gratitude and love goes out to my mother, Ratnaningsih Lelly Tjaturputranty, who is the greatest woman I have ever met and has made me the person I am today. For that, I am forever in debt to her. I thank her for her unwavering support, selfless love, fountain of wisdom, and ultimate belief in me. This thesis is dedicated to my mother.

Publications

Journal Articles

M. Lim, H. Ye, N. Panoskaltsis, E.M. Drakakis, X. Yue, E.G. Cass, A. Radomska, A. Mantalaris. (2007). Intelligent bioprocessing for haematopoietic cell cultures using monitoring and design of experiments. *Biotechnology Advances*. 25 (4): 353-368.

M. Lim, H. Ye, M. Plazcek, A. Mantalaris. (2007). Stem cell bioprocessing: Manufacturing cells for clinical applications. *BioWorld Europe*. S1 Issue: 10-13.

M. Lim, H. Ye, X. Yue, E. M. Drakakis, E. G. Cass, N. Panoskaltsis, A. Mantalaris. (2008). Towards information-rich bioprocessing: generation of spatio-temporal profiles through the use of design of experiments to determine optimal number and location of sensors – an example in thermal profiles. *Biochemical Engineering Journal*. 40 (1): 1-7

A. Radomska, S. Singhal, H. Ye, M. Lim, A. Mantalaris, X. Yue, E. M. Drakakis, C. Toumazou, A. E. G. Cass. (2008) PEG-modified ion selective electrode for monitoring metabolic activity during the growth and cultivation of stem cells. *Biosensors and Bioelectronics*. 24(3): 435-441.

X. Yue, E. M. Drakakis, H. Ye, M. Lim, A. Mantalaris, N. Panoskaltsis, A. Radomska, A. E. G. Cass. (2008). A real-time multi-channel monitoring system for hematopoietic stem cell culture process. *IEEE Trans. On biomedical circuits and systems*. 2(2): 66-77.

Book Chapters

M. Lim, H. Ye, N. Panoskaltsis, A. Mantalaris "Optimal expansion and differentiation of cord blood stem cells using design of experiments: a case study on erythropoiesis" Handbook of Cardiac Stem Cell Therapy. I. Dimarakis, P. Menasche, N. A. Habib, M. Y. Gordon eds. Imperial College Press. London, UK.

M. Lim, A. Mantalaris "Development of a design of experiment methodology: Applications to the design and analysis of experiments" Advances in Tissue Engineering. J. Polak ed. Imperial College Press. London, UK.

Contents

List of Figures

List of Tables

Abbreviations

3D	Three-dimensional
ADC	Analog-to-digital converter
ALL	Acute lymphocytic leukemia
AML	Acute myelogenous leukemia
AMV	Avian myeloblastosis virus
ANOVA	Analysis of variance
APS	Ammonium persulfate
ATP	Adenosine triphophate
Ba	Basophil
BCA	Bicinchoninic acid
BFU	Burst forming unit
BMP	Bone morphogenetic protein
BSA	Bovine serum albumin
CCD	Central composition design
CFU	Colony forming unit
COOH	Carboxylic acid
DEPC	Diethylpyrocarbonate
DMEM	Dulbecco's Modified Eagle's Medium
DOE	Design of experiments
dNTP	Deoxyribonucleotide triphosphate
E	Erythroid

ECM	Extracellular matrix
Eo	Eosinophil
EPO	Erythropoietin
ELISA	Enzyme-linked immunosorbent assay
ESC	Embryonic stem cell
FBS	Foetal bovine serum
FITC	Fluorescein isothiocyanate
FL	FLT-3 ligand
G-CSF	Granulocyte-colony stimulating factor
G-CSFR	Granulocyte-colony stimulating factor receptor
GEMM	Granulocyte-erythrocyte macrophage and monocytes
GM-CSF	Granulocyte-macrophage colony stimulating factor
GPA	Glycophorin-A
GUI	Graphic user interface
GVHD	Graft-versus-host disease
HEMA	Hydroxylethylmethacrylate
HIM	Haematopoietic inductive microenvironment
HLA	Human leukocyte antigen
HPLC	High-pressure liquid chromatography
HSC	Haematopoietic stem cell
IGF	Insulin growth factor
IgG	Immunoglobin
IL	Interleukin

IMDM	Iscove's modified Delbecco's Medium
ISA	Industry standard architecture
ISE	Ion selective electrode
ISM	*In-situ* microscopy
PLS	Partial least squares
PBD	Placket-Burman design
PBS	Phosphate buffered solution
PCI	Peripheral component interface
PCR	Polymerase chain reaction
PC	Phycoerythrin cyanide
PDMS	Polydimethlysiloxane
PEG	Polyethylene-glycol
PMMA	Polymethylmethacrylate
P/S	Penicillin/streptomycin
PVC	Polyvinyl-chloride
MDS	Myelodysplastic syndrome
Meg	Megakaryocyte
MDGF	Macrophage-derived growth factor
Micro-CT	Micro-computed tomography
MIR	Mid-infrared resonance
MLR	Multiple linear regression
MNC	Mononuclear cells
MSC	Mesenchymal stem cell

MTS	3-(4, 5-dimethylthiazol-2-yl)-5-(3-carboxymethoxyphenyl)-2-(4-sulfophenyl)-2H-tetrazolium
MTT	(3-(4, 5-dimethylthiazolyl-2)-2, 5-diphenyltetrazoilium bromide
NIR	Near-infrared resonance
NK	Natural killer cell
NMR	Nuclear magnetic resonance
NOD/SCID	Non-obese diabetic/severe combined immunodeficient
PE	Phycoerythrin
RSM	Response surface method
RT	Reverse transcriptase
RTD	Resistive temperature devices
RWV	Rotating wall vessel
SCF	Stem cell factor
SDS-PAGE	Sodium dodecyl sulphate polyacrylamide gel electrophoresis
SEP	Standard error of prediction
SPR	Surface plasmon resonance
TEMED	N, N, N', N' tetramethyl-ethylenediamine
THF	Tetrahydofuran
USB	Universal serial bus
YSI	Yellow Springs Instruments

CHAPTER 1

Introduction

Haematopoiesis is the process of blood formation. Each day, the human body produces and replenishes about $5x10^{11}$ blood cells for the average adult[1]. When the process of haematopoiesis malfunctions, various types of blood-related malignancies and disorders, such as leukaemia and anaemia result. One of the potential cures that have been tested clinically is haematopoietic stem cell (HSC) transplantation[2,3], which involves the transplantation of HSCs derived from, primarily, the bone marrow and, to a lesser extent, peripheral blood or umbilical cord blood. Though the procedure is still considered somewhat high risk due to the many possible complications, such as graft-versus-host disease (GVHD)[4,5], HSC transplantation offers the only potential cure or long-term remission for many different types of haematological conditions. Human umbilical cord blood stem cells have recently gained in popularity due to their reduced risk in immune rejection and GVHD occurrences but also due to their ease of collection and wider availability of usage for

minorities. However, cord blood stem cells are limited by the volume and number of cells available in a single cord blood unit. *In vitro* expansion and differentiation of cord blood stem cells have, therefore, been investigated in order to increase the cell number available, thus increasing the chances for a successful transplantation. Use of expanded HSCs for treatment of blood types diseases, for transfusion or for post-chemotherapy patients has been successful in various cases[6-8]. However, mechanisms controlling HSC fates *in vitro* are still poorly understood and not well defined; operation of a bioprocess that ensures quality and consistency of *in vitro* manipulated HSC products for clinical applications is therefore still difficult to achieve. Research efforts continue to further the characterisation of these complex bioprocesses in order to improve yield and quality of the cellular product that will meet high clinical standards.

The manufacture of stem cell engineered products suited for clinical applications also requires reliability, productivity, and reproducibility of the bioprocess operation. This not only demands a thorough understanding and definition of the bioprocess of interest, it also requires the necessary tools to perform tight process control[9]. However, current stem cell culture practises still lack the technology that can perform process monitoring in real-time to provide the necessary information for achieving tight process control[9]. This thesis will give an overview of some of the problems currently faced in HSC bioprocessing and aims to provide potential solutions that will bring about significant contributions for the future of stem cell research and bioprocess operation.

1.1 THESIS OUTLINE

Chapter 2 begins with a background of the biology of HSCs, the importance and use of umbilical cord blood stem cells, and the expansion and differentiation of HSCs *in vitro*. This is followed by an introduction to design of experiments (DOE) which includes a background of basic DOE designs, process characterisation, and optimisation methods. The chapter ends with a brief review of a selection of currently available measuring and monitoring technology for cell culture studies to underscore the lack and need for a real-time monitoring system. To sum up the overarching needs in stem cell bioprocessing, the overall goal and objectives of this thesis are presented in Chapter 3. Chapter 4 encompasses all the experimental methods and materials used for cord blood stem cell cultures, DOE strategies used for characterisation and optimisation studies, DOE strategy for spatial profiling of analytes, and the real-time monitoring platform designed for stem cell bioprocessing.

Chapters 5 through 8 embody the scientific research behind this thesis. The specific objectives for each chapter are summarised in Table 1.1. Chapters 5 and 6 focus on characterisation and optimisation studies for *in vitro* erythropoiesis of cord blood stem cells using DOE methods. Specifically, chapter 5 demonstrates the use of DOE in process screening, characterisation, and optimisation for a single step culture process. The main objective in this chapter is to demonstrate a systematic DOE strategy that can effectively and efficiently identify and quantify culture parameters in a complex bioprocess. Chapter 6 aims to further process characterisation and optimisation by looking at the effects of time on the cell expansion and differentiation, using again a DOE approach, to determine *in vitro* cell culture process dynamics. Optimisation of *in vitro* erythropoiesis as a multi-step is pursued here. DOE methods can also be used to study spatial variations within a process space, and

this work is demonstrated in Chapter 7, wherein temperature sensors were used to demonstrate the feasibility and robustness of this approach. In Chapter 8, results from the novel multi-channel multi-analyte real-time online monitoring system are presented. This includes biocompatibility/toxicity studies and real-time monitoring data obtained for ammonia, pH, and oxygen sensors. Final thoughts regarding the findings from this thesis and recommended future directions are summarised and concluded in Chapter 9.

Table 1.1 Scientific objectives for chapters 5, 6, 7 and 8.

Chapter	Scientific objectives
Chapter 5	DOE process characterisation and optimisation (single-step optimisation)
Chapter 6	Elucidation of process dynamics using DOE (multi-step optimisation)
Chapter 7	Spatial profiling using DOE
Chapter 8	Real-time monitoring using *in situ* biosensors

CHAPTER 2

Background

2.1 HAEMATOPOIESIS

Blood is one of the most essential components that sustain the human body. As blood circulates in the body, it helps maintain body temperature, fights infections, and nourishes the survival of all organs via the transport of oxygen and nutrients as well as the removal of harmful metabolites. Blood cells in circulation have a short lifespan varying from a few days to several months. As blood cells die, the human body responds through an elegant feedback system, to ensure that blood is continually replenished. This process is called haematopoiesis and it takes place in the bone marrow of healthy adults[10]. The primary function of haematopoiesis is to maintain the homeostasis of haematopoiesis by producing the various cell progenitors, which then terminally differentiate to generate all mature blood cells. This complex and highly regulated process comprises of the processes of self-renewal, proliferation, commitment, differentiation, and cell death.

The site of haematopoiesis, the bone marrow and its haematopoietic inductive microenvironment (HIM), is a complex sinus network consisting of stromal cells, bone cells, growth factors, extracellular matrix (ECM) and the residing haematopoietic cells[11]. The bone marrow stroma, consisting of stromal cells, macrophages, endothelial cells, and adipocytes, provides structure to the HIM and secretes growth factors that are the key initiators of most haematopoietic cell functions, such as homing, cell adhesion, proliferation and differentiation[11]. ECM macromolecules, secreted by the stromal cells, include proteoglycans, collagen and adhesive proteins such as laminin and fibronectin, which help to localise growth factors and the haematopoietic cells to their specific functional three-dimensional (3D) micro-environmental niches[11]. At these sites, a well-balanced physical, chemical and cellular microenvironment enables regulated processes to occur through a series of cell-to-cell and cell-to-matrix interactions as well as the micro-concentration gradients of the soluble factors.

2.1.1 Haematopoietic cells

All mature blood cells originate from a common stem cell called the haematopoietic stem cell (HSC), which in adults, resides in the stem cell niches of the bone marrow[10]. HSCs are distinguished by their unique properties of self-renewal - they are able to produce a lifetime supply of mature blood cells for the host[12] - and multipotency - their ability to differentiate into different types of blood cells, each with a specific and often distinct function[13] (Figure 2.1). Blood cells can be categorised in three main types: erythrocytes, leukocytes and thrombocytes. Erythrocytes, the red blood cells, are biconcave circular enucleated cells with a distinct affinity to oxygen due to the presence of haemoglobin. Their main function is to carry oxygen from the lungs to the tissues and transport carbon dioxide

from the tissues back to the lungs. Leukocytes, consisting largely of granulocytes, monocytes, and lymphocytes, vary in the shape of their nucleus and the presence of granules in their cytoplasm. Granulocytes, such as neutrophils, have irregular shaped/segmented nucleus while basophils and eosinophils are distinguished by the unique features of their cytoplasmic granules. Lymphocytes usually have a circular/oval nucleus with little/no presence of cytoplasmic granules and can vary significantly in sizes, ranging from 10 to 20 μm[13]. Monocytes are the largest blood cells and measure around 15-22 μm[13]. The nucleus of a monocyte can be round, kidney-shaped or indented and generally stain lighter than other leukocytes. Leukocytes are cells of the immune system. Cells, such as neutrophils, fight bacterial infections, while basophils and eosinophils participate in various inflammatory reactions. B- and T-lymphocytes produce antibodies and cytokines to neutralise bacteria and viruses, while monocytes/macrophages usually engage in phagocytosis, engulfing dead cells and foreign materials as they protect the body against infection. Thrombocytes (platelets) are small cell fragments deriving from megakaryocytes and participate mainly in the blood clotting process.

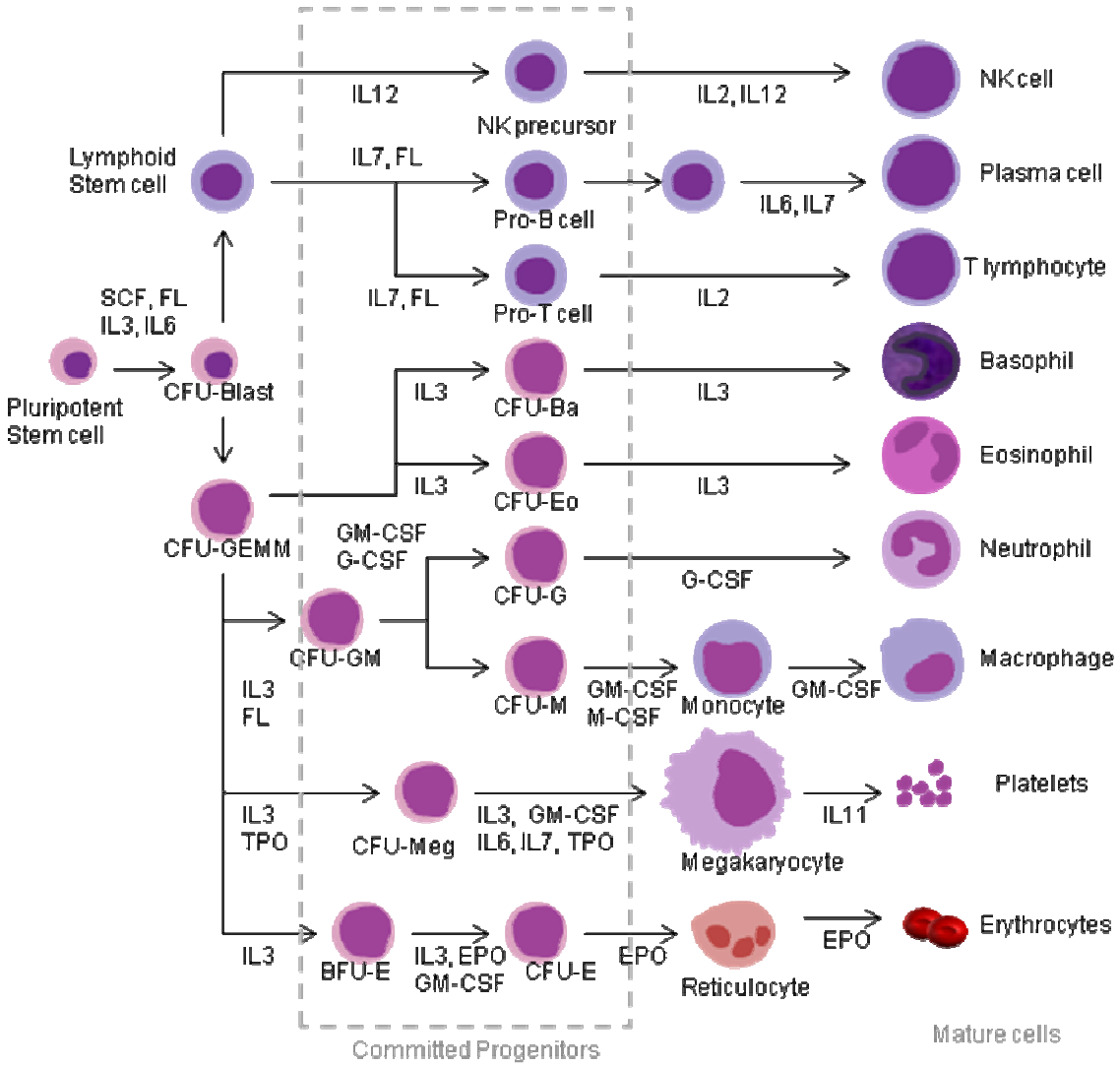

Figure 2.1 The process of haematopoiesis. (Adapted from Kaufman and Anderson 2003) Lineages: B/CFU = burst/colony forming unit, GEMM = granulocyte-erythrocyte macrophage and monocytes, Ba = basophil, Eo = eosinophil, Meg = megakaryocyte, E = erythrocyte, NK = natural killer cell.

Haematopoietic pathways are highly regulated by cytokines/haematopoietic growth factors – a family of glycoproteins that regulate cellular processes by recognising and interacting with specific cell-surface receptors. These cytokines control the proliferation, differentiation, and inhibition of haematopoietic processes, influencing the production of

blood in the body or in *ex vivo* cell culture systems. Figure 2.1 indentifies some of the key growth factors that are involved in the various differentiation pathways of the blood[14]. Progressive differentiation of blood cells to the different lineages often requires the interaction of several growth factors, some of which may be lineage-specific, such as erythropoietin (EPO) which stimulates erythrocyte production and interleukin (IL)-2 which stimulates T-cell production, whilst others such as stem cell factor (SCF), IL-3 and FLT-3 ligand (FL) work across lineage boundaries[12]. Non-lineage specific growth factors often do not act independently, but rather in conjunction with other growth factors to perform the required cellular function. Of these, SCF, IL-3, and FL stimulate the survival and proliferation of early progenitor cells, including HSCs[15]. Others, like the granulocyte-macrophage colony stimulating factor (GM-CSF) and granulocyte colony stimulating factor (G-CSF), help in the differentiation of the myeloid lineages[12,15].

2.1.2 Haematopoietic stem cell markers

HSCs are identified by a number of haematopoietic markers, the most common one being CD34, a 90-120 kDa surface molecule from the sialomucin family (ando). The determination of haematopoietic markers that signifies the true HSC has been controversial as the assessment for long-term self-renewal ability using a reliable assay has not yet been established. Many studies have used the multi-lineage repopulating ability of HSCs in non-obese diabetic/severe combined immunodeficient (NOD/SCID) recipients as a benchmark for identifying the HSC, and have determined that the $CD45^{+}CD34^{+}CD38^{-}$ phenotype as a reliable source[16,17]. However, other researchers have also found that $CD34^{-}$ haematopoietic cells are also capable of SCID repopulating cell activity[18]. Recent studies have indicated that

a haematopoietic phenotype of $CD45^{-}CD34^{-}CD38^{-}Lin^{-}$ cells are capable of long-term culture initiating cell activity and may represent the most immature phenotype identified so far in the haematopoietic lineage[19].

2.1.3 Cord blood stem cells and their therapeutic applications

HSCs are commonly used in transplantation for the treatment of malignant and non-malignant diseases. These include leukaemia, lymphoma, inherited blood, immune, and metabolic disorders, such as Hurler's syndrome, sickle cell disease, and osteoporosis[20]. Sources of stem cells for transplantation include the bone marrow, peripheral blood and cord blood. Each HSC source presents its advantages and limitations[21]. Use of cord blood stem cells has gained in popularity due to the ease of collection, rapid availability, worldwide acceptance, reduced risks of chronic and acute graft-versus-host diseases (GVHD), and greater human leukocyte antigen (HLA) mismatch tolerance[6,22-24]. To date, over 175,000 cord blood units have been banked and are publicly available for transplantation worldwide[24]. Procedures for collecting, banking, and storing cord blood donations are determined by several organisations such as the American Association of Blood Banks, the American Red Cross, Eurocord, NETCORD, and the National Bone Marrow Donor program to ensure the quality and standards of the cord blood units used for transplantation[6]. Thus far, over 8,000 cord blood stem cell transplantation have been performed worldwide with successful treatments performed on 70 different types of diseases including acute lymphocytic and myelogenous leukaemia (ALL and AML, respectively), myelodysplastic syndrome (MDS), Hodgkin and non-Hodgkin lymphoma, neuroblastoma, thalassemia etc[25,26].

Successful cord blood transplantation has been performed on both related and unrelated children and adults. The survival rate post transplantation is generally higher in children than adult patients due to the limited number of cord blood stem cells available in a single cord unit. The recommended minimum dosage for cord blood transplantation is $1.7x10^5$ $CD34^+$ cells or $>2.0x10^7$ total nucleated cells/kg of recipient body weight[24]. However, delayed haematopoietic recovery and lower engraftment success are observed in cord blood transplants in comparison to bone marrow or peripheral blood stem cell transplantations[23]. This can be improved by using higher $CD34^+$ cell dosages; it was found that a cell dosage of $>2.7x10^5$ $CD34^+$ cells/kg reduced transplant related mortality by about four times[6]. However, the major limitation in the use of cord blood stem cell transplantation for adults is the amount of stem cells obtained from a single cord unit which restricts the rate of successful transplantation to mostly children or adults weighing less than 35 kg.

The use of multiple cord blood units for transplantation in adult patients has been attempted and achieved some success. However, continued studies and clinical trials are being conducted to better develop selection criteria and prevent complications that could arise due to the combination of different resources[21,27]. Alternatively, combined use of stem cells with *ex vivo* expanded cord blood cells has also been experimented. Use of *ex vivo* expanded cord blood stem cells provides a promising opportunity for the manipulation of cord blood resources. Transplantation of cord blood stem cells with *ex vivo* expanded cells was intended to accelerate short-term haematopoietic engraftment and reduce the risk of early mortality or graft failure[6,24]. Current methods for expansion of cord blood stem cells include the use of different cytokine combinations in culture. However, *ex vivo* expansion of cord blood stem cells is not straight-forward and the final cellular product must also meet stringent

clinical standards for transplantation purposes. There is also the concern of unwanted stem cell differentiation during the expansion process, which may increase the risk of late graft failures[28]. Directed differentiation of cord blood stem cells to various blood cell types could also provide other potential applications, such as an alternate resource for blood for transfusion[29].

2.1.4 Haematopoietic stem cell culture practices

Traditionally, *ex vivo* expansion and directed differentiation of HSCs have been performed in serum-containing cultures. Many studies have been performed in gas-permeable blood bags and tissue culture flasks/well-plates, which can be sustained for prolonged periods (16 weeks)[30]. The addition of serum provides a rich supplement in nutrients and growth factors that promotes cell proliferation and sustains cell survival, which is particularly applicable to HSC cultures. However, the use of serum presents challenges for clinical applications. Consequently, serum-free culture conditions for *ex vivo* expansion has been explored. However, serum-free cultures typically require the use of large amounts of growth factors or cytokines, at abnormally high concentrations, which renders this approach cost inefficient. Specific roles for different cytokines used in *ex vivo* cultures have been extensively studied and reviewed in past literature[31,32]. Some of the cytokines that have been used for multi-lineage expansion include SCF, FL, macrophage-derived growth factor (MDGF) and granulocyte-colony stimulating factor (G-CSF)[33]. Expansion of specific lineages, such as megakaryocytes, utilises SCF, IL-3, IL-6, IL-9 and thrombopoietin (TPO)[34-36].

Another common method used for culturing HSCs *in vitro* is the stromal-based co-culture system using the murine stroma-5 (MS-5) cell line, HESS-5 cell line, or human bone marrow stroma Stro-1^+ cells to support serum-free cell cultures[37-39]. A comparison between allogeneic and autologous Stro-1^+ mesenchymal stem cell (MSC) populations showed better performance in expanding $CD34^+CD38^+$ cells and higher clonogenic potential of HSCs co-culture with stroma from allogeneic sources[40]. Co-culture systems benefit from stromal cell secreted cytokines and cell-matrix interaction, which enhances cellular activities. However, approval of stromal based cultures for clinical applications can be tenuous, particularly those of xenogenous origin. Preparation of a stromal cell layer for the co-culture system also increases labour, culture time, and complexity of the culturing process. Total cell expansion of progenitors in co-culture systems do not show significant improvement from that achieved in cytokine cultures.

Bioreactors used for expanding HSCs have also been explored. Expansion of cord blood mononuclear cells (MNCs) performed in a rotating wall vessel (RWV) biorector was compared to cell culture in a standard T-flask. Growth performance in the RWV bioreactor was found to be superior to the T-flask as it was able to provide a more homogeneous cell culture environment which enhances contact between HSCs and accessory cells while also optimising the effective utilisation of cytokines[41]. Cells cultured in microgravity (in the RWV) versus earth gravity also showed better engraftment potential[42]. Other types of bioreactors that have been tested for *ex vivo* expansion/differentiation of HSCs include perfused bioreactors, stirred-tank bioreactors, fixed bed, airlift, and hollow-fiber bioreactors[43].

Cytokine-based / 2D cultures do not resemble the *in vivo* environment due to the lack of cell-matrix interactions which has been the basis for many 3D cell culture studies to induce hematopoietic proliferation and differentiation[44,45]. 3D culture systems for creating a culture environment that mimics the bone marrow haematopoietic microenvironment have therefore been attempted. The use of scaffolds to create a 3D culture environment has been tested in various systems. Nanofiber scaffolds conjugated with different amino groups have shown to enhance cell adhesion and affect the expansion outcome of HSC cultures[46]. It has also been shown that a 3D co-culture system developed using stromal cells seeded in non-woven fabrics was more superior to its conventional 2D stromal co-culture in terms of progenitor expansion[47,48]. Additional factors such as extracellular proteins were found to be secreted in the 3D configuration[47]. These studies have shown that *ex vivo* expansion in 3D cultures has several advantages: cellular growth and responses in the 3D configuration appear to resemble that in the *in vivo* system, and the lack of exogenous growth factors also did not inhibit multi-lineage differentiation of cells in the 3D configuration[49,50]. These observations suggest the possibility of eliminating the use of growth factors in haematopoietic cultures which save significant costs in maintaining or expanding haematopoietic resources. However, extraction of cells grown in 3D scaffolds is not straight-forward as it may cause damage to the cells (reduced viability) or achieve only partial dissociation[51].

2.1.5 Culture parameters for *ex vivo* expansion and differentiation

Successful *ex vivo* expansion and directed differentiation of HSCs rely on the careful manipulation of key process variables affecting cellular environment. These include pH, dissolved oxygen and carbon dioxide tensions, nutrients, metabolites, and growth factor

concentrations used for the cell culture (Table 2.1). Culture parameters can greatly affect the growth and differentiation of cells by inhibiting or destroying cells in culture if certain parameters are not maintained at the right levels. It is therefore important not only to understand the effects of each cell culture parameter but also determine the right concentrations and levels that are necessary for a well-balanced cell culture environment.

Table 2.1 Culture parameters affecting HSC cell environment

Physicochemical Factors	Nutrients & Metabolites	Cytokines
pH	Glucose	Stem cell factor (SCF)
Dissolved oxygen tension	Glutamine	Flt3-ligand (FL)
Dissolved carbon dioxide tension	Glutamate	Interleukin (IL)-3, 6, 11
Temperature	Lactate	Thrombopoietin (TPO)
	Ammonia	Etc.

Culture pH, dissolved oxygen and carbon dioxide tensions, and chamber temperature affect the cell's physicochemical culture environment. In standard culture practices, cells are grown in culture at a pH of 7.40, 20% oxygen, and 5% carbon dioxide in a 37^{o}C fully humidified chamber. However, previous studies showed that the inducement of proliferation and differentiation of different blood cell lineages *in vitro* operate at different optima. Specifically, a higher pH (7.60) enhanced the differentiation and maturation of both megakaryocytic and erythroid progenitors[52,53]. In contrast, *in vitro* granulopoiesis was found to operate optimally at a lower pH (7.21); the lower pH enhanced granulocyte colony stimulating factor receptor (G-CSFR) expression which promoted granulocyte proliferation

and differentiation[54]. Oxygen tension is a critical factor in processes of haematopoiesis; in culture, it can greatly affect the expansion of cells by modulating the production of cytokines, surface markers and transcription factors[55]. Oxygen demand varies for different cell lineages at different maturation stages - low oxygen concentration (5%) is better for progenitor cell expansion while high oxygen (20%) promotes the growth of mature megakaryocytes and erythrocytes[53]. Low oxygen tension was also found to enhance granulocyte differentiation[56]. These findings strongly suggest the presence of *in vivo* pH and oxygen gradients where different sites in the bone marrow simultaneously participate in different haematopoietic cellular activities. Very few studies have been conducted on the effects of temperature. Most cell cultures maintained at 37^{o}C achieve healthy cell growth. However, in one study, a slightly elevated temperature of 39^{o}C was found to enhance megakaryopoiesis in CD34-enriched cord blood cultures[57]. The above findings highlight the fact that process variations in the cellular environment affect different cell populations and their behaviours *in vitro*.

Availability of nutrients and removal of unwanted metabolites in a cell culture is important for supporting basic cellular activities and maintaining the overall healthiness of the cells. Serum containing culture medium provides a multitude of nutrients that supports HSC proliferation and differentiation. However, the lack a defined serum as well as serum variability, pose significant limitations. Serum-containing cultures are therefore not ideal for expanding/differentiating cells that will be used in clinical applications. Instead, defined serum-free media are used for these purposes. Traditionally, in mammalian cell cultures, nutrient and metabolite concentrations are frequently monitored to ensure optimal cell growth and production of cellular products[58-62]. Nutrients and metabolites frequently monitored in cell culture bioprocesses include glucose, glutamine, glutamate, lactate, and ammonia.

Glucose and glutamine, the main sources of carbon and nitrogen respectively in metabolic pathways, provide essential components and energy to the cells such that they can participate and perform various cellular activities. In contrast, lactate and ammonia are the by-products of cell metabolism and need to be maintained at low levels so that they do not become toxic to the cells. High levels of lactate or ammonia inhibit cell growth and extreme levels can cause both apoptotic and necrotic cell death[63]. In general, ammonia is more toxic than lactate; levels of ammonia must therefore be closely monitored to prevent damage to the cells. In a study of mouse embryonic stem cell (ESC) culture, ammonia levels were maintained at below 3mM to ensure healthy cell growth and prevent any inhibitory effects on the cell culture[64]. Monitoring of key nutrients and metabolites in a bioprocess operation is essential for maintaining the right balance of these factors to run at optimal conditions.

Growth factors and cytokines provide key functional signals to the cells and regulate processes such as self-renewal, survival, proliferation, and differentiation of HSCs. Each growth factor/cytokine has various unique functions, both positive and/or negative in nature, and can act on either a specific cell lineage or multiple lineages. Early acting cytokines/growth factors that have been identified for the survival and expansion of haematopoietic stem and progenitor cells include SCF, FL, IL-3, IL-6, and IL-1[65-67]. Other cytokines responsible for the differentiation of progenitor cells into specific lineages include TPO which stimulates megakaryopoiesis and thrombopoiesis[35,68], EPO which triggers erythropoiesis (the production of red blood cells)[69,70], GM-CSF which controls the differentiation of myeloid progenitors and production of granulocytes, and IL-5 which regulates eosinophil production[71]. The selection of the growth factors/cytokines for *in vitro* HSC cultures, their concentration and the combinations in which they are used, can

significantly affect stem and progenitor cell activity, differentiation and expansion[72,73]. Many investigators have attempted to study and characterise these effects for the *ex vivo* expansion and differentiation of HSCs[32,67,72,74-76]. However, traditional approaches have been mostly based on dose-response methods that are limited to a one factor at a time analysis[77]. Interactions between different growth factors and other process parameters such as nutrients and metabolites cannot be defined using these methods. A much more robust mathematical approach is required to identify and quantify each effect and their respective interactions in order to tailor culture processes for optimal production of a specific haematopoietic cell population.

A balanced combination of all the above factors (pH, oxygen, nutrients, metabolites and growth factors etc.) contributes to the cellular environment of an *ex vivo* culture. Ideally, a cell culture environment resembling that of the *in vivo* process is desired. However, due to the heterogeneity, complexity, and the transient nature of the *in vivo* cell environment, determining process requirements that mimics the *in vivo* process is not a straightforward task. Utilisation of robust mathematical methods such as DOE is necessary to provide a better understanding and characterisation of the *in vitro* process. This will facilitate the elucidation of complex cellular mechanisms and provide process information that is needed to define an *in vitro* cell culture environment.

2.2 DESIGN OF EXPERIMENTS

DOE is a highly effective and efficient methodology for investigating a process of interest in order to obtain the maximum amount of information about the process using

minimum effort (*i.e.*, experimentation)[77]. In traditional experimental approaches, such as the dose-response methodology, a process is studied one factor at a time; meaning each factor is varied individually while other factors in the process remain unaltered. This approach has several limitations: (1) it does not reveal process interactions between different factors and (2) it often does not paint the "true" picture of the process and can therefore result in misleading conclusions[78]. The optima obtained from dose-response experiments are often not the true optima of the process[77]. In contrast, DOE allows us to study a process under greater scrutiny and precision. The availability of different types of DOE designs allows a tailored approach to the needs/goals of the experiment. A distinct advantage in using DOE is its ability to reveal both individualistic and interactive effects of a process using the minimum number of experimental runs[77]. This saves significant time and operational costs, but more importantly, it reveals a complete and accurate picture of the process which allows the experimenter to determine the process optima. As a result, DOE is widely used in many different types of industrial applications such as chemical and semiconductor processing. Comparison studies, screening experiments, response surface studies, and regression modelling can be performed using different DOE designs.

To date, use of DOE for cell culture studies is still rather limited; much of the research continues to rely on traditional dose-response methods. However, a small number of investigators who have used DOE for studying *in vitro* HSC cultures include the use of fractional factorial designs to perform screening experiments[79,80], and the use of central-composite or full factorial designs to perform process characterisation[35,76]. In the study performed by Yao and colleagues, concentrations of nine different growth factors and eight different serum substitutes were optimised via two-level factorial designs and the method of

steepest ascent, which resulted in 27-fold expansion of $CD34^+$ cells in serum-free conditions after one week[80]. In another study investigating megakaryocyte maturation, 13 different cytokines were screened using the Placket-Burman design (PBD) followed by characterisation using a two-level factorial design[35]. It was found that TPO in the presence of SCF, IL6 and IL3 significantly stimulated *in vitro* megakaryopoiesis while EPO and IL-8 inhibited megakaryocyte maturation[35]. Use of DOE for performing characterisation studies provided a 3D process representation describing cytokine effects and interactions for the process of interest. However, full process characterisation which considers all the process factors including physicochemical parameters, nutrients, metabolites, and growth factor concentrations has not yet been established. Due to the complexity of their interactions, process investigation of these factors in combination is not straight-forward. The successful application of DOE methodologies to resolve the complexity in HSC cultures will not only yield invaluable information for HSC bioprocessing but also provide a novel approach for other cell culture studies.

2.2.1 DOE experimental strategy

Complex systems, such as those encountered in the cell culture can be undertaken using a systematic approach through a series of DOE methods (Figure 2.2). This systematic approach breaks down a highly complex problem into sections and provides solutions to the problem in a sequential manner which ultimately allows the experimenter to develop a realistic process model from the knowledge obtained at each stage of the process. This approach involves three main steps: screening, characterisation, and optimisation, which are performed sequentially using the appropriate experimental design(s) chosen at each stage[81]

(Figure 2.2). The objective in the first stage, *screening*, is to identify factors that have a significant influence on the process, and accurately discriminate against factors that have little or no influence at all. Hence, the ultimate goal of the screening process is to quickly (using the minimum number of experiments) and effectively identify critical factors within the range of operation. In the second stage, *characterisation*, the goal is to obtain a more detailed and quantitative description about the process by way of 3D surface response plots to describe process characteristics. This is achieved by designing experiments for the parameters previously identified in the screening step so that both main and interactive contributions of the critical parameters are revealed. In *optimisation*, various approaches can be taken to reveal the optimal operating regimens for the critical process parameters investigated and yield the best conditions for a target process. In this case, multiple objectives can be defined and a common ground between the various requirements can be maximised using an iterative process from tools in the DOE software. These characteristics show how DOE is efficient for studying complex systems involving multiple factors and having multiple output considerations. The outcome of this systematic framework is a reproducible and statistically valid elucidation of bioprocesses that do not require *a priori* assumptions for the process of interest.

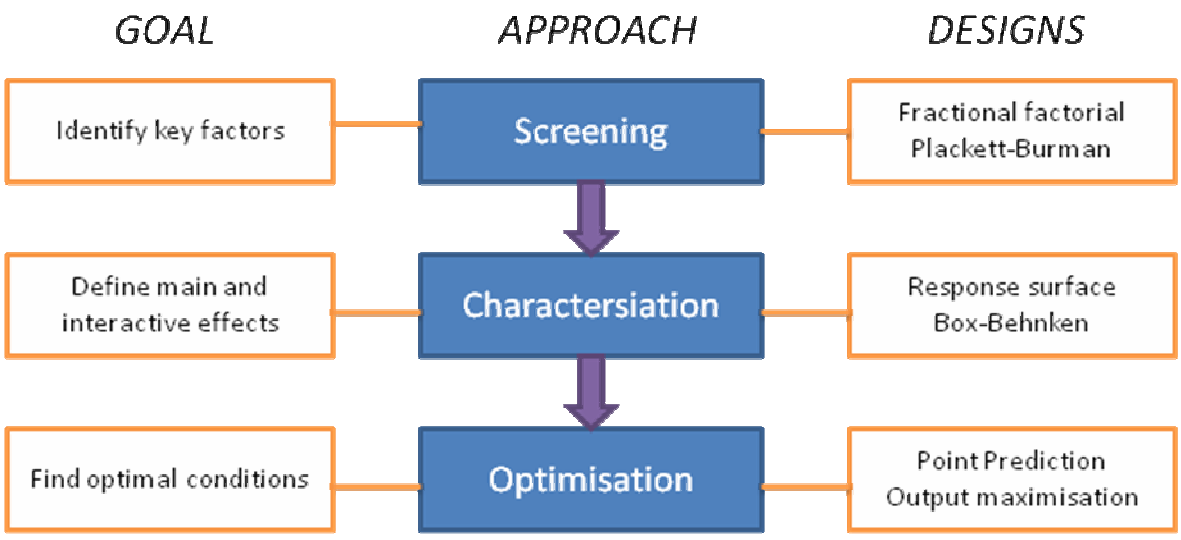

Figure 2.2 Proposed DOE approach for studying complex cell culture systems

2.2.2 Factorial Designs

Two-level factorial designs are the basic building blocks for many DOE designs and are therefore the most commonly applied design method. Factorial designs are very effective in studying both main and interactive effects rendering them extremely useful for response surface studies or process modelling[82]. A basic two-level full factorial design involves all the possible combinations of the high and low values of the various independent process factors under investigation and yields a total number of 2^n experiments for n number of factors. Specifically, in a two-factor factorial design, the design points relate to the four corners of a square, representing full coverage of the experimental space, and yields four (2^2) experimental runs. Similarly, a three-factor factorial design yields eight (2^3) experimental runs and is depicted by points in a cube (Figure 2.3a). Basic two-level factorial designs are

mainly used to study linear relationships between process factors and their responses but are still capable for revealing both main and interactive effects independently. Other variations of the factorial design for the purpose of screening and response surface modelling using second-order models will be discussed in the following sections.

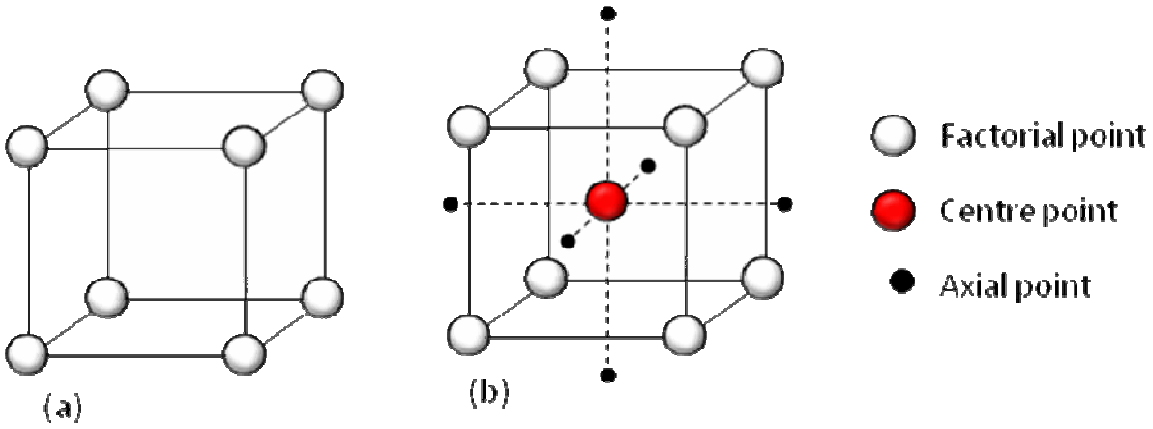

Figure 2.3 Types of DOE designs. (a) A basic two-level three-factor factorial design consists of eight experimental conditions (b) A three-factor centre-composite design (CCD) consists of eight factorial points, a centre point and six axial points.

As previously discussed, most cell culture bioprocesses involve a multitude of parameters. This increase in the number of factors in an experimental study results in a rapid increase in the number of DOE experimental runs required in a full factorial design. For instance, in a seven-factor experiment the required number of experimental runs would be 2^7, which equates to 128 experiments. This is a significantly large number of experiments to perform, which can be costly, labour intensive and extremely time-consuming, thus making full factorial designs an impractical option for process screening. Often when a large number of factors (more than five) are involved, screening is performed and two-level fractional

factorial designs are used to identify the influencing parameters. Fractional factorial designs derive from full factorial designs, where only a fraction of the full design is used to perform the screening. The assumption made in these designs is that higher-order interactions are often negligible, therefore only the main factors and low-order interactions are estimated in the design. The number of experimental runs are reduced in this case as factors in the design, both the main and interactive effects, are aliased with each other.

The effectiveness of the fractional factorial design depends on the resolution of the design which are defined as Resolution III, IV, and V[82,83]. A Resolution III design is one that has no main effects aliased with another main effect but they are aliased with two-factor interactions. Hence, Resolution III designs allow the estimation of the main effects, but the latter is biased by two-factor interactions. A Resolution IV design has no main effects aliased with another main effect or a two-factor interaction, but two-factor interactions may be aliased with each other. In practice it means that Resolution IV designs allow the estimation of main effects which are unbiased by two-factor interactions, although two-factor interactions in such designs are not estimable. Finally, a Resolution V design is one that has no main effects or two-factor interactions aliased with each other. Hence, Resolution V designs allow the estimation of both main effects and two-factor interactions independently. Higher-order interactions, three or more interactions, are usually assumed to be negligible. In conclusion, a design with a higher resolution represents a more thorough design since fewer factors are aliased with each other, but require a greater number of experiments. In most screening studies, a Resolution IV design is sufficient to perform accurate screening as the main factors are not aliased with any two-factor interactions, which are often significant in most processes. A table of experiments required for full and fractional factorial designs is

displayed in Figure 2.4. As symbolised by the colours, experimenters can proceed with Resolution V designs in great confidence (green); Resolution IV designs should be used with caution (yellow); Resolution III designs should be avoided (red) as much as possible.

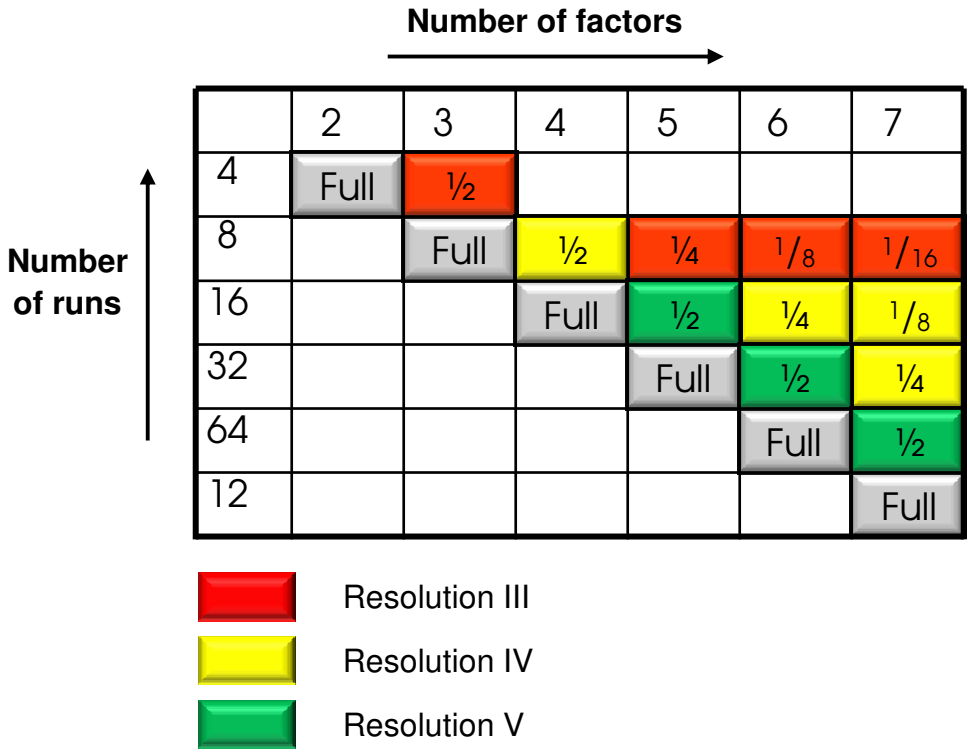

Figure 2.4 A matrix of full and fractional factorial designs and the number of experiments required for each design. (Adapted from Design Expert 6.0)

2.2.3 Response surface modelling

The most common design used for characterisation studies is the central composite design (CCD). The CCD derives from two-level factorial designs with additional axial points and a centre-point integrated into the basic 2^n design. The centre-point is used to estimate the curvature in a second-order model and is replicated for estimating pure experimental error. Axial points are used mainly to estimate the quadratic terms in a second-order model[82]. CCDs

are therefore used for modelling 2nd order response surface curves. The position of the axial point depends on α, the axial distance, which varies according to the extent of the region of operation of the various process variables. The value of α can range from 1 to $\sqrt{n}$, where n is the number of factors in the experiment. The choice of α value affects the design rotatability, which relates to the robustness and stability of the design. A rotatable design is one that provides equal variance in the estimation of predicted values at any two locations in the design space[82]. A CCD with an α value of $\sqrt{n}$ is referred to as a spherical design and is nearly rotatable or considered rotatable. A CCD with an α value of 1 is a cubodial or face-centred design. Though they are not rotatable, face-centred designs are often applied in many experimental studies where operating ranges are restricted but are still very effective in providing full process characterisation for the defined process regime. Another popular design is the Box-Behnken design, which is an independent quadratic design using three levels on each factor including a centre-point. But unlike the factorial designs, it takes the midpoints on the high and low end of the process space. This avoids any single experimental process to be at the extreme values of all the process factors, which can be useful in situations where there is a process limitation. The centre-point is also used here for the estimation of error and curvature. Other available designs include other spherical response surface method (RSM) designs and Equiradial designs[82].

2.2.4 Optimisation methods

Optimisation of process conditions can be performed via several methods. One of the most commonly used methods is the location of a stationary point in the response surface model[84]. This stationary point can represent a maximum response, a minimum response or a

saddle point[84]. The ultimate goal in the RSM is generally to obtain an optimum in the process under investigation and the generation of a 2nd order model allows ease in the identification of these regions. Another commonly used method is the method of steepest ascent[80,84] which is a process that guides the experimenter to move in the direction of maximum increase in the response[84]. Although this method is not as precise as the RSM, it allows one to quickly identify process conditions close to the area of optimal operation.

2.2.5 DOE for cell culture applications

With the availability and diversity of a wide array of DOE designs, many different applications can be found for the elucidation and optimisation of complex cell culture bioprocesses. The variety of DOE designs also provides flexibility in the design and approach of an experimental study and allows the experimenter to test the system using different methods. Use of DOE, as mentioned before, is a highly efficient and effective method for the study of complex systems; process screening can be performed using minimum effort (number of experiments) saving significant time and labour costs. Most importantly, the approach to the definition of cell culture bioprocesses is no longer at random or based on tedious single-factor analysis as DOE readily provides a systematic, reliable and effective approach toward the investigation and optimisation of complex cell culture bioprocesses, and produces information rich data/models that can be used for predicting cell culture outputs. Such precision and quality of information is necessary for achieving a well-defined culture environment that produces consistent cell culture products meeting high clinical standards.

2.3 PROCESS MONITORING TECHNIQUES

Process monitoring and process control of a bioprocess operation is necessary to ensure the quality and reproducibility of the product output. Cell based products intended for clinical applications, in particular, demand the highest quality and purity. In order for us to deliver stem cell therapies from the bench-top to the bedside, a tight control of the bioprocess operation is essential. Online, real-time process monitoring provides vital information that is needed to perform accurate control of the bioprocess of interest. Current monitoring techniques for cell culture bioprocesses, though extensive, have not been widely applied to stem cell cultures. Simultaneous monitoring of key process variables is limited to only certain parameters such as pH and oxygen. In this section, we will discuss existing monitoring and measurement tools applicable to the various process variables of interest: (a) pH, dissolved oxygen tension, carbon dioxide tension, and temperature; (b) nutrients and metabolites; (c) growth factors/cytokines; and (d) cell viability and concentration. Table 2.2 summarises the major measurement and/or monitoring techniques currently used for various applications which will be discussed in the following sections.

Table 2.2 Summary table of monitoring and measurement techniques for cell culture studies

Technique	Applications	Advantages	Disadvantages
Electrochemical Sensors	pH, O_2	Fast, easy to use Large pH range	Electrical/magnetic interferences Frequent calibration needed Invasive method Fouling and biocompatibility
Optical sensors	pH, O_2, CO_2	Fast, easy to use No electrical or magnetic interferences	Turbidity issues Limited pH range
Biosensors	Metabolites Cytokines	Easy to make and use	Limited enzyme stability Frequent calibration Invasive method Sterilisation issues
Commercial bioanalyser	Metabolites, pH, O_2, CO_2	Easy to use Accurate, reliable, quick Available as online systems	High / costly maintenance Bulky instruments as online systems
HPLC	Metabolites	Highly accurate and reliable Wide application Possible online system	Long sample analysis time Mostly applied as an off-line method
NIR Spectroscopy	Metabolites	Rapid analysis Multi-analyte measurement Can be used as online system	Signal overlap Broad bands Poor sensitivity
NMR Spectroscopy	O_2 Metabolites Cytokines Cells	Non-invasive Rapid analysis Obtain O_2 and cell distribution A wealth of information	Labelling required ^{15}N & ^{31}P NMR; low sensitivity Signal to noise issues Very expensive
Immunoassays (ELISA)	Cytokines	Well-established method Highly sensitive Accurate and reliable Wide range of applications	High reagent cost Large sample volume Labour-intensive Not an online method
Multiplex immunoassays	Cytokines	High throughput Highly sensitive More cost-effective Small sample volumes	Initial setup cost Cross-reactivity
Flow cytometry	Cytokines Cells	Multi-cellular quantification Single cell analysis Sorting capabilities High throughput Wide application	Expensive equipment Not suitable as online method
Cell counters	Cells	Fast, accurate, reliable Fully automated Easy to use	Limited applications
In situ microscopy	Cells	Good stability Automatic control and image analysis	Limitations in differentiating cell types Large amount of image data
Micro-CT	Cells	Non-invasive Non-destructive	Qualitative analysis Radiation exposure
Raman	Cells	Non-invasive Relatively little sample preparation	Low sensitivity High concentrations required

2.3.1 pH, oxygen, carbon dioxide, and temperature

The most common devices used for monitoring pH and oxygen are electrochemical sensors. The basic operation of an electrochemical sensor consists of a working electrode and counter electrode separated by a layer of electrolyte. The main advantages of electrochemical sensors are its sensitivity, simplicity and low cost. Sensors are also reliable over a wide range of values. They are therefore frequently used in many industrial applications and suitable for *in situ* process monitoring. Unfortunately, they do not show long-term stability for continuous monitoring in cell culture bioprocesses and require frequent recalibration during the bioprocess operation. Furthermore, electrochemical sensors are susceptible to both electrical and magnetic interferences, and are sensitive to changes in the electrolyte levels.

An alternative to electrochemical sensors is optical sensors, which rely on the absorbance or luminescence of an indicator dye immobilised in a cellulose or polymeric type support[85,86]. Since optical sensors are based on optics, they do not suffer from any magnetic or electrical interference but suffer from optical interferences due to turbidity or bubbles inside bioreactors. On the positive side, they offer fast measurements, excellent resolution, good sensitivity, stability, and are non-invasive to the cell culture environment. Long term performance of optical pH and oxygen sensors has been demonstrated for up to 120 and 180 days, respectively[87,88]. Multi-analyte sensors have also been designed to monitor pH, oxygen and carbon dioxide simultaneously[86,89]. However, due to its optical limitations and high sensitivity, probe position can sometimes influence the results obtained in different experiments. The pH range for optical sensors is also limited by the sensitivity of the indicator dyes used, which is typically over 2-4 pH units. Most cell cultures operate within pH 7-8 and will therefore not be limited by the narrow range of the optical sensors.

Nuclear magnetic resonance (NMR) spectroscopy is an extremely powerful, long-established and well known technique in analytical chemistry. The depth and resourcefulness of this technology has rendered it as one of the best tools for studying physical, chemical, and biological properties of simple or complex compounds. Its powerful imaging capabilities make it a distinctly unique methodology. Scientists have manipulated this advantage for the characterisation of oxygen distribution within a cell culture system[90,91], which was accomplished employing ^{19}F NMR. Unlike the use of sensors, ^{19}F NMR spectroscopy is capable of measuring the oxygen partial pressures inside the bioreactor. This technique is based on signal relaxation time of perfluorocarbons, which depends on oxygen concentration. Images of ^{19}F relaxation times can also be generated to provide the spatial distribution of oxygen within the bioreactor. This technique requires F-labelling through the addition of a perfluorocarbon emulsion into the reactor system, which, due to the biocompatibility of the perfluorocarbons, does not have any negative effects on the cells or culture system[90,92]. However, high equipment costs and the need for skilled operators deter many from using this technique.

Temperature measuring devices are divided into three basic groups: thermocouples, resistive temperature devices (RTDs) and thermistors. These contact devices are typically designed as probes which can be inserted into the bioreactor. Thermocouples are most commonly used as they give the fastest response and are highly economical. They are well suited for high temperature environments and microscopic applications. Unfortunately, they suffer from low sensitivity, poor stability, and exhibit a non-linear behaviour. RTDs, on the other hand, are the most stable and accurate temperature measurement devices. They exhibit a more linear behaviour, have a broad operating range, and show good repeatability, which

makes them applicable in many industrial applications[93,94]. However, they are expensive devices that have a slower response time and lower sensitivity[94]. Slow response time will not limit cell culture monitoring since fast and drastic changes are not expected to occur within the bioreactor system. Response time in cell culture environments are generally in the order of several minutes. Finally, thermistors, though not as commonly used as thermocouples or RTDs, are suited for low cost applications over small temperature ranges. But despite their economical advantages and fast performance, thermistors exhibit non-linearity and have a limited measuring range. They are also comparatively more fragile devices than their counterparts.

2.3.2 Nutrients and Metabolites

High-pressure liquid chromatography (HPLC) is frequently used for metabolite analysis in industry and academia due to its widespread applicability for studying many different types of compounds. It has the ability to analyse multiple analytes simultaneously while at the same time yielding high resolution and highly reproducible measurements. The high pressure system also has added advantages over traditional liquid chromatography columns, making processing time much quicker. However, standard processing time for conventional HPLC still requires around 60-90 minutes and is therefore not applicable for real-time measurements. Instead, it is more suited as a reliable off-line measurement tool or as a comparison to other analytical methods. Although HPLC cannot support real-time measurements, it can be applied as an online system for simultaneous measurement of multiple analytes to obtain continuous data from the process operation[95]. The automated online system provides the advantage of requiring less labour than performing multiple off-

line analyses and is useful for capturing transient effects that may otherwise not be detected from off-line measurements[95].

Biosensors are popular analytical devices for the recognition of biological compounds, pathogens, and toxic compounds. In cell culture applications, they are mostly used for nutrient and metabolite measurements and can be applied to a wide range of biological compounds. The most common type of biosensors designed for metabolites is primarily enzyme-based via electrochemical or optical detection[96,97]. Detection limits of glucose biosensors typically range from 4-150 μM and has a sensitivity of 0.2-1.0 μA/mM[98]. Biosensors are often used in cell culture bioprocess monitoring as *in situ* sensors which make them a relatively straight-forward application. However, the design of a stable sensor that can survive for an extended period in cell culture remains a challenge as they are prone to fouling and do not operate well particularly in serum-containing cell culture environments. Most *in situ* biosensors do not last for longer than 24 hr in a continuous cell culture environment[99]. *In situ* biosensors therefore have severe limitations in operational stability and biocompatibility. The more common setup for online applications is the incorporation of flow injection analysis (FIA) where a sample is taken through a sample port so the sensor is not in direct contact with the process medium[61,100,101]. This protects the sensors from fouling and allows the calibration of sensors to be performed conveniently without disrupting the process operation[101]. Despite the apparent advantages in application design, ease of use, and reliability, one major drawback is enzyme instability. Enzymes are highly specific yet subject to denaturation making them unsuitable for continuous long-term (>7 days) monitoring. Recalibration and enzyme replacement are often necessary. Efforts to enhance enzyme stability via the integration of new materials and improved immobilisation techniques have

been made to extend their operational lifetimes, improve sensor sensitivity, response time and detection limits[102-104].

Commercial bio-analysers, such as the Yellow Springs Instruments (YSI) bioanalyser and the BioProfile (Nova Biomedical) analyser, are some of the more commonly used instruments for mammalian cell culture studies which provide good measurement performance for routine practises. These systems are capable of measuring various nutrient and metabolite parameters such as glucose, glutamine, glutamate, lactate and ammonia, electrolytes such as sodium and potassium, and pH, dissolved oxygen and carbon dioxide. Commercial bioanalysers are easy to operate, self-calibrating and can perform readings within 2-3 min. Commercial bioanalysers are retrofitted for automated sampling to perform online bioprocess monitoring. The typical measuring range for glucose and lactate in a Bioprofiler is 0.2-15 g/L and 0.2-5 g/L respectively. However, commercial bioanalysers are extremely expensive to maintain and require a regular change of reagents in order to support and maintain the equipment's performance. As an off-line system, they provide a good reference point and are often used for performing routine measurements. As an online system, bioanalysers can be utilised for bioprocess monitoring and control of nutrient/metabolite concentrations of cell cultures[58].

Near-Infrared (NIR) spectroscopy offers an attractive alternative to biosensors for performing rapid, simultaneous measurements of multiple analytes in real-time[105,106]. Typical sensitivity of NIR spectrometers has a standard error of prediction (SEP) range of 0.5-1.0 mM. However, the distinct advantage of NIR spectroscopy is its ability to provide chemical information about the compounds, and not just their concentrations. Various configurations are possible for real-time monitoring: in an online system, samples are drawn directly from

the bioreactor in an automated loop[107], while an in-line/*in situ* system assumes direct contact typically via a probe[105,108]. Alternatively, the most non-invasive method is to place an external probe outside the bioreactor through a window or by means of a fibre coupling scheme[109]. NIR spectroscopy requires low maintenance during operation and no sample pre-treatment. Disadvantages of NIR spectroscopy include overlapping of signals, which tend to occur when bands are broad instead of distinct peaks. This makes monitoring of analytes at low concentrations difficult, particularly when the sensitivity and resolution here is not as high as other analytical systems. Other potential problems arising from long-term monitoring are likely due to environmental changes caused by temperature and optical interferences[105]. The development of reliable calibration models, often based on multivariate statistics, is therefore necessary to cope with process variations. This ensures that the system is more robust and sustainable over longer periods. Another instrument that is closely related to the NIR is the mid-infrared (MIR) spectrometer which interrogates in the mid-IR range. These regions are sometimes preferred as they reveal stronger absorbance and more distinct peaks[108]. However, MIR spectrometers are more expensive and are therefore less cost-effective.

The use of NMR spectroscopy to study cell metabolism is made possible through ^{1}H, ^{13}C, ^{15}N, and ^{31}P NMR techniques which trace C-, N- and P-metabolites and their respective intermediates[110-112]. These metabolites include glucose, lactate and glutamine. Cell metabolism is not only important in assessing the cell's physiological and energy status, it has also been recently suggested that metabolic rates could relate to HSC self-renewal[113]. One of the distinct advantages of NMR spectrometry is its ability to trace pathways and the fate of metabolites since it not only provides us with existing substrate concentrations, but

concentrations of intermediates and final products. This reveals the kinetics involved in various processes and allows the control of nutrients and toxic by-products in a biological system. Despite the wealth of information it can produce, instrumentation setup and data analysis for NMR are not straightforward. This technique also requires labelling of metabolites in order to trace their pathways and, in continuous cultures, often large amounts of labelling substrates may be required. The use of this technique is further hampered by the high cost of the equipment which is typically 5-20 times more expensive than NIR spectrometer or HPLC systems.

2.3.3 Cytokines

The golden standard for quantifying extracellular concentration of cytokines, hormones, and antibodies is the enzyme-linked immunosorbent assay (ELISA). The most common form of ELISA is the colorimetric or chemiluminescent sandwich ELISA, which is widely available commercially. ELISA is highly specific and sensitive, and requires only a small amount of sample for detection. Detection limit for a highly sensitive commercially available kit is in the range of 10-50 pg/ml depending of the protein of interest. Sensitivity limits can be as low as <1.0 pg/ml. Unfortunately, due to its long procedure (3-5 hours), ELISA can only be used as an off-line measurement reference. This technique also requires large amounts of substrates and consumables. Analysis of multiple analytes via ELISA is therefore not only time-consuming but can be rather costly[114].

In the last five years, platforms for multiple cytokine analysis have became readily (commercially) available. The multiple cytokine analysis technology exist in two basic formats: multiplex sandwich ELISA such as FAST Quant (Schleicher & Schuell) and bead

based immunoassays such as Luminex (Luminex Corporation). The use of multiplexing technology in these assay platforms offers significant advantages in cost and time savings over standard ELISA, by enabling the investigation of multiple analytes simultaneously[115,116]. This not only reduces significant time and cost but also allows the identification of patterns in analyte concentrations. Current systems such as the Luminex xMAP technology allow the identification of up to 100 analytes. Multiplex bead based immunoassays offer the same sensitivity and specificity as ELISA. However, the possibility of crosstalk in multiple immunoassay platforms is more likely to occur which can result in higher chances of a false positive or false negative[116]. The initial setup and equipment cost can be rather expensive and time-consuming but is more cost-effective as a long-term investment. Growing interest in understanding biological systems as an entity calls for the detection of an array of cytokines simultaneously making these systems more and more indispensible.

Intracellular flow cytometry is a detection method that allows simultaneous identification of intracellular cytokine and cell surface markers[117,118]. The unique advantage in flow cytometry is its capability for single cell analysis which allows the identification of key functional subsets in a cell population and is therefore an attractive tool for detecting cytokine production within a cell population[119,120]. Though the technique is not as sensitive as methods such as the ELISA, sample preparation is much more straight-forward and less time-consuming as there is no isolation procedures required for target purification[121]. Flow cytometry allows the detection of multiple cytokines in a single sample and multicolour staining facilitates co-expression investigation with surface markers as well as high throughput analysis of samples. Furthermore, cells can be sorted into specific cell populations which enable additional analysis of pure populations of the desired cells. Limitations of this

technique include high auto-fluorescence caused by permeabilisation and the inability of certain antibodies to work on fixed/permeabilised cells.

Despite many advantages offered by the powerful techniques described above, online, real-time monitoring is not possible through these methods. Currently, optical biosensors based on surface plasmon resonance (SPR) technology are capable of the online, real-time monitoring of cytokine concentrations. Biosensor assays are also easier to develop than immunoassays and are able to detect molecules as small as 200Da. More importantly, optical biosensors can provide biomolecular kinetic information such as binding constants, relative affinities and rate constants[122,123]. Such information is not only useful in identifying specific biomolecular interactions but can also reveal process mechanisms as has been illustrated by the kinetic studies of IL-5 and GM-CSF involving complex-receptor interactions[124,125]. However, limitations in this technique include the stability of the sensors and high usage of consumables[122]. The sensitivity and accuracy of this technique is also not as good as other quantitative methods such as ELISA or real-time polymerase chain reaction (PCR).

2.3.4 Cell tracking and monitoring

Cell enumeration by vital dye exclusion is the most common and straightforward cell quantification method used in a laboratory. Cells are stained with a vital dye, cells that are dead stain positive against the dye, and are subsequently counted using a haemocytometer through a microscope. The method is relatively quick and easy to perform, and allows visualisation of the cells. However, when a large number of samples are involved, it can be laborious and time-consuming. This technique is also subjective to the operator's judgment which can create high operator-to-operator variability in the results thus compromising its

accuracy. Furthermore, the dye exclusion method only distinguishes live-dead cells and not proliferating cells. Additional cell proliferation assays such as the bromodeoxyuridine (BrdU) labelling kit which measures the amount of cells in the S-phase (DNA-synthesis) is required to determine the number of proliferating cells in a cell culture. Other assays such as those based on the reduction of a tetrazolium salt compound (3-(4, 5-dimethylthiazolyl-2)-2, 5-diphenyltetrazoilium bromide (MTT) or 3-(4, 5-dimethylthiazol-2-yl)-5-(3-carboxymethoxyphenyl)-2-(4-sulfophenyl)-2H-tetrazolium (MTS) by metabolically active cells measures metabolic activity of cells in culture.

Quantification of a large number of samples through manual counting is highly non-practical, automated cell viability analysers such as the Vi-CELL series (Beckman Coulter) is necessary for processing large volume of samples quickly and accurately. The Vi-CELL technology performs a trypan blue dye exclusion assay using video imaging of the flow-through cell and provides the cell concentration, viability count, and real-time cellular images simultaneously. The system is fully automated and is useful for bioprocess monitoring. Another common cell counting system is the Coulter Counter, which provides absolute counts on cell populations for cell sizes as small as 0.4 μm up to 1200 μm on the Multisizer 3 Coulter Counter (Beckman Coulter). Use of Coulter counters provides accuracy, speed, versatility and excellent precision of results. However, these instruments are limited to cell counting purposes.

Alternatively, a much more versatile technique is flow cytometry, which provides an accurate quantification of cell population and cell numbers[126]. The power of flow cytometry is in its ability for single cell analysis and the use of laser technology. Excitation of each and every single cell through the laser beam allows the capture of forward scatter, side scatter and

various fluorescent emissions. This makes the differentiation of different cell type population possible and various types of cellular analysis can be performed simultaneously. Specifically, cell immunophenotyping, cell population distribution, DNA/cell cycle analysis and the identification of many other structural and functional parameters, such as membrane integrity, gene expression and protein content, can be obtained by flow cytometry[127]. A further key advantage is its ability to differentiate and sort cell populations at very high acquisition rates of up to 50,000 cells/sec. Currently, flow cytometry is mostly used as an off-line technique. Although online flow cytometry is possible, the equipment setup is complicated and highly inconvenient. Problems associated to fouling and contamination can also arise from sample withdrawal.

In situ microscopy (ISM) has significant advantages in cellular tracking: to monitor cell growth, cell movement, and even cell differentiation in real-time. It is a relatively straightforward technique that has shown good system stability and robustness for online real-time measurements. Its application has been successful in real-time monitoring of mammalian cell cultures and can be set up to perform automatic control and image analysis[128,129]. Though the application is straightforward, instrumentation setup for the culture system requires effort, which can be rather costly. The design of a robust cell recognition algorithm is also critical for the use of this technology and can pose several challenges. Cells that are too close together or have unusual morphology will become more challenging to identify. The amount of image data acquired from continuous real-time monitoring is enormous and will therefore require a significant amount of effort to perform data analysis.

Micro-computed tomography (micro-CT) is an extremely useful technique for bone tissue engineering to study bone growth, repair, vascular growth and biomaterial scaffolds.

This technology has been applied to monitor mineralisation and *in vitro* cell development within 3D scaffolds[130,131]. In these studies, cells were initially grown in media and seeded into various scaffolds. Weekly scans were then taken to monitor the matrix production and cellular growth within the matrix. These tests were successful in evaluating scaffolds used for bone tissue engineering applications and assessed the cell attachment, differentiation, and mineralisation *in vitro*. The use of micro-CT for these types of cell culture studies offers a quick and non-destructive method that requires minimal sample preparation as compared to histological studies. However, CT scanners are very expensive and computed tomography is still considered a moderate to high radiation diagnostic method; high resolution radiation between 100-1000 mGy can prove to be harmful. Currently, the effects on cells from direct exposure have not been thoroughly evaluated though a study has shown that repeated micro-CT scans (up to 5 scans) did not have any negative effects on mineralised matrix production nor inhibited cellular function of the cells within the scaffolds[130]. This application is particularly useful in the study of cells grown in a 3D environment.

NMR spectroscopy is a powerful and resourceful analytical tool that has been extended to the study of cell distribution. This is accomplished by diffusion weighted ^{1}H NMR and ^{31}P NMR used in combination to determine cell concentration distribution[132]. Diffusion weighted ^{1}H NMR produces images that correlate to intracellular and extracellular water molecules, which are assigned according to intensity. Intensity represents cell density and cell presence is confirmed by ^{31}P NMR data measuring the adenosine triphosphate (ATP) signals. ^{31}P NMR spectroscopy is used extensively in measuring ATP signals and phosphate-containing metabolites. This provides an indication of the cell's activity and energy status. However, the resolution and sensitivity of ^{31}P NMR in detecting the nucleotide pools is found

to be relatively low, and the analysis of living cells often suffers from high noise levels. The high equipment cost, sophisticated instrumentation setup, and need for skilled operators add to its disadvantage for bioprocess applications.

Raman spectroscopy has also been used to study the *in vitro* differentiation of stem cells[133]. Via this technique, RNA and DNA peaks of the cells are identified; the magnitude of the nucleic acid peaks indicates stages of cell differentiation. The application of this technique is straightforward and requires little sample preparation. It is a non-invasive method that enables the monitoring of cells *in situ* and in real-time[133]. However, the sensitivity of the spectrometer is low compared to other spectroscopic methods and requires sufficiently high cell concentration of the sample to provide a reliable reading. Furthermore, only a limited number of cells can be analysed using this technique, which does not render it suitable for quantitative analysis.

2.3.5 Need for cell culture monitoring

The extensive overview of various cell monitoring and measurement techniques presents an array of technology currently available for the analysis of a multitude of factors concerning a cell culture. The use of these techniques provides a wealth of information to appropriately determine characteristics of the culture, cell behaviour, and cell product; some of these tools have since become indispensible in standard cell culture practises. However, there are many limitations as to whether each technique can be applied for continuous monitoring. Gene or protein analysis for example is currently not possible as a continuous method and sophisticated tools such as the NMR or HPLC for metabolite analysis are often too expensive or highly inappropriate as online systems; they are therefore not useful for

continuous cell culture monitoring or process control. The procedure of taking samples from a cell culture is also limited by labour requirement and the quantity of cell culture media needed for each sample analysis. Culture monitoring in current practises is therefore not readily available and result in cell cultures being carried out in a sub-optimal process environment, compromising the outcome of the cellular product. One of the major requirements in the delivery of clinical grade cell/tissue-engineered products is the production of a consistent, reliable and high-grade biological product. Process control of cell culture bioprocesses is therefore necessary for high-throughput and consistent bioprocess operation that can bring results from a laboratory-based research into a manufacturing production. This brief review highlighted the lack of an appropriate, convenient, and cost-efficient monitoring system for cell culture bioprocesses which will ultimately impede research discoveries to be delivered to the needs of patients.

CHAPTER 3

Goal and Objectives

3.1 MOTIVATION

Ex vivo expansion and directed differentiation of HSCs have many applications in HSC transplantation, transfusion, and cellular therapy. This tremendous contribution can bring about potential cures for many blood-related diseases, disorders and malignancies, and provide an alternative resource for blood. One such resource in high demand is the red blood cell with around 40 million pints transfused annually and demand continues to increase[134]. Successful *in vitro* manipulation of HSCs toward mature blood cells such as the erythrocyte is therefore an invaluable resource as blood donations do not meet these demands. However, process complexities due to a large number of influencing factors such as pH, oxygen, glucose, lactate and cytokines[12,32,69,135], its transient nature (process dynamics), and the interplay of various processes such as self-renewal, proliferation, cell division[136], differentiation and apoptosis[137] make the manipulation of HSCs *in vitro* difficult. The lack of

knowledge in the nature of the process hinders precise definition of optimal extracellular process conditions necessary for the HSC bioprocess. This includes the identification of key cytokines and their specific concentrations needed to drive a stem cell culture bioprocess of interest. The production of stem cell products suitable for clinical applications requires precise process definition affecting cellular behaviour[9]. The second challenge that is faced subsequently is the translation of these results from a laboratory based research into patient therapy. Products used for clinical applications require quality and consistency of the highest demand. Cell culture bioprocesses that is used for the manufacture of clinical products require a highly defined culture system and bioprocesses that can be controlled optimally and reproducibly to meet good manufacturing practises[9]. However, due to the lack of process definition of these complex cell culture bioprocesses and the lack of real-time monitoring technology that is practical and economical for process control, delivery of manipulated HSC products as a viable therapy has not yet been achieved. Successful translation of stem cell products requires the integration and cooperation of basic scientific discoveries with pioneering engineering applications[138].

3.2 GOAL AND OBJECTIVES

The overall goal of this thesis is to deliver engineering solutions via statistical design methods and advances in monitoring technology necessary to translate results from the laboratory into a manufacturing facility. The specific objectives are:

(1) to develop a systematic framework using a robust statistical method, such as DOE, for the identification and definition of critical culture parameters required for an optimal bioprocess operation and

(2) to design and implement an online real-time *in situ* monitoring platform that will allow simultaneous monitoring of multiple process analytes for bioprocess control.

Control of stem cell culture bioprocesses to ensure quality and reproducibility of the product requires both process knowledge and real-time information of a cell culture bioprocess operation. Use of a robust and efficient experimental design strategy, such as DOE, is necessary to obtain a quantitative characterisation of complex stem cell culture bioprocesses. To this end, characterisation and optimisation can be achieved by: (1) the development of a simple and systematic approach for studying complex HSC cultures, (2) demonstration of the effectiveness and efficiency of DOE methods in optimising a single-step culture and (3) the development of a DOE strategy to reveal process kinetics. As a case study, the *in vitro* erythropoiesis of cord blood stem cells will be taken to demonstrate the success of DOE methods in HSC process optimisation.

The development of a robust monitoring platform that will allow real-time, online, *in situ* monitoring of multiple process analytes such as pH, glucose, oxygen and ammonia is necessary for bioprocess control. Development of a cell culture monitoring platform that is suitable for HSC or other cell cultures will include: (1) the design of biocompatible, functionally stable, miniaturised sensors suited for long-term cell culture monitoring, (2) the design of a unique multi-channel (many channels), multi-functional (many analytes) and multiplexable (stackable/expandable) data acquisition system that will allow simultaneous monitoring of different process analytes and (3) the design of a simple perfused bioreactor

system for HSC cultures. The successful integration of these three components will permit real-time, online, *in situ*, and long-term monitoring of culture parameters for any cell culture bioprocess of interest. Due to the diversity of expertise required in this project, a collaborative effort between the Biomedical Institute, Bioengineering department, and Chemical Engineering department at Imperial College London was established.

CHAPTER 4

Materials and Methods

Chapter 4 encompasses all the experimental methods and materials used in this thesis which include: (1) the work involved in using DOE which includes process characterisation, (2) spatial profiling in a bioreactor, and (3) the work involved in the development of a novel real-time online monitoring platform for stem cell bioprocessing. The main focus in section 4.1 is in the development and implementation of DOE strategies for the characterisation of cord blood stem cell differentiation. DOE strategies are divided into two parts: Characterisation I and Characterisation II. Part I focuses on the implementation of a simple strategy in approaching a complex process problem while part II attempts to integrate a factor of time and defining its influence on a culture process. Basic cell culture procedures and cellular analysis are also included in this section. Section 4.2 contains the experimental work and DOE design setup used in spatial profiling. A simple temperature study was performed as an example to illustrate and test the proposed DOE design and strategy. Section 4.3

contains all the work involving the uniquely designed online real-time monitoring platform which includes the development of the sensors, the data acquisition system and the bioreactor system suited for haematopoietic stem cell culture.

4.1 PROCESS CHARACTERISATION OF *IN VITRO* ERYTHROPOIESIS

4.1.1 Cord blood $CD34^+$ Isolation

Cryopreserved human umbilical cord blood was obtained from the London Cord Blood Bank (London, UK), in accordance with regulatory and ethical policies (Harrow Research Ethics Committee No. 05/Q0405/20). Cryopreserved human cord blood cells were thawed in a 37^{o}C water bath and gently aspirated from the blood bag using a 10 ml syringe and 18G needle. The aspirated cord blood is placed drop-wise into two 50 ml centrifuge tubes, each containing 30% (v/v) foetal bovine serum (FBS; GIBCO Invitrogen) and Iscove's Modified Dulbecco's Medium (IMDM; GIBCO Invitrogen) and centrifuged at 180g for 10 min. Supernatant is gently aspirated using a sterile Pasteur pipette and the remaining cells were re-suspended in 30% (v/v) FBS and IMDM solution. This wash procedure is repeated twice and cells were collected into a single 50 ml centrifuge tube. MNCs were isolated from whole cord blood cells using Ficoll-Paque PLUS (Amersham BioSciences) via density-gradient centrifugation. Cord blood cells were suspended in 2% (v/v) FBS and IMDM, and the Ficoll-Paque PLUS solution was gently layered under the cell suspension before being centrifuged at 400g for 35 min. The middle buffy coat layer which contains the $CD34^+$ and mononuclear fraction was gently removed using a sterile Pasteur pipette.

Freshly isolated MNCs were incubated with CD34 microbead kit reagents (Miltenyi Biotec GmbH) which contain an FcR blocking reagent and microbeads conjugated to monoclonal mouse anti-human CD34 antibody for 30 min at 4°C. After incubation, cells were subjected to microbead selection using high-gradient magnetic field in the MidiMACS and MiniMACS separators (Miltenyi Biotec GmbH). Cells were first passed through a 70 µm nylon mesh to remove any clumps before being applied into the MACS column. A typical purity of 92-96% in $CD34^+$ cells was obtained after two column separations. The $CD34^+$ fraction was measured by flow cytometry (see section 4.1.4.3). A simplified diagram illustrating cord blood extraction, density centrifugation and isolation procedure is shown in Figure 4.1.

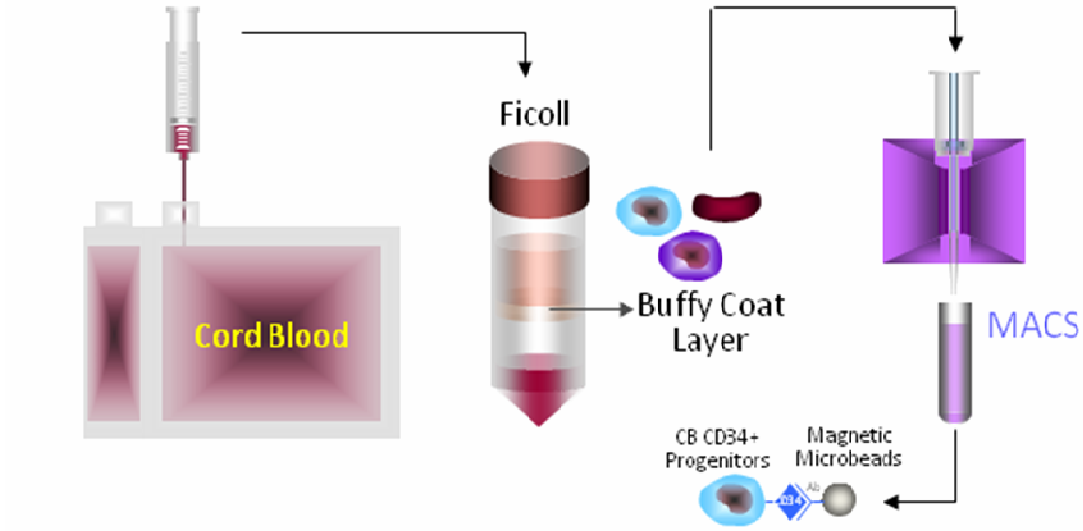

Figure 4.1 Cord blood isolation procedure. A flowchart of the isolation process which includes cord blood extraction, Ficoll-Paque density gradient centrifugation, and magnetic bead $CD34^+$ isolation. (Courtesy of Hwang, YS)

4.1.2 DOE Methods

4.1.2.1 Characterisation I: Basic DOE Strategy

Cell culture experiments driven by DOE were divided into three basic steps: screening, characterisation, and optimisation. In the screening step, seven different cytokines were selected from previous literature as those being more often utilised and showed some effects on *in vitro* erythropoiesis[70,139-141]. They include SCF, FL, IL-3, IL-6, GM-CSF, TPO and EPO. These cytokines make up seven independent process factors in the screening experiment, and a Resolution IV fractional factorial design was used to determine the significance of each cytokine of interest. A resolution IV design was chosen as it allows an accurate estimation of individual effects, without being convoluted with other individual effects or two-factor interactions[83]. The screening experiment generated 16 independent experimental conditions and four additional centre point replicates were included for pure error estimation (Table 4.1). Cord blood $CD34^+$ cells were seeded at a density of $2x10^4$ cells/ml in each well containing the different DOE defined cytokine-cocktail media. After ten days, cells were evaluated for total cell expansion and red blood cell maturation. DOE analysis was performed on day 10 cells so as to ensure sufficient differentiation of the cell population that is distinctive to the effects of the respective cytokines. The significance of each cytokine is determined by the coefficient plots and half-normal plots obtained from the DOE analysis.

For the characterisation study, results from the screening experiment which identified SCF and EPO as the only two cytokines affecting the process, was utilised to create a two-factor face-centred CCD. The face-centred CCD encompasses all factorial points, a centre point and axial points with an α–value of 1.0[82]. Three centre replicates were included for pure

error estimation and this design generated a total of 12 experimental runs. Cells were cultured for up to ten days prior to evaluation. The experimental data obtained for this CCD was fitted to a 2nd order polynomial model. Results were analysed using analysis of variance (ANOVA) and the response surface plots for each response of interest, cell expansion and red cell maturation, were plotted using MODDE 7 (Umetrics).

Table 4.1 Screening experiment for *in vitro* erythropoiesis of cord blood stem cells: Seven growth factors which include early-acting, mid-acting and late-acting growth factors were SCF, IL3, IL6, FL, TPO, GM-CSF, and EPO.

Std	Run	SCF ng/ml	IL3 ng/ml	IL6 ng/ml	FL ng/ml	TPO ng/ml	GMCSF ng/ml	EPO IU/ml
1	7	0	0	0	0	0	0	0
2	17	100	0	0	0	100	0	5
3	2	0	100	0	0	100	100	0
4	6	100	100	0	0	0	100	5
5	1	0	0	100	0	100	100	5
6	3	100	0	100	0	0	100	0
7	14	0	100	100	0	0	0	5
8	10	100	100	100	0	100	0	0
9	16	0	0	0	100	0	100	5
10	12	100	0	0	100	100	100	0
11	18	0	100	0	100	100	0	5
12	20	100	100	0	100	0	0	0
13	4	0	0	100	100	100	0	0
14	8	100	0	100	100	0	0	5
15	15	0	100	100	100	0	100	0
16	19	100	100	100	100	100	100	5
17	5	50	50	50	50	50	50	2.5
18	13	50	50	50	50	50	50	2.5
19	11	50	50	50	50	50	50	2.5
20	9	50	50	50	50	50	50	2.5

Optimisation of the process parameters was done by determining the overlapping regions of both responses, maximising both total cell expansion and red cell maturation simultaneously. This determines a region of operation where the most optimal cytokine concentration necessary for each factor can be found. The selected values for cytokine concentration were subsequently verified in a separate study and repeated (n = 6) in a 16-day cell culture. DOE design software used for generating all the experimental runs and for analysing the data were Design Expert 6.0.1 (StatEase) and MODDE7 (Umetrics). All 3D response surface graphs were obtained from MODDE7 while the ANOVA tables were generated from Design Expert.

4.1.2.2 Characterisation II: Defining the influence of time

The time factor in a cell culture is defined as the feeding frequency and time-points in a cell culture. Feeding frequency determines how often culture media needs to be replaced. Time-points in the culture determine when a change in culture conditions i.e. cytokine concentrations needs to occur. As an initial step, a screening study was performed to determine the significance of feeding frequency and change in culture conditions at a random time-point. A feeding frequency of two days versus four days was tested and a random time-point, day 6 of the culture, was taken into consideration for this experiment. A four-factor full factorial design was created and the process variables included three numerical factors – feeding frequency, SCF and EPO, and one categorical factor, change of media in relation to culture time-point.

In the second part of this study, a more distinct definition of time-point is required. At this stage, the *in vitro* process was defined based on growth kinetics which is characterised by

the lag phase, the growth phase, and the stationary phase/plateau. Though the *in vitro* process is reflective of both proliferation and differentiation simultaneously, it was difficult to delineate these effects. This study is a first attempt to characterise process dynamics, the use of growth kinetics was simply to provide a starting ground for dividing process phases. In the first phase (lag phase), slow growth was observed and this occurred during the first six days of the culture period. The second phase, the exponential/growth phase, was defined as cell culture from day 6 to day 10; this is when the highest growth rate of HSCs was observed. Finally, by the end of the culture (day 10-16), cell proliferation began to retard and the growth rate eventually reached a plateau. Cytokines used in this characterisation study included SCF and EPO; both were previously established in part I of the DOE characterisation study. In addition, a third cytokine, the insulin growth factor-II (IGF-II) was added as a mid-acting growth factor. IGF-II has been previously known to enhance *in vitro* growth of mature and primitive erythroid progenitors[142,143] and showed promising growth performance in cell culture studies[144]. Concentration ranges selected for SCF, IGF-II and EPO were from 10-110 ng/ml, 0-100 ng/ml and 0.1-5 IU/ml respectively. A face-centred CCD was used to characterise and optimise growth conditions for each phase of the culture. Six centre replicates were included in each study, which yielded a total of 20 experiments in each characterisation study to be performed sequentially throughout the cell culture. An example of the DOE experimental matrix required for each phase of the culture is presented in Table 4.2.

Experimental results in terms of fold expansion, viability and GPA expression for each DOE experiment were evaluated using Design Expert 6.0.1. Experimental results for each characterisation study were fitted into a 2nd order polynomial model via multiple linear

regression (MLR) to obtain the best fit to a model. Each DOE characterisation experiment was repeated two-three times to compare DOE models generated for each phase of the culture and to determine repeatability of models between different cord units. ANOVA tables summarised the results for each model and significance of the models in each DOE study. Response surface curves were generated to show a quantitative illustration of their relationships. Cytokine concentrations were subsequently optimised for each phase of the culture by maximising cell growth expansion and were subsequently verified (n = 3) for growth performance, clonogenic ability and surface antigen expressions.

Table 4.2 DOE-designed experimental run for three process factors

Std order	Run order	SCF (ng/ml)	IGF-II (ng/ml)	EPO (IU/ml)
1	20	10	0	0.1
2	7	110	0	0.1
3	8	10	100	0.1
4	18	110	100	0.1
5	5	10	0	5
6	16	110	0	5
7	1	10	100	5
8	10	110	100	5
9	19	10	50	2.55
10	2	110	50	2.55
11	3	60	0	2.55
12	11	60	100	2.55
13	15	60	50	0.1
14	13	60	50	5
15	14	60	50	2.55
16	9	60	50	2.55
17	12	60	50	2.55
18	4	60	50	2.55
19	6	60	50	2.55
20	17	60	50	2.55

4.1.3 Cord blood cell culture from DOE study

Freshly isolated cord blood $CD34^+$ cells were cultured in 10% (v/v) FBS and IMDM plus the growth factor cocktail defined by DOE. Cells were cultivated in 24-well plate systems (Corning) at a seeding density of $2\text{-}5x10^4$ cells/ml and fed every three days starting from day 4 of the culture by completely replacing the old culture medium for characterisation study I (Chapter 5). For characterisation study II (Chapter 6), cells were fed every two days after day 4. All cultures were maintained in a fully humidified chamber at 37^oC, 5% carbon dioxide and 20% oxygen environment. Cytokines used for screening in characterisation study I included recombinant human SCF, IL-3, IL-6, FL, TPO, GM-CSF (all from GIBCO Invitrogen) and EPO (R&D systems). Results from the DOE experiment indicated that the optimal cytokines and concentrations to be used in this single-step study (Chapter 5) were 75 ng/ml SCF and 4.5 IU/ml EPO. Cytokines used in characterisation study II were SCF, IGF- II (Peprotech) and EPO. Cord blood $CD34^+$ cells (> 95% purity) cultured in a three-step (multi-step) cytokine cocktail optimised from the DOE results were as follows: 50 ng/ml SCF, 100 ng/ml IGF-II and 3.00 IU/ml EPO from day 0 to day 6; 110 ng/ml SCF, 17 ng/ml IGF-II and 3.75 IU/ml EPO from day 6 to day 10; 74 ng/ml SCF and 3.98 IU/ml EPO from day 10 to day 16.

4.1.4 Cellular Analysis

4.1.4.1 Cellular growth

Cellular growth and cell viability were evaluated at each passage during the culture. Cells were manually counted using a haemocytometer under the Leica DM-IL inverted phase

microscope (Leica). Cell viability was determined by a dye-exclusion method using Erythrosin-B stain solution (ATCC) which stains only dead cells reddish-pink. Fold expansion, defined by the increase in total cell numbers from the starting population, was one of the main criteria that guided the DOE studies.

4.1.4.2 Cell staining

Morphology of the cultured cells was observed on a cytospin. The cytospin is a cell preparation technique where cells are spun onto the microscope slide for staining/observation purposes. A cell suspension of $1x10^6$ cells/ml was prepared in PBS and 100 µl of the cell suspension was loaded into a well in the cytospin assembly. Cells were spun for 3 min at 100g. The cuvette and filter in the cytospin assembly was then gently removed to avoid any damage to the fresh cytospin and the slide was air-dried for 5-10 min in preparation for immunohistochemistry. Cells were stained with either Wright-Giemsa stain (Sigma-Aldrich) for nuclear-cytoplasmic differentiation or Brilliant Cresyl-Blue stain (Sigma-Aldrich) for reticulocytes identification. Wright-Giemsa stain was performed in a Coplin jar via the dip-method. Slides were dipped for 10 sec in Wright-Giemsa stain and subsequently dipped in deionised (DI) water for approximately 2 min. For reticulocytes staining, cells were first mixed with Brilliant Cresyl-Blue stain in a microcentrifuge tube and incubated for 15-30 min at 37^{o}C before making the cytospin. Cells were visualised on the Olympus BX51 microscope (Olympus UK Ltd) and images were captured using the DP50 camera (Olympus UK Ltd). Fluorescence microscopy was also used to verify the expression levels and distribution of cellular surface antigens for CD45 and GPA. Staining procedures for surface antigens is described in the next section. The F-view unit (Soft Imaging System GmbH), a high

resolution cooled CCD digital camera, was used for capturing images in fluorescence microscopy.

4.1.4.3 Flow cytometric analysis

Surface expression of cultured cells for CD45, CD71, and GPA were analysed via flow cytometry using the Epics-Altra (Beckman Coulter) flow cytometer, equipped with a 488 nm Argon (Ar) laser. At each cell culture passage, 0.5-1.0x10^6 cells were harvested and incubated at 4^{o}C for 30 min with directly labelled anti-human CD45-fluorescein isothiocyanate-immunoglobin G_1 (FITC-IgG_1), CD71-phycoerythrin-IgG_{2a} (PE) and Glycophorin-A-phycoerythrin cyanide-5 (GPA-PC5)-IgG_{2b} antibodies (all from BD Biosciences) in PBS buffer containing 2% (v/v) FBS and 0.1% (w/v) sodium azide (Sigma-Aldrich). Negative controls were cells which are not stained with any antibodies. Isotype controls for each fluorescent signal (FITC, PE and PC5) were made up using FITC-IgG_1 isotype control, PE-IgG_{2a} isotype control and PC5-IgG_{2b} isotype control (all from BD Biosciences). Freshly isolated $CD34^+$ cells were stained with CD45-FITC-IgG_1, CD34-PE-IgG_1 (BD Biosciences) and CD38-PC5-IgG_1 (Beckman Coulter). Their corresponding isotype controls were FITC-IgG1 isotype control, PE-IgG_1 isotype control (BD Biosciences) and PC5-IgG_1 isotype control (Beckman Coulter). After staining, cells were washed twice with PBS buffer prior to analysis. If fixation is required, cells were normally fixed in 0.2% (w/v) para-formaldehyde solution and stored in 4^{o}C for 24 hr prior to analysis. Freshly isolated $CD34^+$ cells from cord blood units were also evaluated for CD45-FITC-IgG_1, CD34-PE-IgG_1 (BD Biosciences) and CD38-PC5-IgG_1 (Beckman Coulter) expression. Data acquisition using the Epics-Altra is typically performed immediately or within three days following

fixation, and a total number of 30,000 ungated events was recorded for each sample. Data analysis and off-line colour compensation for the FITC-PE, PE-PC5, PE-FITC, and PC5-PE fluorescent panels were performed using WinList (Verity).

4.1.4.4 Clonogenic assay

In vitro clonogenic assays for the erythroid (colony-forming unit-erythroid; CFU-E and burst-forming unit-erythroid; BFU-E), granulocyte-macrophage (CFU-GM), and multi-lineage (CFU-GEMM) cells were assessed using methylcellulose-based media, MethoCult GF H4434 (Stem Cell Technologies) which is supplemented with recombinant human SCF (50 ng/ml), GM-CSF (10 ng/ml), IL-3 (10 ng/ml) and EPO (3 IU/ml). For freshly isolated $CD34^+$ cells, 500-1,000 cells were seeded into 35 mm culture plate and for cord blood cultured cells, 500-20,000 cells (depending on the day of culture) were seeded into each plate. Seeding densities are optimised according to the clonogenic ability of the cells as recommended by the manufacturer's technical manual (Stem Cell Technologies). All assays were performed in duplicates. Plates were scored after 14-16 days of incubation in a fully humidified chamber at 37^oC.

4.1.4.5 RNA analysis

The total RNA from cord blood cultured cells was isolated using the RNeasy Mini kit (Qiagen). First, cells were disrupted in buffer RLT supplemented with 1% β-Mercaptoethanol and homogenised in a QIAshredder spin column, centrifuged at maximum speed for 2 min. Ethanol was then added to the cell lysate to promote binding of RNA to RNeasy membrane. Total RNA that bound to the membrane column was washed twice with Buffer RW1 before

ethanol was removed using buffer RPE. RNA was then eluted in a 1.5 ml collection tube using RNase-free water. RNA quantification was performed on a UV spectrometer and the A_{260}/A_{280} ratio of greater than 1.70 is required to ensure quality of RNA sample.

Total RNA was reversed transcribed into complimentary DNA (cDNA) using the reverse transcription system (Promega). First, 1 μg of each sample was prepared with Diethylpyrocarbonate (DEPC) water in a microcentrifuge tube and heated at 70°C for 10 min. RNA samples were centrifuged at maximum speed for 5 sec and cooled in ice for 5 min. The running cocktail consisting of 4 μl $MgCl_2$ (25 mM), 2 μl RT 10x buffer, 2 μl deoxyribonucleotide triphosphate (dNTP) mix (10 mM), 0.5 μl ribonuclease inhibitor (Rnasin), 0.6 μl avian myeloblastosis virus reverse transcriptase (AMV RT) (15 U) and 1 μl random primers (0.5 mg) was then added to each sample to make up 20 μl of sample volume. All samples are then placed in a thermocycle program that ran for 10 min at room temperature, 40 min at 42°C and 5 min at 4°C. The final cDNA samples were stored at -20°C.

cDNA pools were amplified using the Platinum Taq DNA-polymerase (GIBCO Invitrogen) in a G-Storm GS1 thermal cycler (Gene Technologies Limited) for 30 cycles. Each sample contains 45.6 μl of mastermix, 1 μl of each primer (sense and anti-sense), 2 μl of cDNA sample and 0.4 μl of Taq polymerase. PCR mastermix consisted of 5 μl 10x PCR buffer, 1.5 μl $MgCl_2$ (50 mM), 1 μl dNTP mix (10 mM) and 38.1 μl of DEPC-treated water. Sequences of the gene-specific primers for RT-PCR can be found in Table 4.3. Temperatures for each amplification step were optimised specifically for each primer (50.4°C for α-haemoglobin; 59.3°C for β-haemoglobin, 56.9°C for γ-haemoglobin; 53.0°C for GATA-1; 56.9°C for HOXB4; 53.0°C for GAPDH). The denaturation step was performed at 94°C for 30 sec, and the annealing/extension step was at 70°C for 1 min for all primers. K-562 cells

(ATCC) were used as the positive control for this test for γ, β and α–haemoglobins and GATA-1, while HL-60 cells (ATCC) were used as the negative control.

RT-PCR samples were processed via agarose gel electrophoresis for separation and visualisation. Agarose gel was made by mixing 2 g of agar with 100 ml of 1x TBE solution, dissolved in a microwave and adding 10 µl of EtBr (10 µg/ml) just before being casted to solidify. Solidified gel is then transferred to the electrophoresis system. Samples were prepared by mixing 2 µl of Blu/Orange loading dye and 10 µl of RT-PCR sample. A DNA reference sample consisting of 5 µl of 100bp DNA ladder and 1 µl of Blu/Orange loading dye was also made up. Samples were loaded quickly into each well in the gel and subjected to electrophoresis at 80 V for the first 10 min and 110 V for 50 min. Gels were visualised in a gel-documentation system (Dyversity; SynGene).

Table 4.3 Gene-specific primers used to characterise cord blood cultured cells

Gene of interest	Forward sequence	Reverse sequence
α-haemoglobin	CACGCGCACAAGCTTCG	AGGGTCACCAGCAGGCAGT
β-haemoglobin	CAAGAAAGTGCTCGGTGCCT	GCAAAGGTGCCCTTGAGGT
γ-haemoglobin	TGGCAAGAAGGTGCTGACTTC	TCACTCAGCTGGGCAAAGG
GATA-1	CAGGTACTCAGTGCACCAAC	TGGTAGAGATGGGCAGTACC
HoxB4	CCTGCATGCGCAAAGTTCA	AATCCTTCTCCAGCTCCAAGA
GAPDH	GCAGGGGGGAGCCAAAAGGG	TGCCAGCCCCAGCGTCAAAG

4.1.4.6 Protein analysis

Cord blood $CD34^+$ cells (day 0) and cultured cells from days 7 and 14 were collected for Western Blot analysis. Cells were centrifuged into a cell pellet and stored at -20^{o}C till analysis. Frozen cell samples were lysed in 150 ul of cold RIPA lysis buffer (Santa Cruz

Biotechnology), incubated at 4°C for 30 min and centrifuged 10,000 RPM for 15 min to pellet the cell debris. Protein-containing supernatant was collected for protein quantification.

Total amount of protein was quantified using the bicinchoninic acid (BCA™) Assay Kit (Peirce Biotechnology). The BCA quantification method is based on the reduction of Cu^{2+} ions to Cu^{1+} by proteins in an alkaline environment which causes the formation of a blue-coloured complex. The highly sensitive and selective colorimetric reagent, BCA, reacts with the Cu^{1+} cation to form a BCA/copper complex which exhibits a strong linear absorbance at a wavelength of 562 nm. Bovine serum albumin (BSA) was used as a known protein standard and diluted at various concentrations in phosphate buffered solution (PBS) ranging from 0-500 µg/ml to create a standard curve. 25 µl of each sample is loaded onto a 96 well plate followed by 200 µl of BCA working reagent. Plates were covered and incubated in an orbital shaking incubator at 37°C for 30 min and then read on a microplate reader at a wavelength of 560 nm. Protein concentrations in each sample were quantified against the BSA standard curve.

From each sample, 40 µg of proteins were loaded onto each lane of the gel in sodium dodecyl sulphate polyacrylamide gel electrophoresis (SDS-PAGE). Protein samples were mixed with 2x SDS-PAGE sample buffer which consisted of 0.125 M Tris-HCl at pH 6.8, 4% SDS, 20% (v/v) glycerol, 10% β-mercaptoethanol and 0.005% (w/v) bromophenol blue. The sample mixture was heated at 95°C for 10 min for protein denaturation and placed in ice prior to gel loading. A protein ladder consisting of a range of proteins from 40-200kDa was included in each gel.

SDS-PAGE gels were prepared individually using the gel assembly kit for a 10-well gel. A 12.5% resolving gel was made by mixing 4.81 ml of resolving buffer, 4.16 ml of

Protogel acrylamide mixture (National Diagnostics), 1 ml 0.9% ammonium persulfate (APS; VWR) and 15 µl of TEMED (N, N, N', N' tetramethyl-ethylenediamine; VWR) and gently poured into gel assembly, allowing it to polymerise for 15-20 min. The gel is finished off with a stacking gel layer and allowed to further polymerise for about 45 min. The stacking gel consists of 2.03 ml stacking buffer, 0.6 ml Protogel acrylamide mixture, 0.3 ml of 0.9% APS and 8 µl of TEMED. One-dimensional SDS-PAGE was performed in the EC120 mini veritical gel electrophoresis unit (Thermo Electron) and a constant voltage of 110 V was initially applied for 15 min or till the sample passes the stacking gel before a constant voltage of 150 V was applied for another 45 min or until the dye reached the bottom of the gel. Gels are allowed to equilibrate in 1x transfer buffer for 30 min before they are blotted onto 0.2 µm nitrocellulose membranes. Protein blotting was performed in the C140 Mini Blot Module (Thermo Electron) at a constant current of 30 mA for 50 min. The blotted membrane was then air-dried for at least 1 hr at room temperature prior to immunostaining.

Western blot analysis of β and γ-haemoglobins (Santa Cruz Biotechnology), and GATA-1 (R&D Systems) were used to assess erythrocyte maturation determined by its expression at the protein level. GAPDH (Abcam) was used as the housekeeping gene. Red blood cells collected from cord blood were used as positive controls for β, γ–haemoglobins, and K562 cells were used as the positive control for GATA-1. HL-60 cells were used as negative controls for all proteins of interest. Protein membranes were then incubated overnight at 4^{o}C in the primary antibody and 1 hr at room temperature for the secondary antibody. The primary antibody dilution for the haemoglobins and GATA-1 was 1:200 and 1:20000 for GAPDH. Secondary antibodies were conjugated to horseradish peroxidase (HRP) and a dilution of 1:10000 was used for each antibody. Proteins were detected using the

SuperSignal West Pico chemiluminescent substrate (Pierce Biotechnology), a highly sensitive enhanced chemiluminescent substrate for detecting HRP on immunoblots. Western blot images were captured in the Dyversity gel-documentation system (SynGene) using the Genesnap program (SynGene).

4.2 SPATIAL PROFILING USING DESIGN OF EXPERIMENTS

4.2.1 Culture chamber and experimental setup

Culture chamber designed for HSC process monitor was a 2D perfused system that is identical in size to a standard 6-well culture plate. Specifically, the cylindrical chamber had a diameter of 31 mm and a height of 9 mm with two inlets and two outlets for perfusion at opposite ends (Figure 4.2a). The inlets are positioned at 1.0 mm from the bottom of the chamber while the outlets are positioned 1.0 mm from the top of the chamber (Figure 4.2b). This was designed so as to minimise the loss of cells due to perfusion and optimise the availability of fresh media to the cells. The material used to fabricate this chamber is polymethylmethacrylate (PMMA/Perspex) with the exception of the top cover, which is made of polydimethlysiloxane (PDMS), a soft and flexible mould that allows insertion of the sensors directly into the culture chamber via an 18G needle. Sensors were placed as close as possible to the bottom of the chamber, without touching the base; the estimated height of the sensing tip was approximately 1 mm above the base of the chamber. The chamber was then filled with 8 ml of water which was at 18-19^{o}C. The maximum capacity of the culture vessel was 9 ml.

Three experimental setups were employed to simulate different cell culture scenarios. In the first scenario, a single heating element was used to represent a single large cell colony being present in a static culture environment (Figure 4.3a). In the second scenario, two heating elements were used to represent two large cell colonies in a static culture (Figure 4.3b). In the third scenario, two heating elements were used to represent two cell colonies in a perfused culture operating at a flow rate of 0.01 ml/min. This equates to 14.4 ml of media exchange per day which is considered a high perfusion rate for this culture system. A high perfusion rate was selected to further demonstrate the applicability of this DOE approach under conditions that would result in a homogeneous environment more rapidly. The liquid used for perfusion was water measuring at 18-19^{o}C. All experiments were repeated three times and the centre point in the DOE design was used to obtain an estimate for pure error. Figure 4.3 (a) and (b) depict the positions of the heating elements for the single (lower heating element only) and dual heat source set-ups. All three experiments were monitored using DOE- and randomly-generated sensor placement designs as described below. Temperature readings were obtained every 10 sec for up to 10 min.

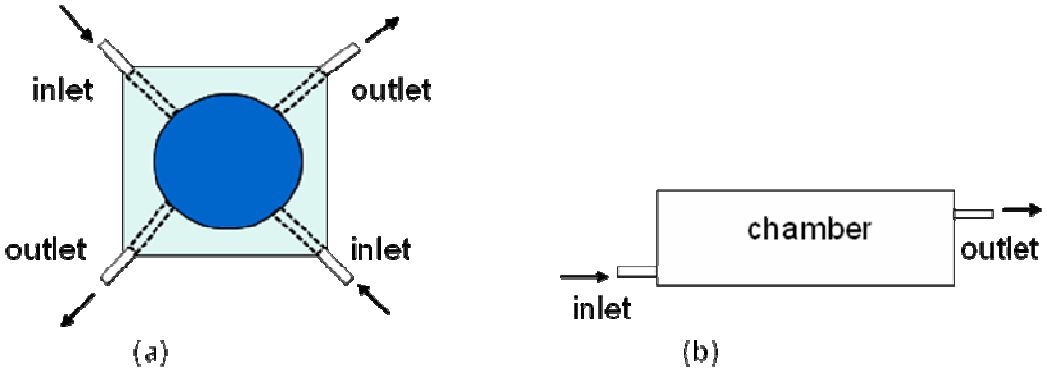

Figure 4.2 Design of bioreactor system for haematopoietic cell cultures. (a) Top view of the bioreactor (b) Side view of culture chamber

4.2.2 Temperature sensors and heating elements

Temperature sensors used in this experiment were the IT-21 series, Type-T flexible implantable thermocouple probes (Physitemp Instruments Inc.) along with the Thermes high accuracy industry standard architecture (ISA) based data acquisition system (Physitemp Instruments Inc.) which has 16 data input channels. The data acquisition system has a resolution of 0.01^{o}C, a reading accuracy of 0.2^{o}C in the ambient temperature range of 15 to 35^{o}C, and a stability of +/- 0.1^{o}C. Multiplexing capability of this system allows continuous readings of 16 channels per second. Temperature sensors have a diameter of 0.406 mm, they are flexible, and can be inserted through the PDMS cover of the bioreactor using an 18G needle. The sensors are fairly fragile but very fast responding. The latter provides a good basis for capturing small temperature variations.

Heat sources to the chamber were provided by high density penny-bottom cartridge heaters (Tempco Electric Heater Corporation) that have an integrated thermocouple and a diameter of 6.35 mm. Side-walls of the cartridge heaters were surrounded by a ceramic block to minimise heat loss sideways to the environment while directing most of the heat upwards into the bioreactor. Heating elements were placed at the bottom of the bioreactor to generate point heat sources inside the culture chamber. Heating elements were set at 69-70^{o}C for all experiments and controlled by a basic PID controller (Tempco Electric Heater Corporation).

4.2.3 Design of experiment parameters

Response surface method (RSM) is a commonly used and highly effective method for defining 2nd-order polynomial relationships[82]. As described previously in Chapter 2, the

model consists of a standard 2^{nd}-order quadratic equation used to fit experimental points in the design. In this case, a basic CCD consisting of four factorial points, a centre point, and four axial points was chosen. The α-value, depicting the position of the axial points, of this two-factor design was chosen to be 1.414 which covers the entire 2D process space of the cell culture chamber. The factor variables defining the design space is expressed in terms of the x-axis and y-axis in the 2D area of the culture chamber. The design matrix was created based on these criteria, and the number and position of the sensors were obtained, as shown in Figure 4.3c. Nine DOE sensor positions were determined for this face centred CCD design. DOE software used to generate the experimental points and for data analysis was MODDE 7.

As a comparison to the DOE method, two random designs for the positioning of sensors were chosen. In the first design (Figure 4.3d), five sensors were utilised and placed in the centre (one sensor) and the periphery (four sensors) of the culture chamber. In the second design (Figure 4.3e), seven sensors were employed and placed in the centre (one sensor), middle section (two sensors), and the periphery (four sensors) of the chamber. These two random designs were compared to the DOE-generated designs for effectiveness. Finally, a validation experiment for the DOE design was performed by placing three additional sensors at random (Figure 4.3f). These sensor positions were used to compare with the predictions obtained from the DOE analysis to experimental data. The verification experiment was performed for the single heating element experiment (Figure 4.3a).

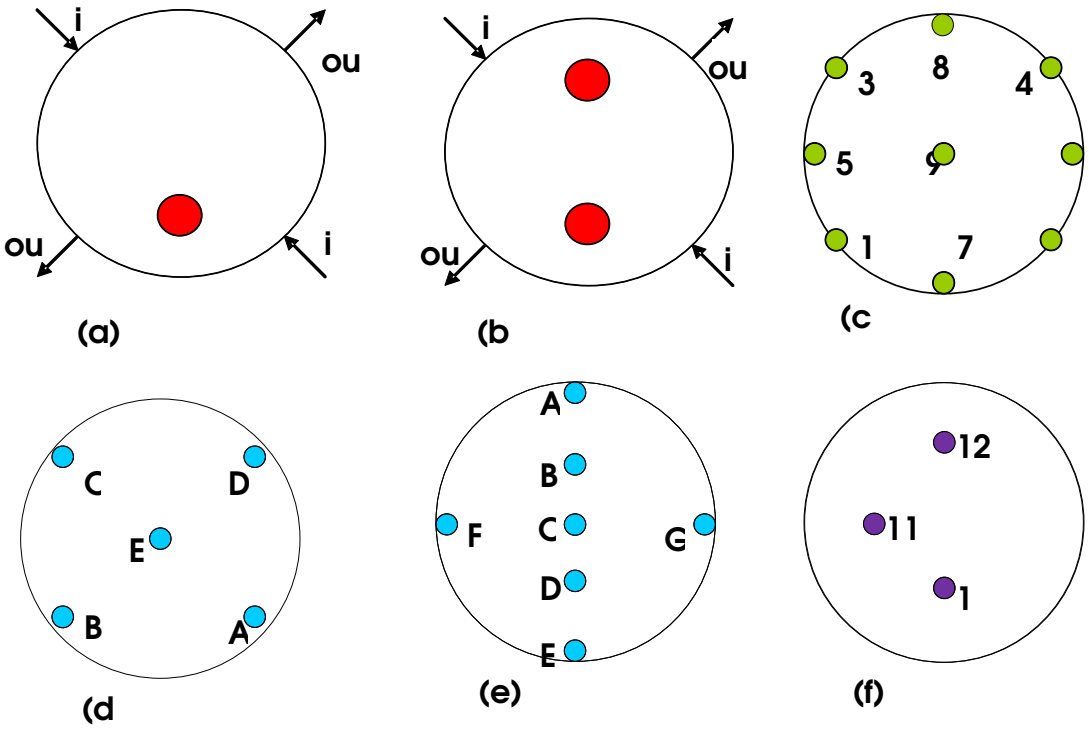

Figure 4.3 Placement of heating elements and sensors. (a) Single heating element (b) Dual heating element (c) Nine DOE-design sensors (d) Five random positions (e) Seven random positions (f) Sensor positions for verification study.

4.2.4 Data analysis

Temperature variations across the 2D culture chamber were estimated via MLR into a 2^{nd} order polynomial model using MODDE 7. The agreement of fitness to the model was determined by the R^2 values. The p-value and lack of fit, describing the validity of the model, were obtained by ANOVA analysis. Contour maps showing the temperature spatial profiles for the 2D culture chamber were generated from the fitted model via point prediction. Point prediction values can be generated in the DOE software. Predicted values from the model were subsequently graphed using SigmaPlot (Systat Software Inc.) to generate spatial and temporal contour distributions for each temperature experiment in the single heating element,

dual heating elements, and perfused system settings. Finally, additional points in the DOE validation experiment for a single heating element setup were compared to model results at a 95% confidence interval.

4.3 ONLINE REAL-TIME PROCESS MONITORING

4.3.1 Development of pH, oxygen, and ammonia sensors

4.3.1.1 pH sensor

pH electrodes were fabricated via electrochemical deposition of iridium oxide thin films on Pt electrodes in galvanostatic mode. The main advantages of the iridium oxide electrodes are the wide pH range, low potential drift, super-nernstian response, good response time, and low sensitivity to redox pair interferences. The basic response of anhydrous iridium oxide films to pH is due to an Ir(III) to Ir(IV) redox transition associated with the reaction and has a slope of 59 mV/pH. However, hydrated iridium oxide exhibits a super-Nernstian response, resulting in a slope of approximately 90 mV/pH, which corresponds to better sensitivity of the sensor. Finally, the hydrated iridium oxide films were coated with a Nafion layer which prevents its instability to anions and enhances its resistance to biofouling. Size of the sensor is around 250 μm.

4.3.1.2 Oxygen sensor

The oxygen sensors are basic amperometric oxygen transducers comprising of a Pt electrode coated with PDMS. The porous and hydrophobic PDMS layer allows permeation of

gases but restricts the passage of other soluble electroactive species which makes it possible to monitor the oxygen level without interference from reactive species such as H_2O_2. Since PDMS is highly hydrophobic, proteins will easily adsorb onto the surface of this material and the biocompatibility of this material is compromised. However, the adsorbed layer of protein is also permeable to small molecules such as oxygen and will therefore not change the analytical response of the amperometric sensor.

4.3.1.3 Ammonia sensor

Ammonia sensors fabricated for the monitoring studies were polyvinyl-chloride (PVC)-based ion-selective electrodes (ISE). The polymeric membrane consists of 3.2 mg of ionophore (Nonactin), 128.2 mg of plasticiser Di-n-octyl sebacate (DOS), and a combination of 6.0 mg of polyethylene-glycol (PEG) and 62.6 mg of PVC-carboxylic acid (COOH) polymers dissolved in 1.2 ml of tetrahydrofuran (THF)[145]. The polymeric membrane was doped in PEG to improve surface resistance to protein adsorption and PVC-COOH to increase charge negativity on the polymer surface favouring protein repulsion. ISE membranes were made using disposable pipette tips dipped into casting mixtures and dried for 24 hr at room temperature. The tiny flexible membrane which solidifies at the bottom of each pipette tip forms the sensitive part of the ammonia electrodes. The internal electrode consists of an Ag/AgCl wire which was made by treating Ag wire for 20 min in 0.1 M $FeCl_3$ solution. Ag/AgCl wire was subsequently immersed into the internal filling solution and attached to the open end of the pipette tip using Parafilm. The size of the ammonia sensor is around 300 μm.

4.3.2 Data acquisition system and software

The data acquisition system designed for the real-time online monitoring platform consists of potentiometric, amperometric and ohmic modules which can be multiplexed for up to eight independent modules, as displayed in Figure 4.4. This multi-channel and multi-parametric measuring system will allow continuous acquisition of many different analytes simultaneously in real-time. Each module can monitor up to 16 channels and consisted of a 16-bit analog-to-digital converter (ADC) with input voltage range of 0-5 V at a 0.076 mV resolution[146]. The different types of modules were designed to meet the requirements of different types of sensors such as the amperometric, potentiometric or ohmic sensors. Data acquisition modules were controlled by a host PC through Universal Serial Bus (USB) connections. The software for configuring, collecting, managing and processing data was uniquely designed for cell culture bioprocessing using LabVIEW 7.1 (National Instruments Corporation). An example of the graphic user interface (GUI) front panel display and the configuration sub-panel are shown in Figure 4.5. Additional information regarding the technical specifications of this data acquisition system can be found in the publication by Yue et al.[146].

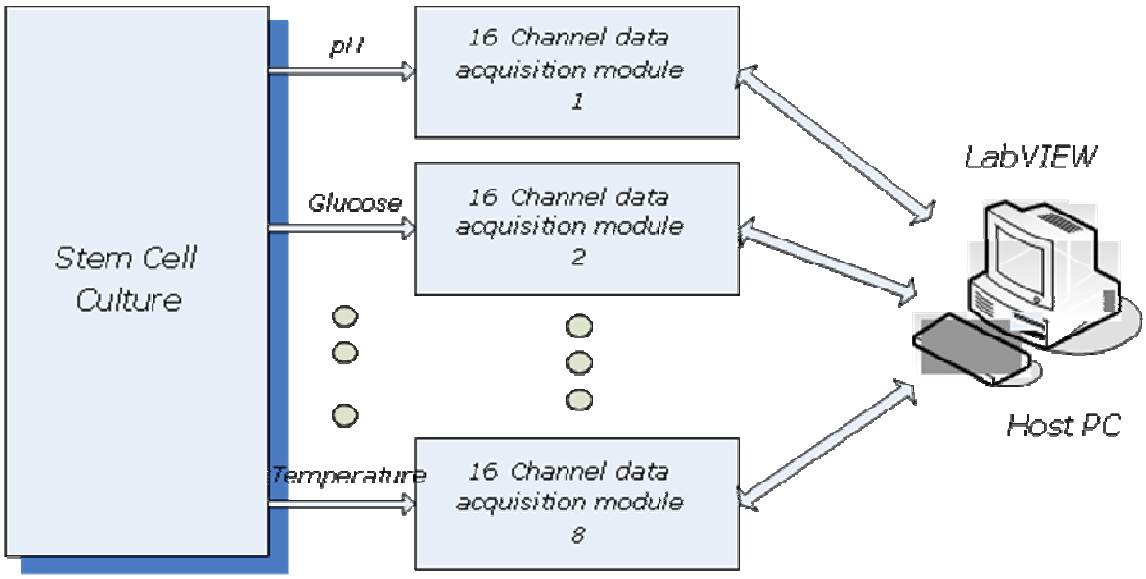

Figure 4.4 Proposed real-time online monitoring platform for stem cell bioprocessing

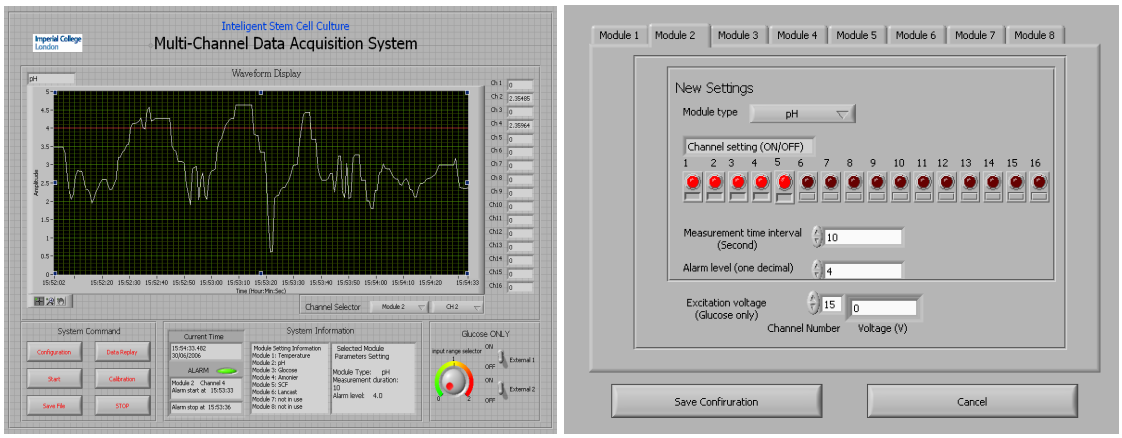

Figure 4.5 GUI front panel display (left) and configuration sub-panel (right)

4.3.3 Bioreactor and cell culture conditions

The bioreactor designed for HSC bioprocessing has been described in section 4.2.2 and is a simple perfusion system consisting of a cylindrical chamber with two inlets and two outlets for the exchange of media (Figure 4.6). Material used to fabricate the culture chamber is PMMA which is biocompatible for cellular growth. An example of a bioreactor in cell culture with several sensors placed for process monitoring is demonstrated in Figure 4.6. Various cells lines were used to test sensor performance in different cell culture conditions/environment, this included human leukemic cell line HL-60 cells (ATCC), NIH/Swiss mouse 3T3 fibroblast cell line (ATCC) and Shh Light II mouse fibroblast cells (ATCC). Media used for culturing leukemic cell line consists of 20% FBS (v/v) in IMDM and 1% penicillin/streptomycin (v/v) (P/S; GIBCO Invitrogen). Media used for culturing mouse fibroblast cells consists of 10% FBS (v/v) in Dulbecco's Modified Eagle's Medium (DMEM; GIBCO Invitrogen) containing 1.5 mg/L $NaHCO_3$ (Sigma-Aldrich) and 1% P/S (v/v). Media used for culturing Shh Light II fibroblast cells consists of 10% FBS (v/v), 0.4 mg/ml G-418 (Sigma Aldrich), 0.15 mg/ml Zeocin (GIBCO Invitrogen) in DMEM. HL-60 cells were cultured at $2x10^6$ cells/bioreactor while mouse 3T3 fibroblast cells and Shh Light II fibroblast cells were seeded at $2x10^5$ cells/bioreactor. Each bioreactor was filled with 3-6 ml of culture media. All cells were grown in static cultures and maintained in a 5% CO_2, 20% O_2 and 37^{o}C fully humidified incubator for up to six days.

For the ammonia experiments, cells were seeded on the same day when sensors were placed into the bioreactor (at the start of the experiment – day 0). Cells were allowed to adhere randomly within the bioreactor and the ammonia concentrations were monitored continuously throughout the culture period. For the pH and oxygen experiments, a slight

modification in the placement of cells was attempted and the fibroblast cells were intentionally seeded onto a specific area in the bioreactor in order to stimulate a region of higher cell density. To achieve this, cells were seeded two days prior to the start of the experiment. A quarter of the PDMS mould was cut out to allow cells to settle only into this area: only a quarter of the bioreactor will be covered with cells (Figure 4.7). Once the fibroblast cells have adhered onto the desired area, sensors were sterilised and placed into the bioreactor to begin continuous monitoring of the analyte of interest.

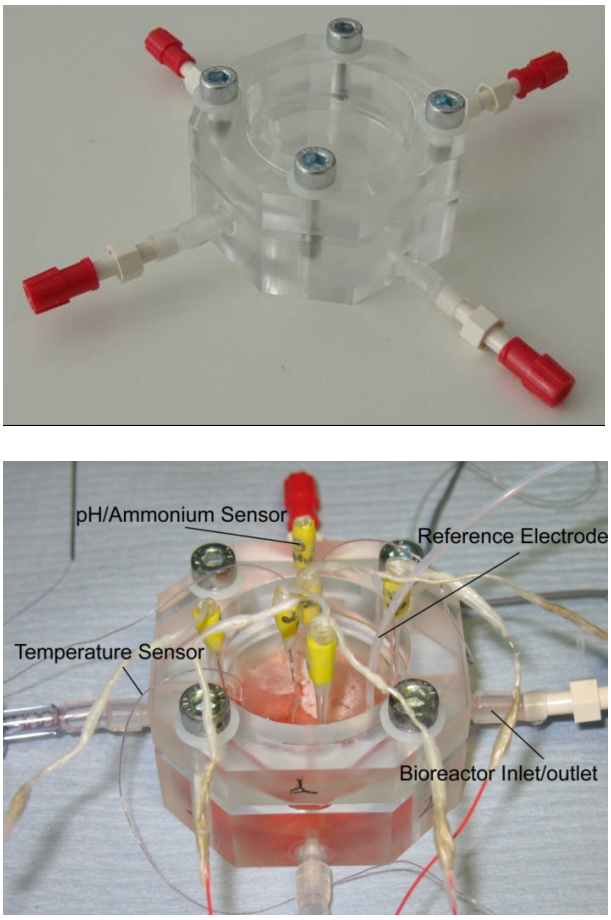

Figure 4.6 Bioreactor designed for HSC bioprocesses (top). Sensor placed in bioreactor with cell culture (bottom)

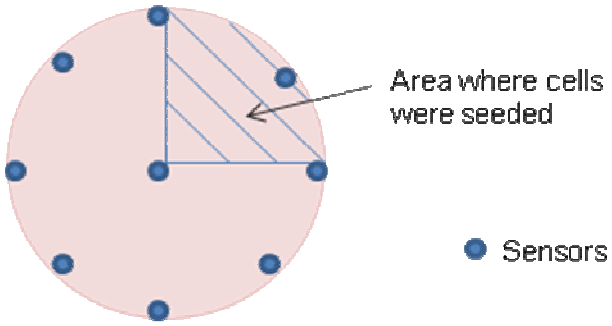

Figure 4.7 Configuration of cell seeding for pH and oxygen experiments. Nine sensor locations based on DOE configuration.

4.3.4 Toxicity study

Each sensor type was tested for its toxicity to cells in culture. Mouse 3T3-Swiss albino fibroblast cells were seeded at a density of $2x10^5$ cells in each bioreactor and cultured in static conditions for up to six days. Each experimental setup consisted of four bioreactors: two bioreactors contained nine real sensors of either pH, oxygen or ammonia, and one or two control bioreactors with no sensors placed inside. At the end of six days, sensors were removed and the growth of cells was observed from its morphology through the Leica inverted-phased microscope, and from manual cell counting using a haemocytometer. Cells were stained with Erythrosin B solution to determine the total cell viability. Cellular growth was compared to the control bioreactor which contained no sensors to determine if sensors had any toxic effects on the cells in culture.

4.3.5 DOE design parameters and data analysis

Sensor placement in the perfused bioeactor system was determined by DOE as described in section 4.2.3. Briefly, spatial dimensions of the chamber were defined by x- and y-coordinates and utilised a CCD which has an α-value of 1.414. This generated a total of nine sensors required to perform a single DOE experiment. Each group of sensors, pH, oxygen and ammonia, were tested and placed in all nine DOE locations for continuous monitoring and spatial profiling. At the end of the culture, cells were counted and examined through the microscope at various locations in the bioreactor. Monitoring data obtained from cell culture experiments were processed in Design Expert 6.0.1 and MODDE 7. In the DOE software, the MLR or partial least squares (PLS) method were used to fit the experimental data into a 2^{nd} order polynomial model to generate spatial and temporal profiles taken at various time-points throughout the culture process.

CHAPTER 5

In vitro erythropoiesis: Process characterisation and optimisation

5.1 INTRODUCTION

Human umbilical cord blood is collected and stored worldwide in both public and private banks for stem cell transplantation and research purposes. One of the main areas of research is the *ex vivo* expansion and directed differentiation of cord blood stem cells toward specific lineages. Successful manipulation of these cells is of great clinical utility; bringing potential therapies for many blood related diseases and providing an alternate resource of blood. Currently, the average cost for processing blood transfusion in the US is reported at $2B per year, this cost is mostly associated to the testing of blood for its safe use[147]. One such resource in high demand is the red blood cell. Direct clinical applications of the red blood cell include transfusion for patients undergoing an operative procedure that will likely result

in major blood loss, patients who may also suffer from impairment in oxygen transport exacerbated by anaemia, or patients undergoing a chronic transfusion regimen or marrow suppressive therapy[148]. *Ex vivo* expansion and differentiation of HSCs toward red blood cells is therefore of great clinical interest. However, due to the complexity of stem cell mechanisms and our limited knowledge in their *in vitro* bioprocesses, successful manipulation of HSCs toward mature lineages that is useful for transplantation or transfusion is still limited by the quantity and quality of stem cell engineered blood products. Quantitative characterisation and optimisation of these *in vitro* bioprocesses has not yet been fully established.

Traditional studies performed on HSC cultures are mostly based on a comparison of the outcomes from combining different cytokines[69,70,75,149] or using a dose-response method to determine the effect of a single cytokine[149]. Typical combinations of cytokines being studied for *in vitro* erythropoiesis include EPO, FL, IL-3, SCF, GM-CSF and TPO. Studies based on comparing random combinations of cytokines and dose-response approaches provide limited information and do not often lead to an optimal process. The study performed by Detmer et al. for example investigated the effect of various bone morphogenetic proteins (BMP-2 to -7) with EPO or IL-3 and EPO, by testing one factor at a time at various concentrations of IL-3 and EPO[149]. The lack of a systematic approach in this process impedes the amount of information that can be extracted from performing the experiments and generally requires a larger number of experiments than DOE methods. The dose-response effect of BMP-4 was subsequently studied in this investigation to determine its effect on $CD34^+$ cells[149]. It is clear from this example that comparison studies and dose-response methods cannot reveal interactive effects between the variables, thus they often do not

provide an accurate account of the process being studied. The approach used in these studies is therefore a highly inefficient and ineffective way of experimentation.

DOE, on the other hand, can bring truthful insights and offer many advantages. DOE not only provides a more thorough and quantitative characterisation of the process but is also a much more efficient way of experimentation using the minimum number of experiments required[83]. The availability of an array of DOE designs allows the experimenter to perform many different types of process investigations, such as screening, characterisation, and process optimisation[82,83]. Previous studies have proven the effectiveness and efficiency of DOE methods for the characterisation of HSC cultures by showing successful screening and optimisation using fractional factorial designs and process characterisation using response surface modelling[35,79,80]. The study performed by Yao et al. used a fractional factorial design approach followed by the path of steepest ascent to optimise media supplements required for a serum-free condition for CB expansion[80]. Cortin et al. used a PBD to screen different cytokines and subsequently characterised the process of megakaryopoiesis using a CCD to obtain a fully developed quantitative model that describes the *in vitro* process[35]. In both methods, screening of a large number of factors was easily achieved and interactive effects from contributing factors were revealed.

Cultures of HSCs, as previously discussed in Chapter 2, can be done through several approaches: from a serum-containing to serum-free and even stromal-based co-cultures. Traditionally, HSC cultures were performed in a serum-supplemented single-step cytokine cocktail wherein concentrations of cytokines are fixed throughout the culture period. In other configurations, multi-step cytokine, stromal-based co-cultures or a combination of both methods, have been experimented. A single-step cytokine culture entails the use of a fixed

combination and concentration of cytokines throughout the culture period while a multi-step cytokine culture uses different cytokines at different concentrations at various stages of the cell culture. This chapter focuses on the use of DOE as an experimental strategy for characterising and optimising process conditions for *in vitro* erythropoiesis of cord blood $CD34^+$ cells in a single step.

5.2 AIM AND HYPOTHESIS

The aim of this study is to develop a simple DOE-based experimental strategy that can be readily applied for studying complex cell culture systems/stem cell bioprocesses. The basic hypothesis is that DOE can improve methods of experimentation in cell culture studies by providing quantitative results and better outcomes from the cell culture i.e. greater proliferation and/or differentiation in the process of interest.

5.3 APPROACH TO STUDY

The general approach is to first develop a simple DOE experimental strategy that can be easily applied to different bioprocesses of interest. The proposed DOE strategy consists of three simple steps: (1) screening of a large number of factors using fractional factorial designs, (2) process characterisation using response surface modelling, and (3) optimisation of process conditions using model-based point prediction. Specific details of the designs used for each step were previously described in section 4.1.2.1. The selection of cytokines that will

be used in this study was based on previous findings, of which the more commonly used cytokines for red blood cell differentiation were chosen. The selected cytokines were: SCF, IL-3, IL-6, FL, GM-CSF, TPO and EPO. The optimised process obtained from the DOE experiments were subsequently verified and analysed for red blood cell markers and phenotypes. These results were then compared to previous findings for a single-step cytokine culture that were not optimised using DOE to determine whether the hypothesis is valid.

5.4 RESULTS

5.4.1 DOE analysis

The DOE screening experiment revealed that SCF and EPO were the only two factors significantly influencing the *in vitro* erythropoiesis of cord blood HSCs. A set of full experimental results reflecting the raw data from this screening study is displayed in Table 5.1. This set of experimental results (all 20 runs in the DOE matrix) was obtained from a single cord blood unit. The screening experiment was repeated one more time using a different cord blood unit and led to the same conclusions as those from the first experimental study. The analysis of this data using DesignExpert 6.0.1 yielded coefficient estimates for each cytokine which is presented in the coefficient plot (Figure 5.1). The coefficient plot shows that the effects of SCF and EPO were not only large in magnitude but also significant ($p < 0.05$) for both the total fold expansion (Fold) and red cell maturation (%RBC) over a 10-day culture. The %RBC represents the percentage of red blood cells in the population which is determined by their GPA expression in the flow cytometer. GPA is a marker for mature red

blood cells and is therefore a good indicator for differentiation of cell population toward the erythroid lineage. All other remaining cytokines in the coefficient plot had p-values > 0.05 which indicate that they are insignificant to the process.

Table 5.1 Full experimental results for screening study (raw data). All 20 experimental runs were performed using a single cord blood unit.

Std	Run	SCF ng/ml	IL3 ng/ml	IL6 ng/ml	FL ng/ml	TPO ng/ml	GMCSF ng/ml	EPO IU/ml	Fold	%RBC
1	2	0	0	0	0	0	0	0	0	0
2	11	100	0	0	0	100	0	5	402.5	67.03
3	6	0	100	0	0	100	100	0	2.335	0
4	15	100	100	0	0	0	100	5	337.5	64.79
5	10	0	0	100	0	100	100	5	0	0
6	7	100	0	100	0	0	100	0	7.45	1.82
7	17	0	100	100	0	0	0	5	4.78	13.44
8	16	100	100	100	0	100	0	0	18.1	6.54
9	13	0	0	0	100	0	100	5	0	0
10	14	100	0	0	100	100	100	0	60.7	1.79
11	4	0	100	0	100	100	0	5	12.35	19.18
12	9	100	100	0	100	0	0	0	34.35	4.1
13	3	0	0	100	100	100	0	0	3.11	5.67
14	20	100	0	100	100	0	0	5	440	59.31
15	1	0	100	100	100	0	100	0	9.2	3.49
16	12	100	100	100	100	100	100	5	405	52.98
17	19	50	50	50	50	50	50	2.5	376	47.01
18	18	50	50	50	50	50	50	2.5	376	46.51
19	8	50	50	50	50	50	50	2.5	475	51.92
20	5	50	50	50	50	50	50	2.5	440	47.81

Factors with a negative coefficient estimate imply that they may have a negative effect on the response; causing a retardation in the expansion and/or maturation capability of the cells. For

example, the effect of GM-CSF on %RBC suggests that the presence of GM-CSF in the culture media will reduce the maximum potential maturation of the cell population resulting in a lower %RBC value than its full potential. The half-normal plots (Figure 5.2) generated from the DOE analysis for both fold expansion and red cell maturation confirm the significance of main effects from SCF and EPO. They also suggest the presence of the two-factor interactive effect (AG).

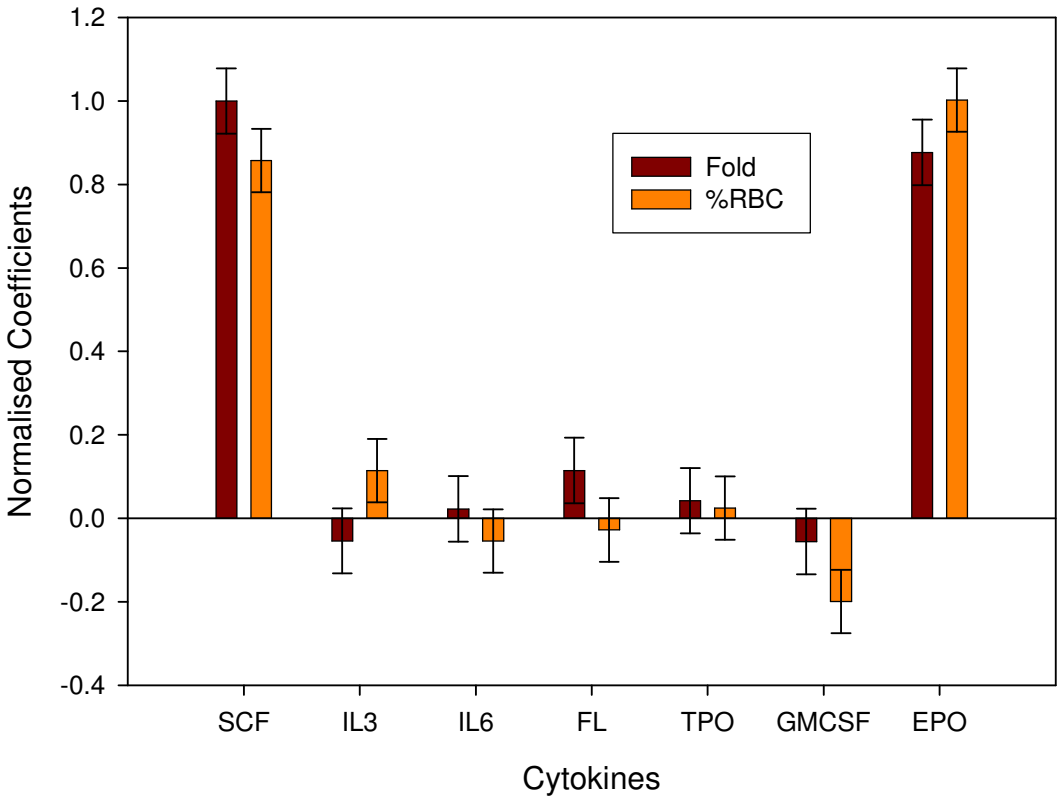

Figure 5.1 Coefficient plots for total fold expansion (Fold) and red cell maturation (%RBC). Only the p-values for SCF and EPO were < 0.05 i.e. significant. The coefficient of each cytokine gives the magnitude of their effect. Coefficients were normalised against the highest coefficient in each group.

(A)

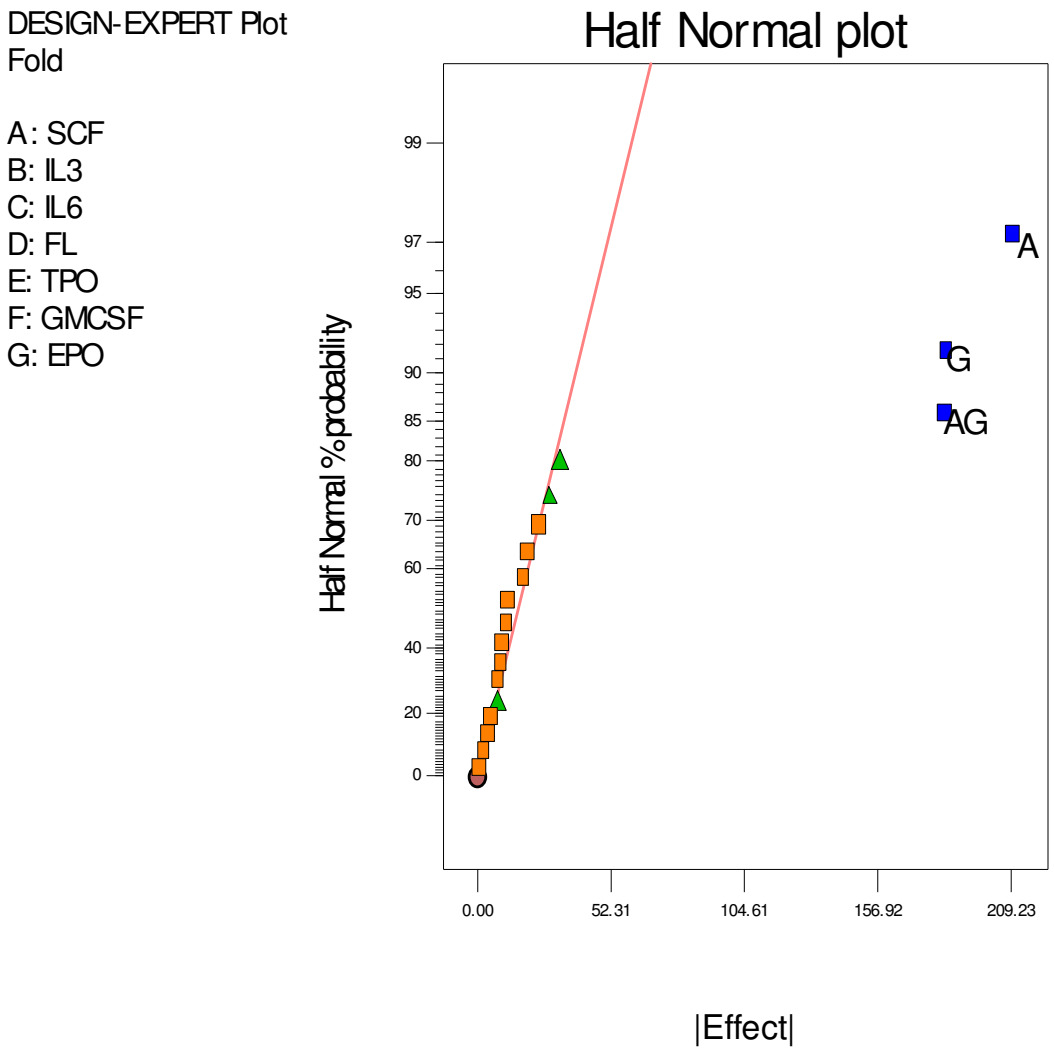

Figure 5.2 (a) Half-normal plot for fold expansion. Significant effects are A (SCF), G (EPO) and AG (SCF-EPO).

(B)

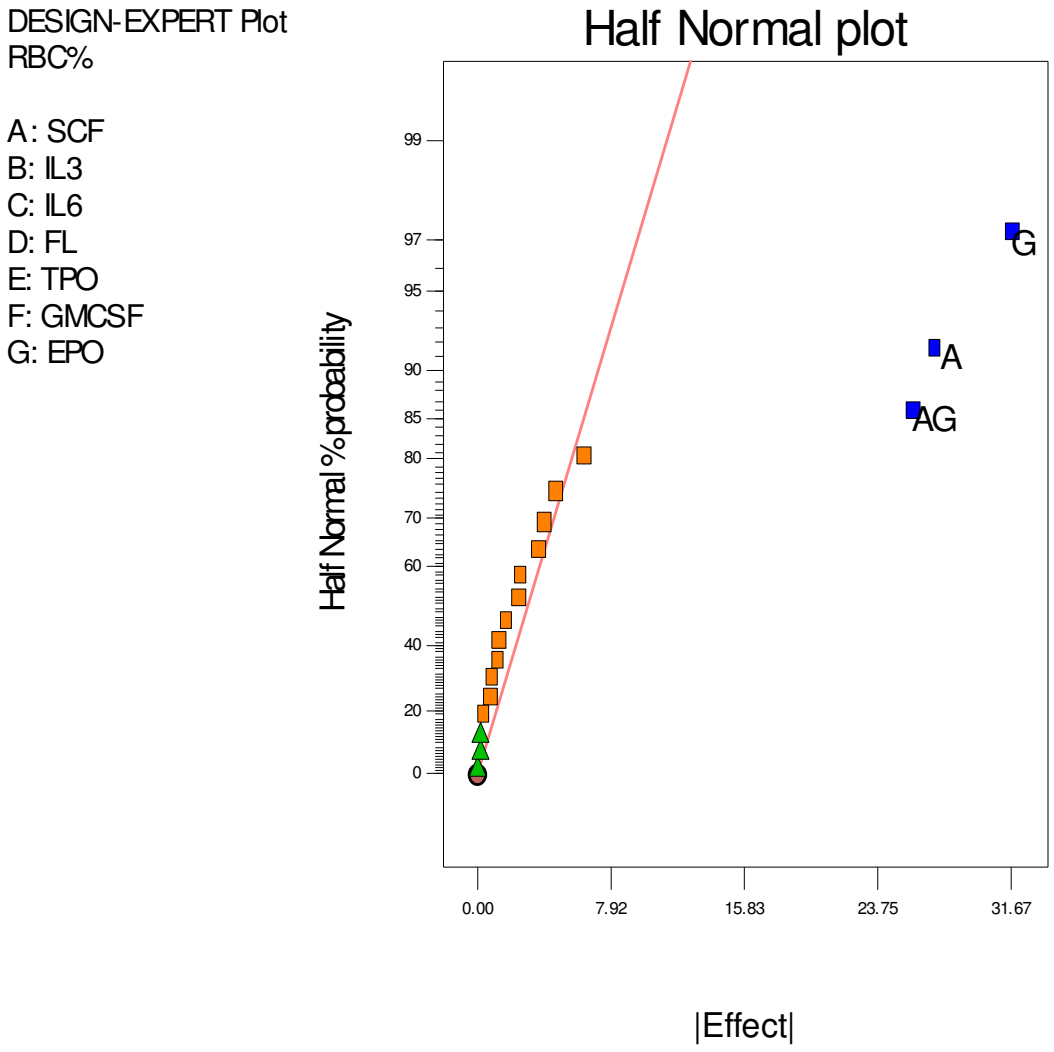

Figure 5.2 (b) Half-normal plot for %RBC. Significant effects are A (SCF), G (EPO) and AG (SCF-EPO).

The characterisation study based on a two-factor face-centred CCD with SCF and EPO produced quantitative relationships that accurately describe the effects of SCF and EPO on the fold expansion and red cell maturation. The resulting output model equations representing these relationships are displayed in Table 5.2 and the full ANOVA analysis of the DOE experimental results is provided in Appendix A. Both models were significant and showed no lack of fit. The resulting models generated three-dimensional (3D) surface response plots for both total fold expansion (Figure 5.3a) and red cell maturation (Figure 5.3b). Coefficient plots (not shown) and 3D surface plots (Figure 5.3a and 5.3b) revealed that the expansion of cord blood stem cells in culture is affected by both SCF and EPO while red blood cell differentiation is affected by only EPO.

Table 5.2 Model equations for characterisation of cord blood $CD34^+$ cells toward erythropoiesis. Factors are: A = SCF and B = EPO

Characterisation for	**R-squared**	**Model Equations (in terms of actual factors)**
Fold expansion	0.9650	$\text{Log(fold + 8.50)} = 1.044 + 0.0499A + 2.269\text{x}10^{-3}B - 4.885\text{x}10^{-4}A^2 + 2.721\text{x}10^{-3}AB$
RBC%	0.9795	$(\%\text{RBC} + 0.67) = 5.546 + 0.0728A + 27.432B - 3.049B^2$

Process optimisation can be done by setting criteria in the desired responses. In order to determine the optimal operating regime and cytokine concentrations required for maximum red blood cell production (i.e. high cell expansion and high %RBC in the cell population), the two response surface plots were overlapped to reveal the region where both optima are met (Figure 5.3c). This region is represented by the area shaded red in Figure 5.3c

and meets the criteria of achieving a fold expansion greater than 1500 and percentage of red blood cells greater than 67%. The optimal cytokine concentrations for the most optimal process operation can then be selected from this overlapping regime; the final DOE cytokine concentrations selected were 75 ng/ml of SCF and 4.5 IU/ml of EPO.

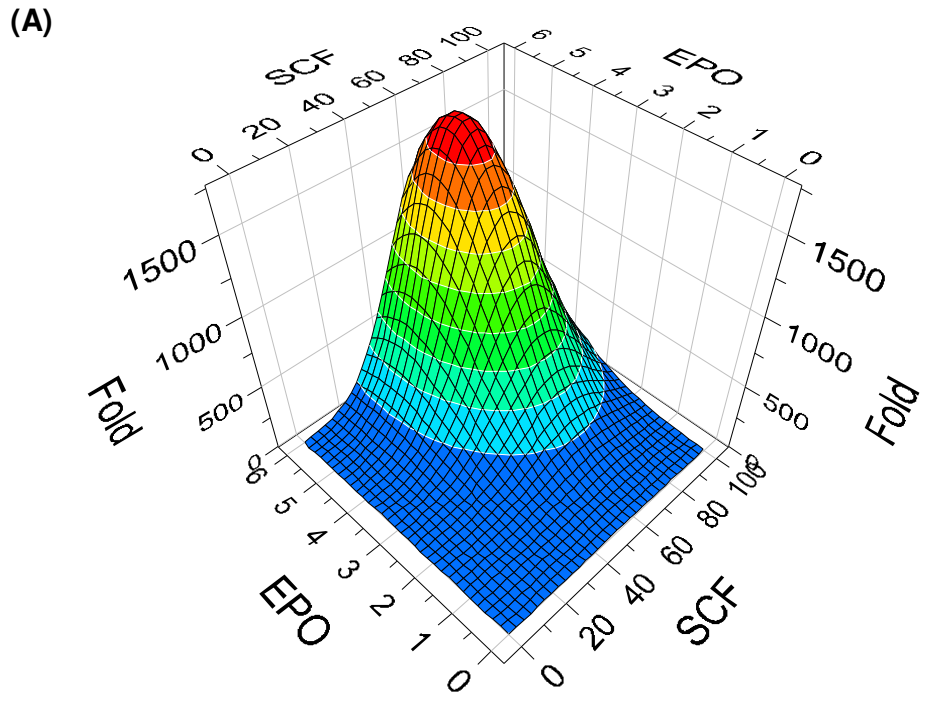

Figure 5.3 (a) Response surface plots for SCF and EPO on total fold expansion. The total fold expansion is defined as the fold of increase over the initial seeding density.

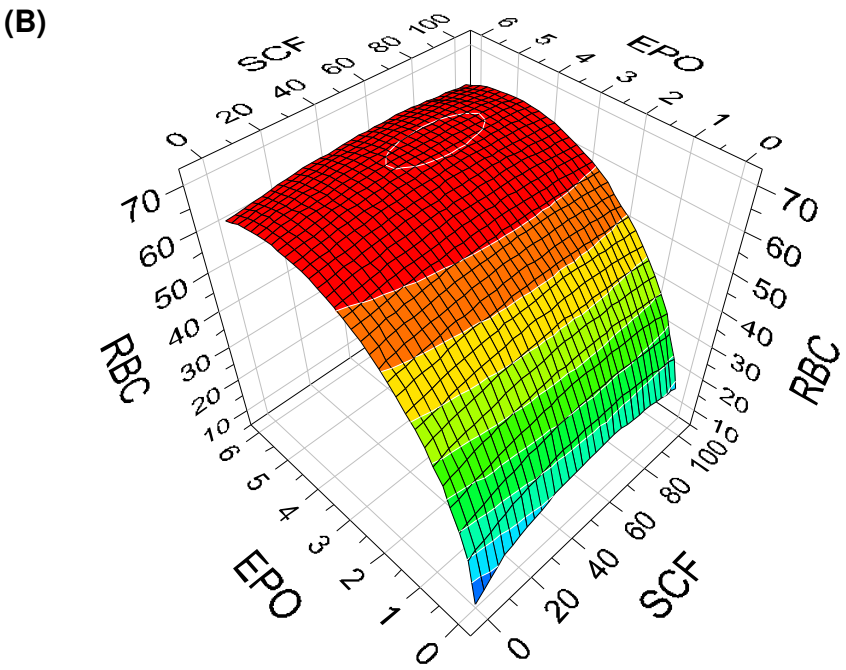

Figure 5.3 (b) Response surface plot for SCF and EPO on red cell maturation. Red cell maturation is defined as the percentage of red blood cells in the population determined by their GPA expression levels detected in the flow cytometer.

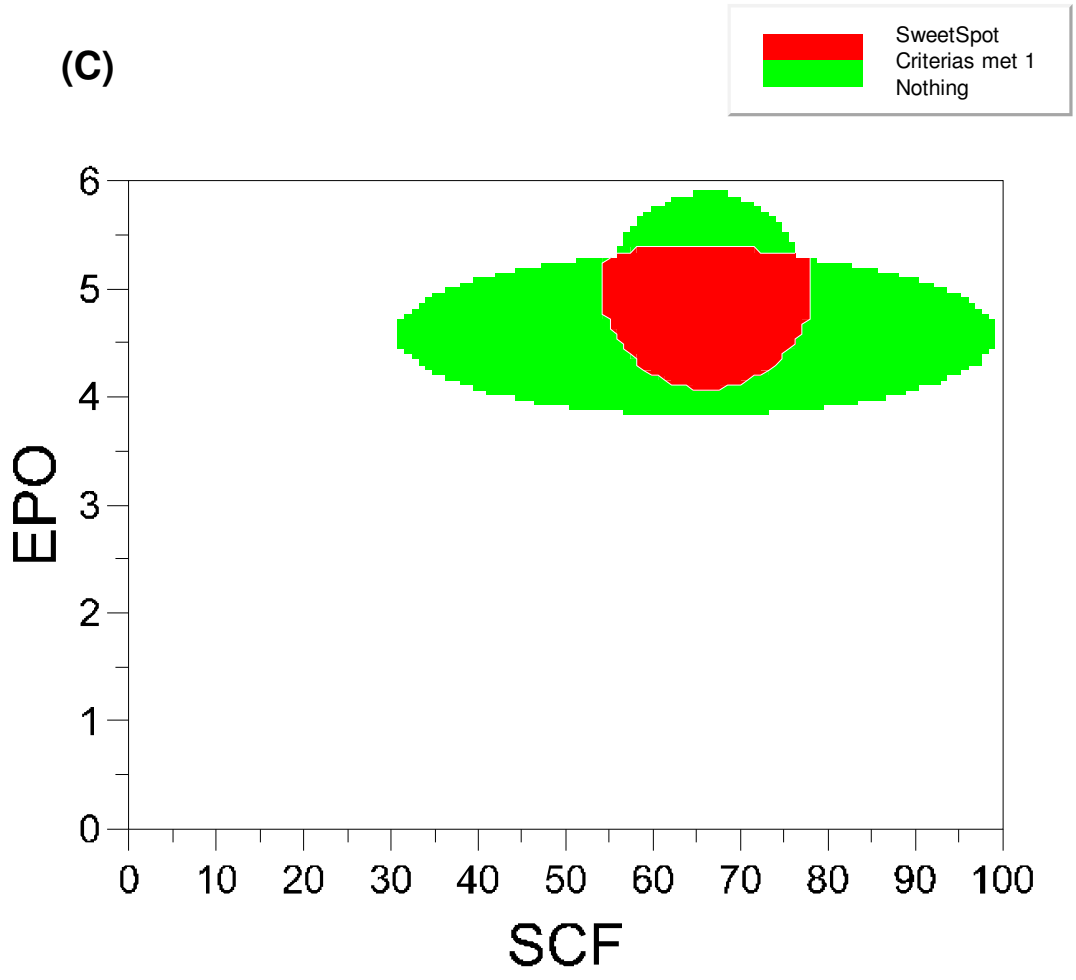

Figure 5.3 (c) Overlapping region for optimal cell expansion and RBC maturation. The sweet-spot (red shaded area) is determined by conditions that meet the following criteria: fold > 1500 and %RBC > 67%.

5.4.2 DOE verification

The DOE optimised cytokine concentrations (75 ng/ml SCF and 4.5 IU/ml EPO) were verified in a 16-day culture (n = 6). Cells were analysed for a pan-haematopoietic marker, CD45, and two erythroid markers, CD71 and GPA. CD45 is generic haematopoietic cell marker but is lost in mature haematopoietic cells including red blood cells. CD71 is a marker for erythroid progenitors and reticulocytes, but is lost when reticulocytes mature into red blood cells[150]. GPA is expressed normally at the stage of erythroblast through mature red blood cells[150]. Accelerated maturation of cord blood stem cells toward the erythroid lineage was evidenced by the rapid increase and high percentage of CD71 and GPA expression (Figure 5.4). By day 4, 80% of the cells expressed CD71 and 26% expressed GPA. By day 7, almost 80% expressed both CD71 and GPA, and a reduced expression of CD45 (from 57% to 26%) was observed (Figure 5.4). On day 13, the expression of CD45 reduced to 2.9% while the expressions of CD71 and GPA reached as high as 97%. The progression of surface antigen expressions for the cord blood cultured cells toward red blood cell maturation can also be observed from the flow cytometry plots (Figure 5.5). Both the 3D and 2D flow cytometry plots are displayed in figures 5.5a and 5.5b respectively. In comparison to other standard cytokine cocktails, a significantly faster maturation is achieved in this DOE cocktail. One such study was compared to the DOE cocktail in Table 5.3; the DOE optimised culture showed higher expressions of CD71, GPA, and lower expressions of CD45 indicating a more mature population of erythroid cells found in both days 7 and 10 of the DOE culture.

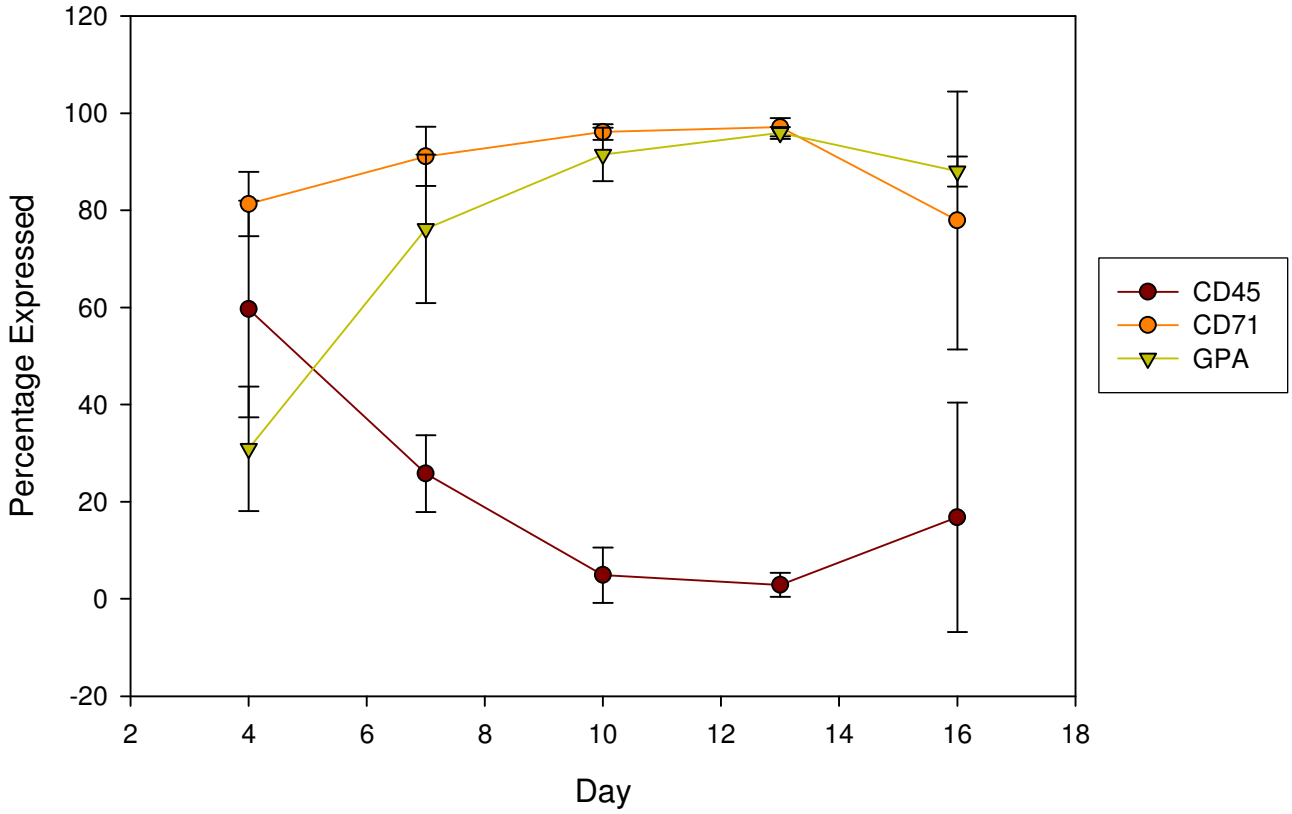

Figure 5.4 The progression of surface antigens (CD45, CD71 and GPA) expressed in the cord blood cultured cells (n = 3-6). A decreasing trend observed in the CD45 expression while and increasing trend is observed in both CD71 and GPA expression.

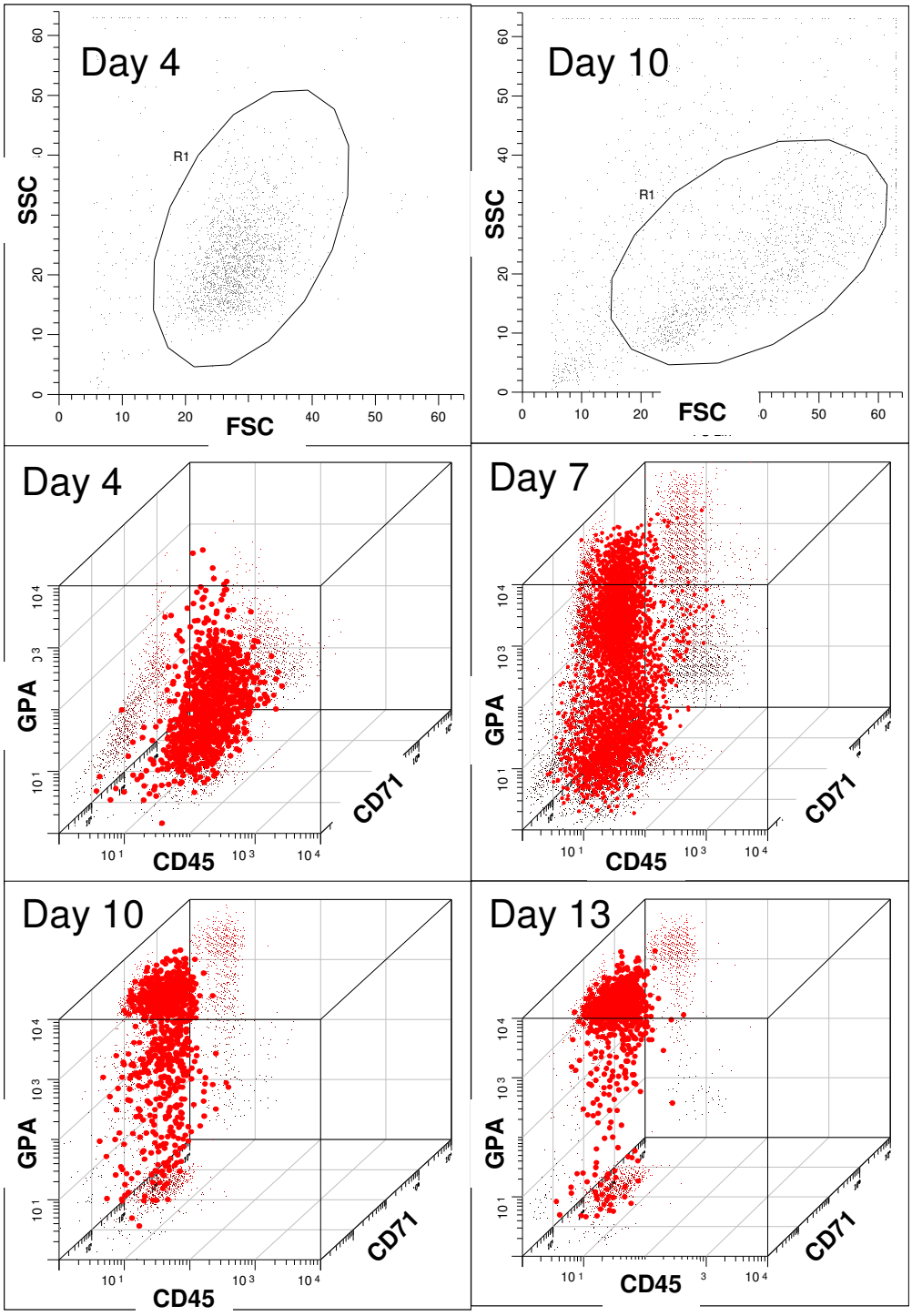

Figure 5.5 (a) 3D flow cytometry plots for cord blood cultured cells in 75 ng/ml SCF and 4.5 IU/ml EPO. FSC-SSC indicates gated population shown in the forward scatter versus side-scatter. Surface antigens CD45, CD71 and GPA are shown in all 3D plots.

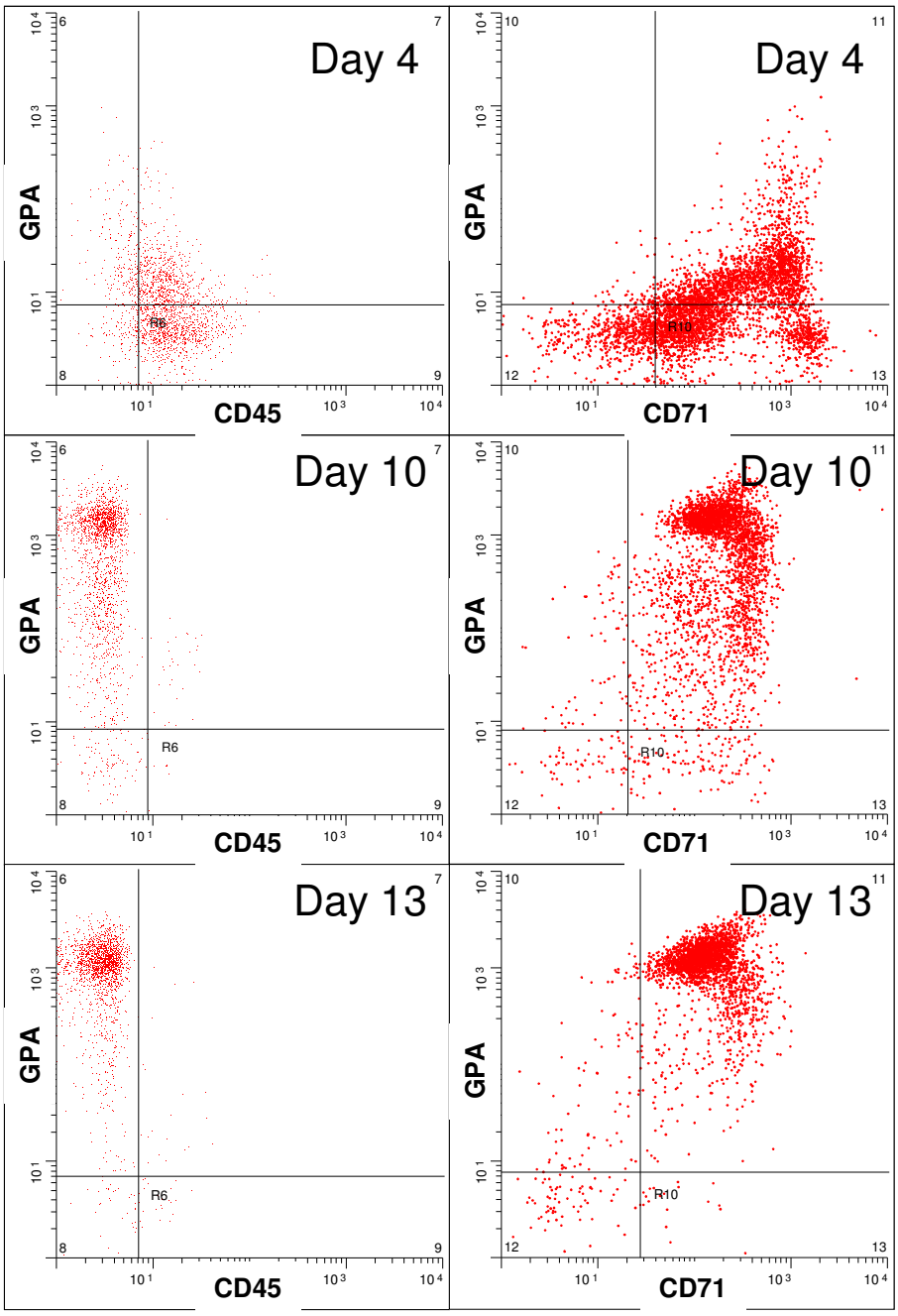

Figure 5.5 (b) Flow cytometry data in 2D plots. Low expression of CD45 observed on days 10 and 13 and high expression of GPA observed on days 10 and 13 versus day 4.

Cells cultured in 75 ng/ml SCF and 4.5 IU/ml EPO yielded high total cell expansion. Cellular growth reached an average total fold expansion of up to 18,307 by the end of 16 days in culture (Figure 5.6a); the maximum fold expansion obtained in one culture was 36,900 and the minimum fold expansion achieved was 3,029. The huge difference observed in cellular expansion between experiments is related to cord-to-cord sample variability. Cellular growth of cord blood stem cells in this cytokine culture followed a typical growth profile which consisted of a lag phase, a log phase, and a plateau. In its log phase, the average growth rate is 7.8 fold per day which equates to a doubling time of roughly 3 hr, a rapid cell expansion. A comparison in the maximum fold expansion achieved in this study to other studies showed an overall improvement of 18-fold than the total average obtained from all studies using a single-step cytokine cocktail. An example of the comparison in growth potential from one such study is shown in Table 5.3. The DOE cocktail achieved 3.5 fold greater expansion by day 7 and 17.8 fold by day 10.

CFU assays relate to the clonogenic capability of the cord blood cultured cells. The assays showed an overall increase in the number of erythroid progenitors, which are the CFU-E and BFU-E colonies, in the first seven days of culture compared to its starting population - $CD34^+$ cells (Figure 5.6b). The BFU-E colonies are earlier erythroid progenitors than CFU-E colonies. The maximum number of total erythroid progenitors was achieved on day 4, reaching over 260 colonies/1000 cells plated. Cells from day 4 showed significantly larger numbers of BFU-E colonies than CFU-E colonies while cells from day 7, a more mature population, showed higher numbers of CFU-E than BFU-E colonies. The total number of erythroid progenitors from day 7 also decreased by more than half of its total

number at day 4. By day 10, only a small number of CFU-E colonies remained in the cell population (less than 20 colonies/1000 cells plated) indicating a small population of immature erythroid progenitors.

Table 5.3 Comparison of DOE cocktail to a standard single-step culture.

	DOE cocktail*	**Standard cocktail***
Day 7 Fold	136	38
CD45	25.8%	89.6%
CD71	91.1%	84.1%
GPA	76.2%	45.5%
Day 10 Fold	1853	110
CD 45	4.9%	96.5%
CD71	96.1%	78.3%
GPA	91.5%	49.5%

**DOE cocktail consists of 10% FBS, 75ng/ml SCF and 4.5IU/ml of EPO in IMDM while the standard cocktail consists of 100ng/ml IL-3, 50ng/ml of FL and 2 IU/ml EPO (results obtained from Kie et al.)*

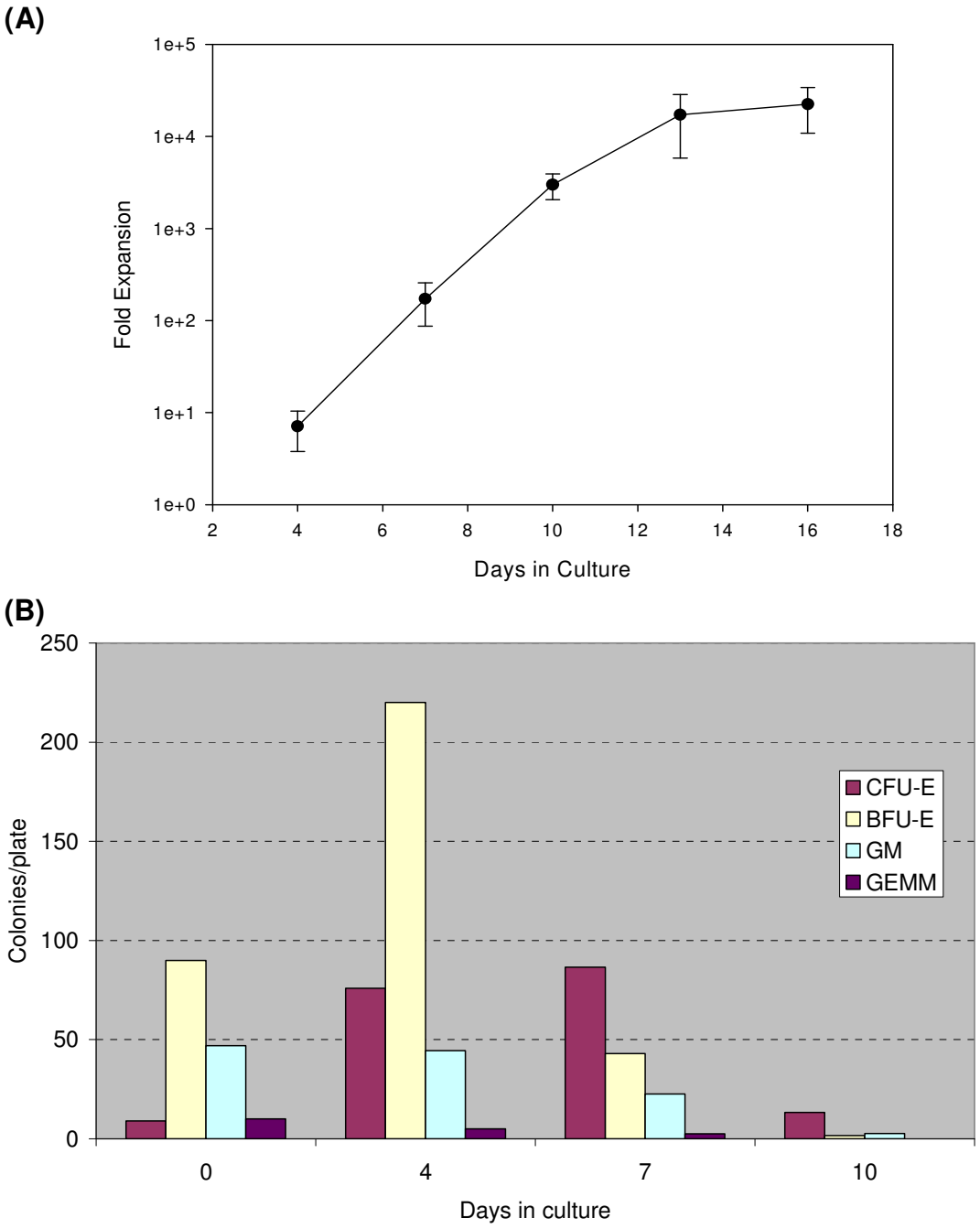

Figure 5.6 Growth profile and *in vitro* clonogenic assay. (a) Cell growth in total fold expansion (n = 6). (b) *In vitro* clonogenic assays were performed at days 0, 4, 7 and 10. Assays were normalised to a seeding density of 1000 cells/plate (n = 2-4).

Red cell maturation was also evidenced in the morphology of stained cells. Indications of red cell maturation such as the expulsion of cell nucleus was observed on day 7 and day 10 cells, and a small number of enucleated red blood cells were observed in day 13 and 16 of the culture (Figure 5.7a). Most cord blood cultured cells were around 15-20 μm in diameter and larger cells (~30-35 μm) resembling reticulocytes were observed from day 7 through day 13. Cells appear slightly larger than normal as they were cytospun onto the glass slide. The presence of reticulocytes is confirmed by brilliant Cresyl-blue staining; reticulocytes stain deep blue as seen in day 13 while other haematopoietic cells do not stain (Figure 5.7b). On day 13, shrinkage in cell size was also observed and a small population of cells measuring ~12 μm and lacking of a nucleus began to appear (Figure 5.7a). Fluorescence microscopy showed a larger number of cells expressing CD45 at the beginning of the culture as compared to those at the end of the culture (Figure 5.7b), consistent with observations made in the flow cytometry data. More importantly, expression of GPA on the cells' surface differed between cells early in the culture versus those late in the culture. Expression of GPA on day 4 cells were granulated and scattered throughout the cellular surfaces while GPA expression on day 13 cells were much more homogeneous on the cell surface and has a brighter intensity on several cells (Figure 5.7c). Surface expression and distribution of GPA on day 13 cells resembled the expression on our cord blood red cell control (Figure A1 in Appendix A).

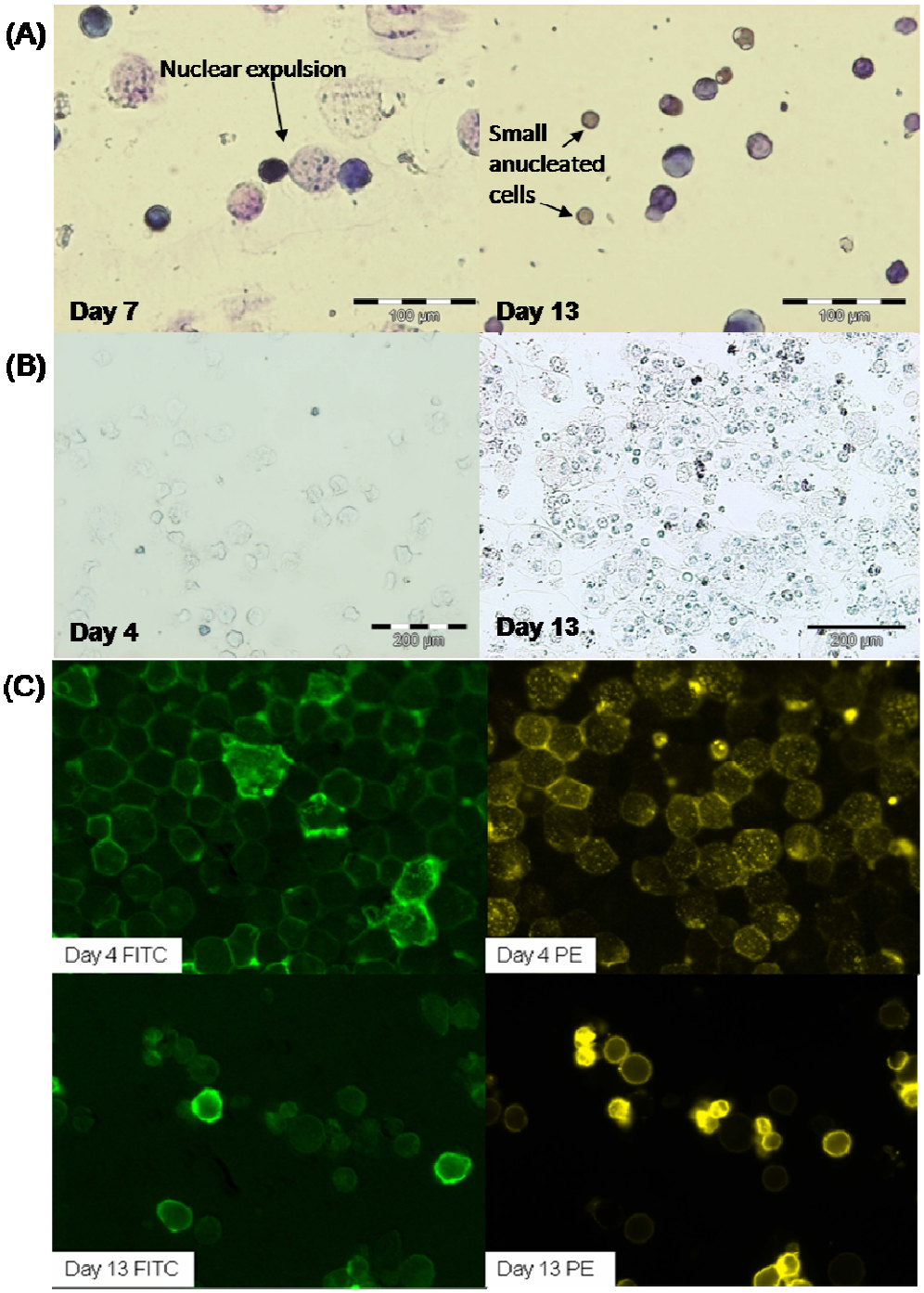

Figure 5.7 Cell morphology of cord blood cultured cells. (a) Giemsa-Wright's stain for nucleic-cytoplasmic differentiation: Day 7 cells (left) and Day 13 cells (right). (b) Cresyl-blue stain for reticulocytes: Day 4 cells very little / no stain; day 13 cells have many dark blue stain. (c) Comparison of CD45 and GPA surface antigen expression using fluorescence microscopy - day 4 versus day 13 cells stained for FITC-CD45 and PE-GPA.

RT-PCR and western blot results confirmed differentiation of cord blood cultured cells toward the erythroid lineage in the gene and protein level. mRNA expressions of γ, β, and α-haemoglobins and GATA-1 were observed from day 6 through day 14 cells (Figure 5.8a). Alternatively, no HOX-B4 expression was observed in any of the cultured cells from day 6 to day 14 indicating a lack of stem cell expression as early as day 6 of the culture. HOX-B4 is a haematopoietic stem cell marker while GATA-1 is a marker for red blood cells. The α and β-haemoglobins are normally expressed in adult red blood cells while the γ-haemoglobin is only found in foetal red blood cells. Expressions of β, γ-haemoglobins and GATA-1 were also present at the protein level, but appeared only at a later stage than their mRNA expressions which was expected. Positive expressions of all three erythroid proteins appeared on day 14 cells and not on day 0 or day 7 cells (Figure 5.8b). Protein expression of β-haemoglobin and GATA-1 was strong; notably the expression of β-haemoglobin (the adult haemoglobin) was stronger in cultured cells than that from cord blood foetal red cells. Conversely, protein expression of γ-haemoglobin (foetal haemoglobin) was weaker in the cord blood cultured cells than that from cord blood foetal red cells (the positive control).

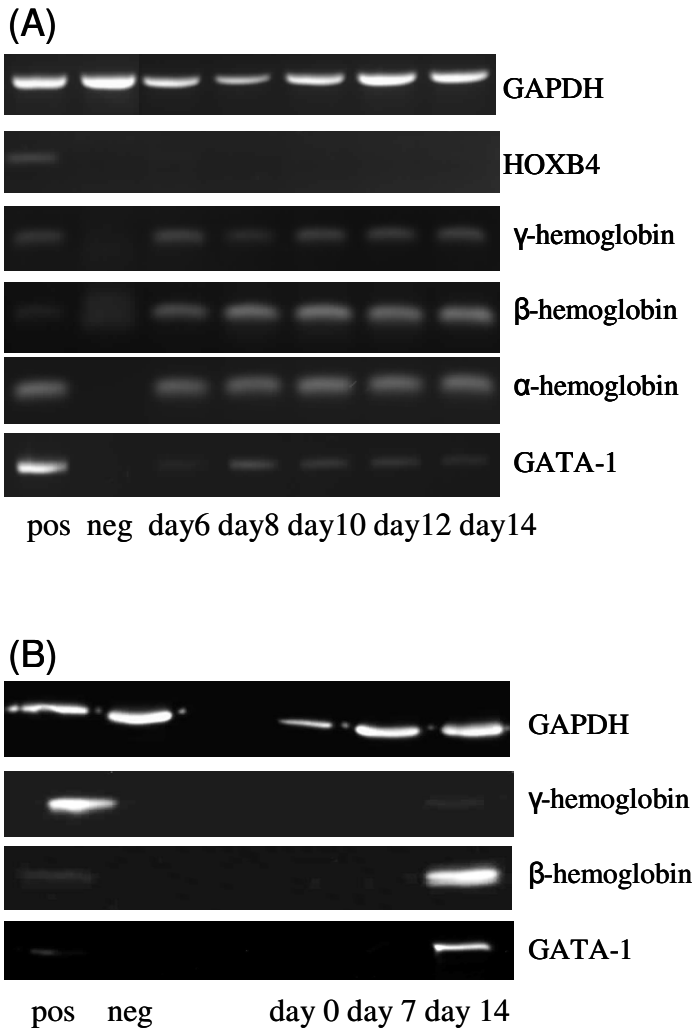

Figure 5.8 Gene and protein expression profiles. (a) RT-PCR results for GAPDH, HOXB4, α, β, γ-haemoglobins and GATA-1. Positive controls: Cord blood $CD34^+$ for HOXB4; K562 cell line for all others; negative controls: HL60 cell line. (b) Western blot results for GAPDH, γ, β-haemoglobins and GATA-1. Positive controls: Cord blood RBC; negative controls: HL60 cell line. Protein expression is reflected at a later stage than mRNA expression and is observed on day 14 but not day 7.

5.5 DISCUSSION

5.5.1 DOE as an experimental strategy

This study has successfully demonstrated the ease and efficacy of DOE as a quick and effective screening, characterisation, and optimisation tool. Specifically, DOE provided a well-illustrated quantitative representation of the relationships between SCF and EPO on the *in vitro* erythropoiesis of cord blood stem cells, and obtained a significant improvement on total cell expansion, with over 18-fold in comparison to other single-step cytokine cocktails, and faster red cell maturation of the cord blood cells overall. A DOE approach to HSC process characterisation and optimisation therefore provides a highly effective and efficient experimental strategy that can be used to tailor the production of clinical grade blood products.

DOE screening methods are excellent tools for investigating a large number of factors and reducing these parameters based on their level of contribution. The fractional factorial design is a commonly used design method for screening due to its ability to accommodate a large number of factors and tailor experiments at different levels of resolution according to the goal of the experiment. In this study, the use of fractional factorial design allowed quick screening of seven different cytokines performed in a single study using 16 experimental conditions. Other investigators, such as Yao et al., have also used such designs for screening and subsequently optimising concentrations of media supplements using the path of steepest ascent[80]. The advantage of my DOE approach in comparison to the study performed by Yao et al. is the production of a quantitative model that can be used to describe the *in vitro* process. Optimisation using the path of steepest ascent is less precise than the development of

a response surface model. However, in both studies, the fractional factorial design has proven to be highly advantageous for the screening of cell culture supplements and cytokines used in various types of culture media and experiments. It has helped to determine key factors rapidly (minimum experiments) and reduces the amount of work required to study and optimise a culture process of interest.

For process characterisation, many different types of designs are available to fit experimental results into a 2^{nd} order polynomial model. In this study, a face-centred CCD was utilised to quantify main and interactive effects of SCF and EPO on cell expansion and red cell maturation. The ANOVA analysis (Appendix A) and response surface plots (Figure 5.2a and 2b) revealed both main and interactive effects of SCF and EPO on cell expansion but only a main contribution from EPO on red cell maturation. This finding is consistent with the current knowledge on erythropoiesis; EPO being the main driver of this differentiation process[151-153]. More importantly, the 3D surface response plots generated from DOE represent a quantitative model on the expansion and differentiation of cord blood stem cells into erythrocytes which has not been previously established. This not only illustrates the exact relationships between the factors and responses, but it also allows us to predict and determine the best operating regimes for the bioprocess of interest, as demonstrated here (Figure 5.2c). A similar approach was taken by Cortin et al. to determine the optimal conditions for *in vitro* megakaryopoiesis of cord blood stem cells. In their study, the group utilised the PBD for screening. The advantage of using this design is the small number of experiments required to screen more than 10 process factors. However, a fold-over (repeat) of the design is necessary to verify results obtained from the PBD study. Still, the PBD can sometimes be confusing due to the number of factors aliased to each other which makes it

challenging to determine real effects from each factor. In this study, since there were only seven factors involved, use of the PBD is not extremely advantageous in terms of reducing the number of experiments required. The resolution IV fractional factorial design proved to be more beneficial in providing the most reliable results using the least amount of effort.

Also of significance is the efficiency of the DOE experimentation process in terms of time and labour savings in comparison to traditional dose-response methods. Since experiments are varied only one factor at a time in most dose-response studies, it would generally require a larger number of experiments to be performed in order to obtain the resolution roughly close to that obtained in DOE studies. For this case study, it would require a minimum of 14 experiments to first determine if each of the factors significantly affects the process and subsequently a matrix of 50 experimental conditions for the two factors, with each factor being varied at five different concentrations. A minimum total of 64 experiments is therefore required using dose-response, and in comparison with the DOE approach which required only 26 experimental conditions in total, clearly shows significant time and labour savings. DOE-based experimentation for process characterisation can be easily applied to any other stem cell bioprocesses of interest to provide a more thorough and quantitative process illustration as performed here.

Although the DOE approach has been successful in screening, characterising and optimising process requirements in a rapid and efficient manner, the outcome from this DOE study still requires high concentrations of cytokines, particularly EPO, to perform an optimal process. Normal physiological levels of serum EPO ranges in the 1.1-27.3 mIU/ml[154], a 100-fold lower concentration than what is typically used in cell culture 1-3 IU/ml. In this study, the optimised DOE cocktail demands a 4.5 IU/ml of EPO, an even higher concentration of

EPO which can result in a costly bioprocess operation. One of the challenges in setting up a DOE experiment is to first determine the range of process operation as this greatly affects the results from the DOE study. The complexity of the cell culture environment adds further obstacles to the optimisation of a bioprocess, other factors such as feeding frequency or glucose concentrations may influence process requirements. In this study, effects of other parameters have not yet been considered.

5.5.2 A comparison: DOE optimised process versus other studies

DOE optimised cytokine concentrations used for this single-step cytokine culture demonstrated significantly better performance in terms of total fold expansion, red cell maturation and clonogenic ability of the cultured cells than previous studies using a single step. Total fold expansion in a typical study achieved 15-1000 fold after 14-18 days in culture[69,70,155]. In this study, as much as 36-fold (average of 18-fold) higher expansion was achieved than the currently best reported study[155]; indicating that the DOE approach has resulted in improved growth factor concentrations and an effective combination. However, when compared to the multi-step cytokine cocktail cultures (those that vary cytokine combinations and/or concentrations throughout the culture period) and co-culture systems, the DOE culture lags by about 10 fold or more. The multi-step and co-culture systems resulted in an average of 200,000 fold expansion in 16 days[144,156,157]. However, co-cultures are not ideal due to the possibility of cross-contamination from stromal sources and are much more labour-intensive than a standard cytokine culture. Interestingly, in one study, no co-cultures were utilised in the procedure and they were still able to achieve significantly higher cell expansion[157]. In this study, the use of erythroid differentiation medium which consisted

of 20% FBS (v/v) was included, however this is not likely to fully explain for the significantly higher expansion achieved in this culture procedure. The multi-step cytokine cultures have shown an effect of timing in which the cells are fed at different growth factor concentrations, on cellular dynamics. Hence, the DOE approach to cellular cultures and bioprocesses used in this study may be strengthened by factoring in time.

Trends in the clonogenic capacity of the cord blood cultures corresponded well with the growth profile and flow cytometry data observed in this study. At the beginning of the culture (day 0-4), enriched $CD34^+$ cells proliferated at an average rate of ~2.0 fold/day and a high level (81.3%) of CD71 expression was obtained by day 4 which indicate a high level of erythroid progenitors and this is reflected in the CFU-assays producing the largest number of CFU-E and BFU-E colonies, and a reduction in CFU-GEMM colonies. By day 7, no CFU-GEMM colonies were found and the population consisted mostly of erythroid progenitors and maturing erythroid cells, as indicated by the increase in GPA expression in cells and reduction in BFU-E and CFU-E colonies. In comparing the clonogenic capacity to other studies, one study using a multi-step culture[144] was used as a close comparison since there were no other single-step cultures that had sufficient CFU data for this comparison. The overall trend observed in erythroid colonies over the cell culture is the same in both cultures. However, the DOE culture achieved higher BFU-E and CFU-E numbers on day 4 and sustained more colonies on day 10 than the multi-step cytokine culture.

In terms of red blood cell maturation observed from flow cytometry data, an even more significant improvement was obtained here. Typical GPA expression of cord blood cultures from previous literature only reached ~15% at day 7 and 80% at day 14 for the single-step cytokine cultures while in this study, 80% of the cells already expressed both

CD71 and GPA by day 7. By day 10, over 90% expressed both CD71 and GPA markers and only 5% expressed CD45, the lost of CD45 expression indicates full maturation of the erythroid cells which is further reflected in the appearance of reticulocytes in the cell culture. The comparison to multi-step cytokine cultures also shown a better performance (maturation of cells) in this DOE optimised culture; the best maturation from the three studies reached ~85% GPA in day 10 and ~89% in day 16. Accelerated maturation as observed in the DOE optimised culture is likely attributed by the high concentration of EPO used for the culture.

5.5.3 Biological significance of study

Cell culture optimised via the DOE method achieved accelerated expansion and maturation simultaneously. Expression of CD71, an early-mid stage erythroid progenitor marker, reached an average of 81.3% as early as day 4 of the culture. The expression of CD71 continues to increase to reflect complete maturation of stem cell progenitors toward the erythroid lineage and a lost in the CD45 expression indicates further maturation of the cell population. Fully functional mature red blood cells however do not express CD71 but only GPA[150]. In this case, the expression of CD71 on day 13 remained very high, indicating complete maturation of red blood cells has not yet been achieved at this stage but by day 16, a 20% lost in CD71 expression was observed but the results obtained from day 16 were somewhat questionable since the variability in CD45 and CD71 expression was large in comparison to the GPA expression. Based on observations from cell morphology, there is still sufficient evidence to indicate the presence of a small population (<10-20%) of red blood cells in day 16 culture. However, the cell population achieved in this DOE culture still mostly

consisted of premature erythrocytes and reticulocytes. The achievement of a high percentage of fully functional red blood cells remains a challenge.

Expression of haemoglobins at the protein level indicates some promising results from this study. The high levels of adult haemoglobin obtained from cultured cord blood cells and low levels of foetal haemoglobin reflect the type of blood cells obtained from this study were that mostly relating to adult red blood cells even though the starting population (cord blood) consisted mostly of foetal red blood cells. Enucleation of red blood cells from embryonic stem cells, on the other hand, often led to the production of foetal blood cells[158]. Adult red cells are more suitable for transfusion. The production of adult erythroid cells in this study is therefore beneficial for the purposes of transfusion.

5.6 CONCLUSION

The overall outcome from this study has been very successful: the DOE approach and proposed experimental strategy efficiently and effectively screened, characterised, and optimised the process under study (*in vitro* erythropoiesis of cord blood stem cells). The optimal DOE cytokine cocktail obtained from this study also generated higher growth potential and rapid differentiation toward the erythroid lineage *in vitro* in comparison to other single-step cytokine cultures. The DOE approach has therefore proven the validity of the proposed hypothesis, showing an improved method of experimentation and achieving significantly better results from the process outcome. These promising results underscore the efficacy of DOE methods not only in process characterisation but in process optimisation. However, DOE optimisation as a single step culture is mostly end-point driven which

explains the accelerated maturation and rapid expansion observed in this culture bioprocess. The process objective in this single-step study was simply to maximum the number of red blood cells by day 10 of the culture. Process dynamics within the culture process has been completely ignored. Chapter 6 presents a DOE approach in an attempt to characterise and optimise the *in vitro* erythropoiesis of cord blood stem cells as a multi-step process considering the factor of time.

CHAPTER 6

In vitro erythropoiesis:

Defining the influence of time in cell culture

6.1 INTRODUCTION

In vitro expansion and directed differentiation of HSCs toward the erythroid lineage is a complex and dynamic process. Optimisation of this process not only entails the identification of process factors, in this case growth factors, but also in determining the concentrations in which they should be added into the culture media. However, for many haematopoietic processes, the need for specific growth factors may be transient through the early, mid, and late stages of the differentiation process. A process such as erythropoiesis *in vivo* requires factors such as SCF and FL as early-acting growth factors, GM-CSF as a mid-acting growth factor and EPO as the late-acting growth factor to produce fully functional red blood cells (Figure 6.1)[159,160].

In chapter 5, the DOE approach was used to perform process characterisation and optimisation for the *in vitro* production and maturation of erythrocytes from cord blood $CD34^+$ cells using only a single step i.e. without varying growth factor concentrations throughout the culture period. Although the DOE-optimised single step process demonstrated significant improvements in comparison to other single step studies, optimisation performed in this single step culture was end-point driven, culture dynamics was not revealed. However, as seen from the *in vivo* process, process dynamics can change drastically throughout differentiation. Process kinetics is clearly quite significant and can greatly affect the outcome of the process. This study seeks to investigate the possibilities in using DOE to reveal process dynamics and further improve cell culture fold expansion using a multi-step cytokine culture.

In vivo, erythropoiesis is distinctly defined by the development of erythroid progenitors from the HSC to the red blood cell (Figure 6.1), and as cells mature, different cytokines are required for the generation of different red cell progenitors[159]. *In vitro* studies have shown that the effects of different growth factors such as SCF and EPO were independent from each other at different stages of erythroid development[161]. Another study showed that early stages of *in vitro* erythropoiesis were EPO-independent and only the later stages were EPO-dependent[160]. These studies support the idea that the *in vitro* expansion and maturation of HSC requires different growth factor conditions at different time-points during their differentiation process. Cytokine conditions for the *in vitro* process should therefore be optimised to meet the requirements of this dynamic process. This chapter discusses the results obtained in determining changes in process requirements for *in vitro* erythropoiesis with respect to time and limitations of the DOE method in resolving cell culture dynamics through the early, mid and late stages of differentiation.

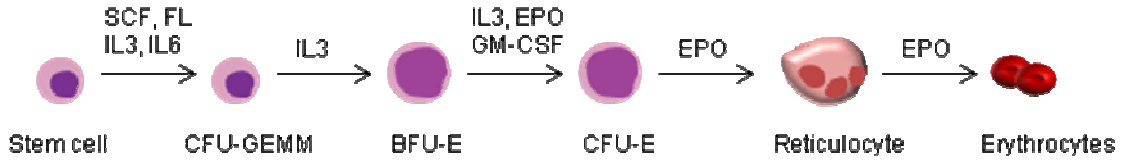

Figure 6.1 Erythropoiesis as it occurs *in vivo.* Production of the red cell begins with the HSC leading to the production of multi-lineage colonies, the erythroid progenitors, the reticulocyte and finally the erythrocyte. Cytokines known to be involved in the various stages of the *in vivo* differentiation process include SCF, FL, IL3, IL6, GM-CSF and EPO.

6.2 AIM AND HYPOTHESIS

The aim in this study is to develop an experimental strategy based on DOE for elucidating process dynamics of an *in vitro* process. The influences of time, such as the feeding frequency and identification of time-points during the culture where cytokine concentrations are varied, on the proliferation and differentiation potential of the *in vitro* erythropoiesis of cord blood stem cells is investigated. The hypothesis is that the influence of time of when the cells are fed and variations in cytokine cocktails and their concentrations can significantly affect the growth potential of cord blood stem cells *in vitro* i.e. a multi-step cytokine culture is better than a single-step cytokine culture and that with the aid of DOE, it is possible to reveal *in vitro* process dynamics effectively. This study will also be used as a measure to evaluate the advantages and disadvantages of an end-point driven versus a kinetics-driven process optimisation.

6.3 APPROACH TO STUDY

The general approach to this study is to divide the culture period into sequential phases, which was subsequently chosen to reflect the growth kinetics (Figure 6.2). First, the influence of time on cell culture kinetics was defined as the feeding frequency and the change in cytokine concentrations at various time-points in the cell culture. These effects were tested in a preliminary screening study. Once the influence of time is confirmed, DOE characterisation at each phase of the culture will be performed to determine cytokine effects and optimal concentrations required. The proposed work flowchart is shown in Figure 6.3. Each DOE characterisation study was performed via RSM using the face-centred CCD. Finally, the final combination of cytokine cocktails used in each phase for this multi-step cytokine cocktail will be tested in different cord blood cultures and these results will be compared to that obtained from the single-step cytokine culture (results from Chapter 5) to determine if the sequential optimisation of each step in the culture has made a significant improvement in the growth performance of this *in vitro* process.

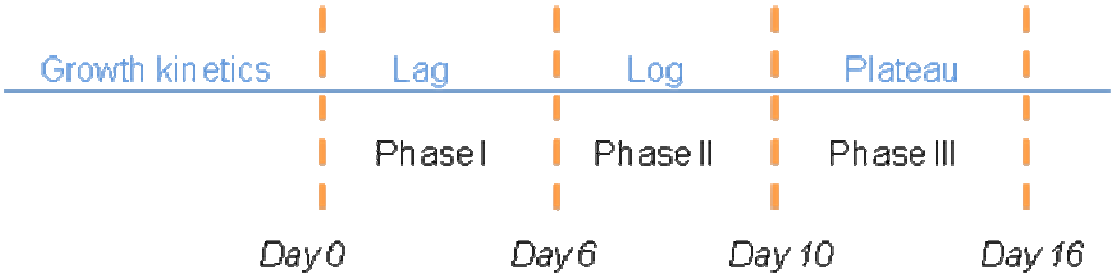

Figure 6.2 Division of culture period into three distinct phases defined by growth kinetics

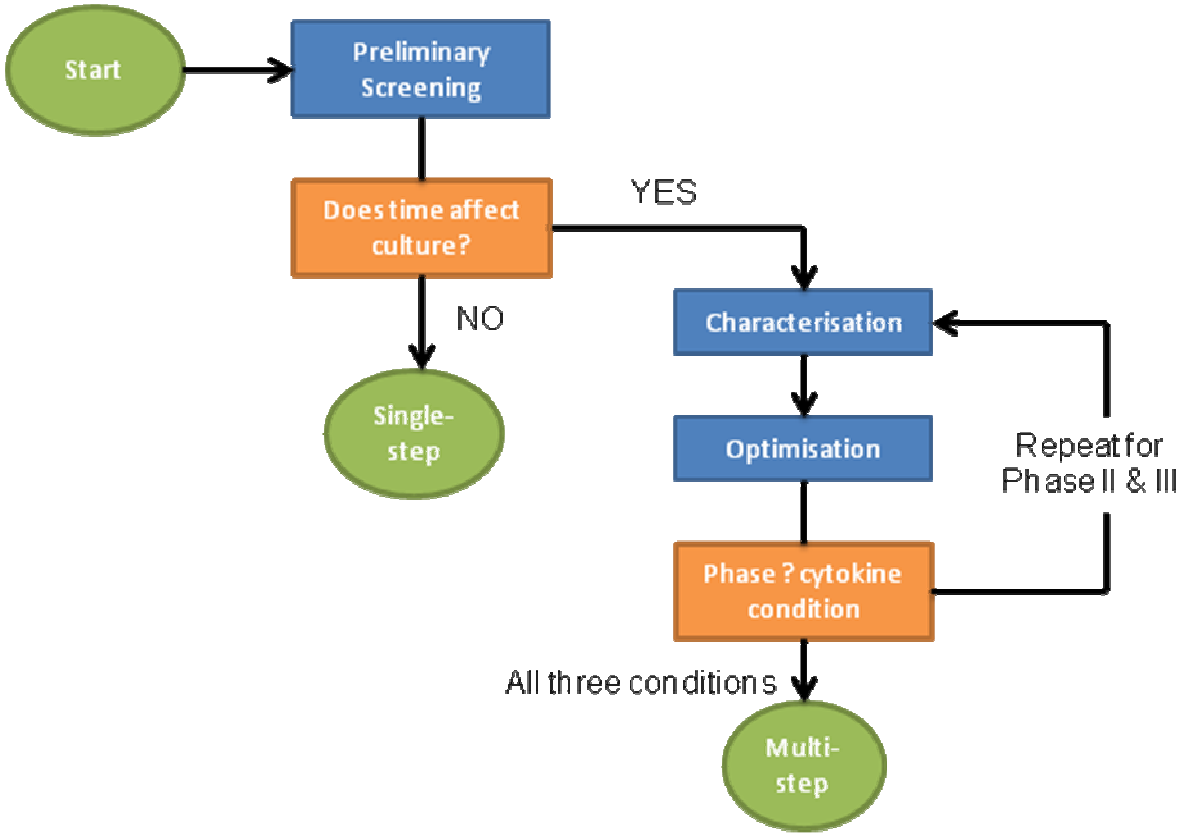

Figure 6.3 Flowchart of DOE experimental strategy for multi-step cytokine culture

6.4 RESULTS

6.4.1 Preliminary screening analysis

The preliminary screening experiment demonstrated that the feeding frequency, change of growth factor concentrations, and the presence of EPO have a significant effect on the total cell expansion over the course of an eight-day culture. The half normal plot for total cell expansion (Figure 6.4a) shows that the most prominent effects arose from change of media and the presence of EPO and a smaller effect came from the feeding frequency. This

indicates that a change in cytokine concentrations in the middle of the cell culture significantly affects cellular expansion. A number of factors also appear to affect the viability of cells, from the half-normal plot (Figure 6.4b) it can be concluded that cell viability was affected by frequency and a combination of two/three-factor interactions, which included frequency-change-EPO, change-SCF, frequency-EPO and change-EPO.

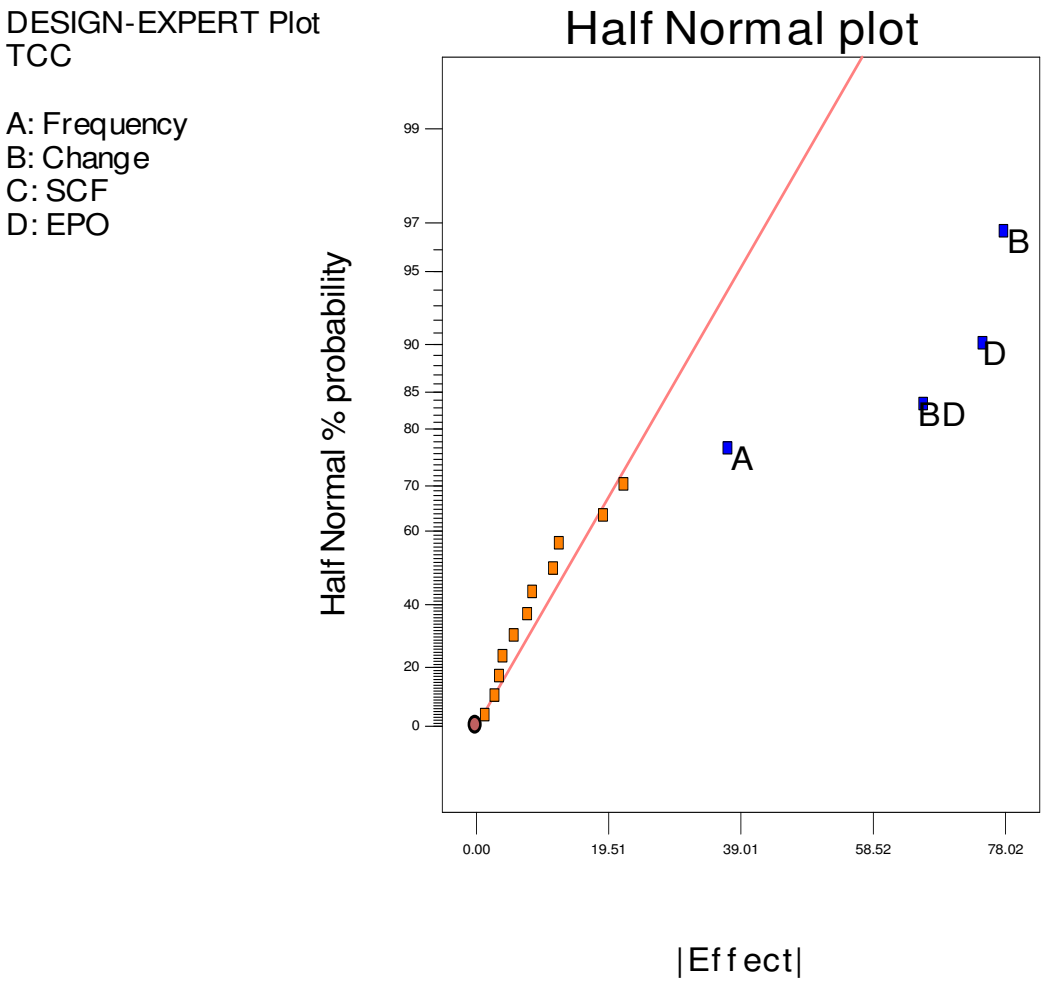

Figure 6.4 (a) The half-normal plot for fold expansion. Factors A, B, D and BD are significant. The x-axis reflects the magnitude of each effect; the y-axis reflects the probability that effect is significant. All other points that lie close to the line reflect random error.

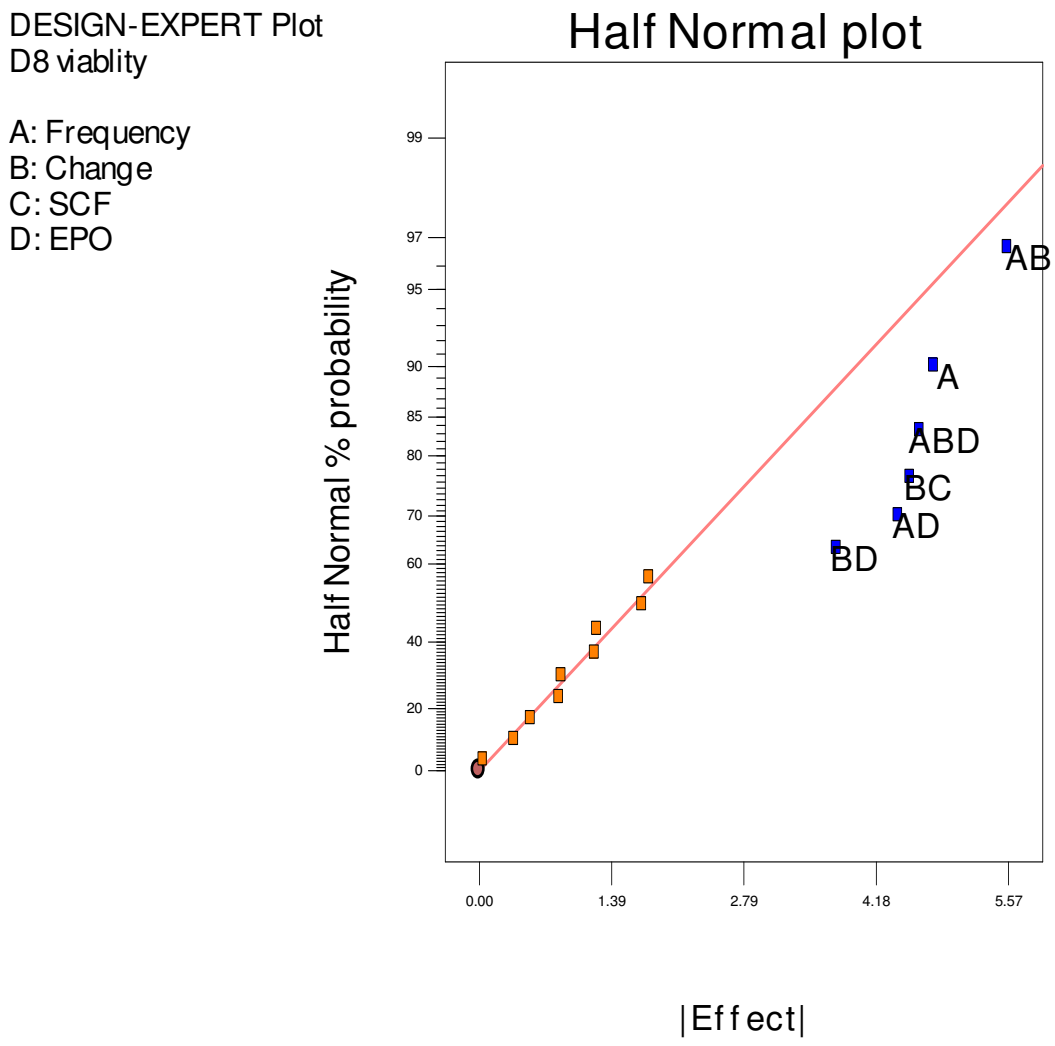

Figure 6.4 (b) The half-normal plot for cell viability. A number of factors appear to influence cell viability; this includes frequency and several two/three factor interactions.

6.4.2 Characterisation and optimisation analysis

Characterisation and optimisation of cellular growth for phases I, II and III were slightly more challenging than previously attempted (Chapter 5) for a single-step cytokine cocktail. Although DOE characterisation for each phase was repeated three times, not all

DOE characterisation studies performed yielded significant models. From those that were significant, the repeats in the models within each phase, in some cases, were slightly different. In phase I, all models showed a general dependency on IGF-II and EPO but no significant effect in changing SCF concentrations on cellular growth (total cell expansion). In the first experiment, a strong contribution from changing EPO concentrations and an interactive effect between IGF-II and EPO were identified but the contribution of IGF-II was not very significant. The experiment was repeated and the results were modelled against variables from the initial findings. In this case, all parameters involved were significant including that of IGF-II. The response surface model generated from the second experiment differed slightly from the first experiment in shape of the curvature toward higher EPO concentrations (Figure 6.5). The optima on each plot also do not lie exactly in the same region although both have a tendency toward higher EPO concentrations. A model describing the relationships for fold expansion in the first experiment was generated by backward elimination and has an R^2-value of 0.7886 and no significant lack of fit ($p = 0.4874$). The model describing relationships in the second experiment has an R^2-value of 0.7546 and no lack of fit ($p = 0.9487$). A summary table for the equations of both models is provided in Table 6.1 and the full ANOVA output can be found in Appendix A. Although the R^2 values for both models were not very high (< 0.90), they were both significant and showed no lack of fit. Optimal cytokine concentrations were optimised based on the model with the best fit (experiment 1) and the optimal operating regime lies in the region of 3-5 IU/ml EPO and varying concentrations of SCF and IGF-II. Two sets of cytokine concentrations were selected from the optimisation list and tested: (1) 70 ng/ml SCF and 5.00 IU/ml EPO and (2) 50 ng/ml

SCF, 100 ng/ml IGF-II and 3.00 IU/ml EPO and showed no significant difference. The cytokine cocktail with lower concentrations of EPO was chosen for economical reasons.

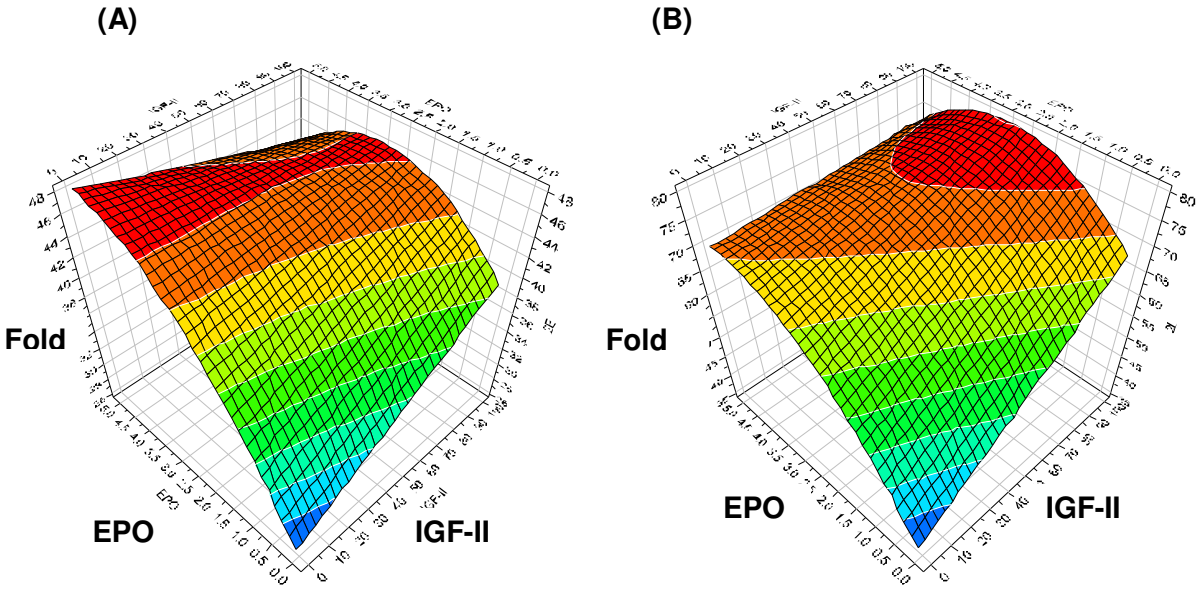

Figure 6.5 Response surface plots for phase I studies: Characterisation for total cell expansion from day 0-6 of cell culture (a) Experiment 1: fold range is 0-48 (b) Experiment 2: fold range is 0-80. Cytokine ranges for both experiments are 0-100 ng/ml IGF-II and 0.1-5.0 IU/ml EPO. Both experiments showed no dependency on SCF and has a tendency toward higher concentrations of EPO (3-5 IU/ml).

In phase II, all three models showed a dependency on EPO and SCF though in one model the effect of SCF was not significant ($p = 0.20$). In the other two experiments, relationships were almost identical as observed by their response surface plots (Figure 6.6) and the optima for each plot lie in the same area. However, the numerical values in each model output differed, which is not surprising, since cord-to-cord variability affects cell

culture performance. In the first experiment, the R^2-value for this model was 0.5972 and has no lack of fit. In the second experiment, the R^2-value was 0.8747 and has no lack of fit. The response surface plots for these two experiments are displayed as a comparison in Figure 6.4; both plots look almost identical. Model equations are summarised in Table 6.1 and the full ANOVA outputs are provided in Appendix A

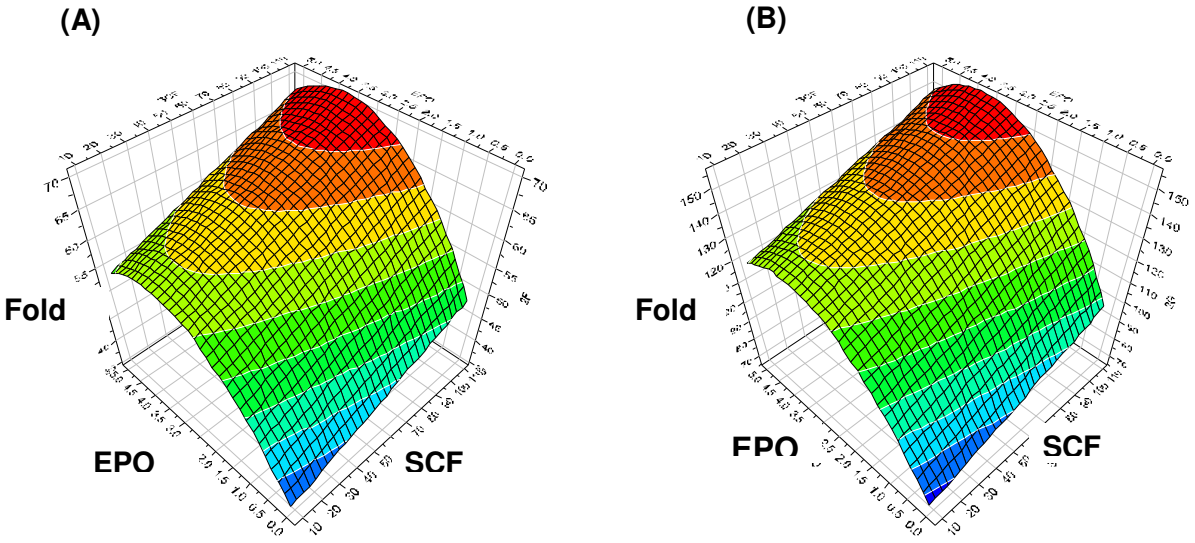

Figure 6.6 Response surface plots for phase II studies: Characterisation of total cell expansion from day 6-10 of cell culture (a) Experiment 1: fold range is 0-70 (b) Experiment 2: fold range is 0-150. Cytokine ranges for both experiments are 10-100 ng/ml SCF and 0.1-5 IU/ml EPO. Plots from both experiments look almost identical and share the same optimal regime of operation.

The final numerical optimisation for phase II was based on the model that gave the best fit (Experiment 2), and this yielded an optimal regime around 110 ng/ml SCF, 0-80 ng/ml IGF-II, and 3.68-3.80 IU/ml EPO. The final concentrations selected for phase II were 110 ng/ml

SCF, 17 ng/ml IGF-II and 3.75 IU/ml EPO. Generation of DOE models in phase II cultures were more consistent than that in phase I cultures.

In the final stage (Phase III), cell expansion was evaluated from day 10 to day 16. Three independent DOE experiments were performed but only one provided results that produced a significant model; the other two experiments did not provide a good fit to any model and showed only a dependency on EPO. In the experiment that provided significant results, fold expansion showed a strong dependency on SCF and EPO concentrations and the model fit has an R^2 value of 0.8620 and has no lack of fit. High concentrations of both cytokines, particularly EPO, appear to enhance cellular growth at this stage. Their relationships are displayed in a response surface graph on Figure 6.7. For the other two experiments, an attempt to fit the data on a model using SCF and EPO showed very poor fit. One of them is shown in Figure 6.7b and the model equations can be found in Table 6.1. Full ANOVA outputs can be found are in Appendix A. As observed from the response surface plots, experiments which did not yield a good model showed no correlation or resemblance to the experiment with a good model. It has also been noted that the maintenance of cell culture up to this stage became more challenging; expansion was significantly slower due to increased maturity of overall cell population thus there is less variation in cellular growth due to changes in cytokine concentrations. A numerical optimisation initially based on cellular growth gave an optima at 74 ng/ml SCF, 0 ng/ml IGF-II and 3.98 IU/ml EPO.

Table 6.1 Summary table of model equations from characterisation studies. A = SCF, B = IGF-II and C = EPO

Experiment ID	Model Equation (in coded factors)
Phase I (Expt. 1)	$Fold = 44.18 + 1.84B + 6.46C - 5.32C^2 - 4.75BC$
Phase I (Expt. 2)	$Fold = 71.10 + 8.92B + 10.27C - 9.57C^2 - 7.21BC$
Phase II (Expt. 1)	$Fold = 62.09 + 6.85A + 9.87C - 10.78C^2$
Phase II (Expt. 2)	$Fold = 135.90 + 15.31A + 26.50C - 28.00C^2$
Phase III (Expt. 1)	$Fold = 10.89 + 1.23A + 2.06C - 2.08A^2 - 2.05C^2$
Phase III (Expt. 2)	$Fold = 3.72 - 0.11A + 0.94C + 1.09A^2$

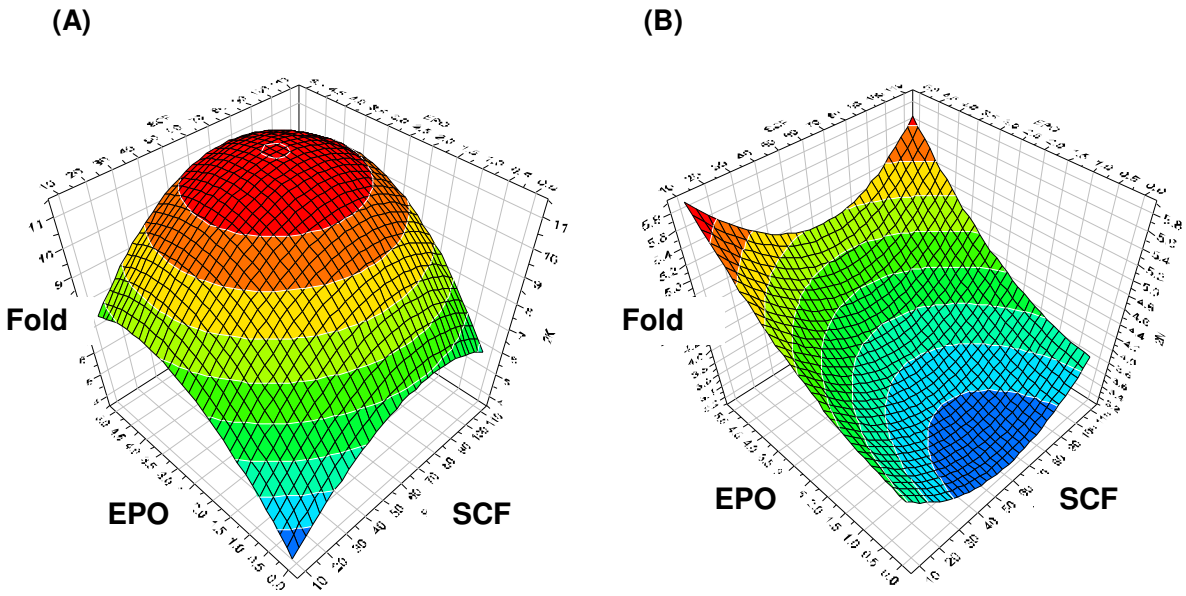

Figure 6.7 Response surface plots for phase III studies: Characterisation of total cell expansion from day 10-16 of cell culture (a) Experiment 1: fold range is 0-11 (b) Experiment 2: fold range is 0-5.8. Cytokine ranges for both experiments are 10-100 ng/ml SCF and 0.1-5 IU/ml EPO. Models with poor fit (experiment 2) showed no resemblance to the model with a good fit (experiment 1).

6.4.3 DOE verification

The three-step DOE optimised cytokine culture achieved an average fold expansion of 27,940 (n = 3) with a maximum fold expansion of up to 64,300 fold achieved in one culture and the minimum fold expansion of 5,400 fold (Figure 6.6a). Cord-to-cord variability caused significant differences in the outcomes of cord blood cultures in the verification study. The unit that produced lowest proliferation had the smallest number of CFU-GEMM colonies from the initial starting population; only 5 colonies versus 25-34 colonies from other cord blood units used in this study. The low CFU-GEMM count indicates a lower proliferative capability of this unit compared to the others, which explains for the low total fold expansion. A comparison in the growth potential of the three-step cytokine culture versus the single-step showed no statistically significant differences due to the large variability in growth performance (Figure 6.8a). However, both the maximum and minimum expansion achieved in the three-step culture are still better than those achieved in the single-step culture: for the minimum fold expansion, the three-step produced 5,400 fold while the one-step produced 3,029 fold; for the maximum fold expansion, the three-step produced 64,300 fold while the single-step produced 36,900 fold.

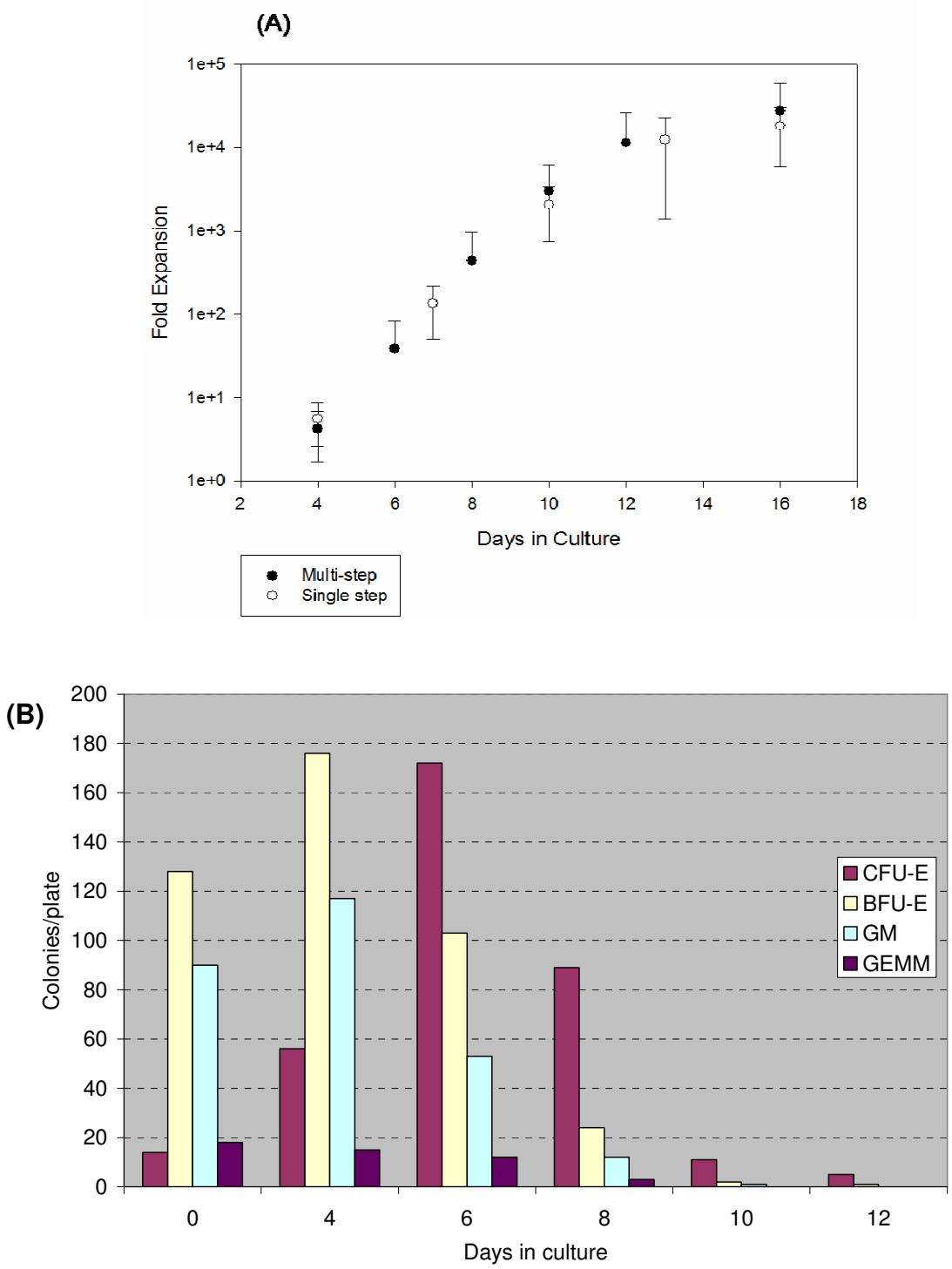

Figure 6.8 Cellular growth and clonogenic capability of cord blood cultured cells in three-step DOE cocktail. (a) Total fold expansion over 16 days; a comparison between the three-step and single-step culture (b) Colonies formed through 12 days.

Clonogenic ability of cultured cells showed increasing colonies toward the erythroid lineage with the largest number of BFU-E and CFU-E colonies achieved on day 6 of the culture (Figure 6.8b). The number of CFU-GEMM and CFU-GM did not seem to decrease as much on day 4 as those observed from the single-step cytokine culture (Figure 5.4) indicating longer maintenance of immature progenitors in this culture. Expression of erythroid surface antigens (CD71 and GPA) is similar to those achieved from the single-step cytokine culture. A rapid increase in CD71 and GPA expression is observed (Table 6.2) with almost 60% expressing GPA by day 6 and over 90% by day 10 of the culture; results were similar to that achieved in the single-step cytokine culture. Cell morphology of cultured cells stained with Wright-Giemsa and brilliant Cresyl blue were also similar to those observed from the single-step cytokine culture. Some of the cells observed during culture on day 16 resembled those of red blood cell morphology, having a biconcave shape (Figure 6.9). Observations from the surface antigen expression, cellular morphology and CFU-assays were consistent with the results made in the previous study (Chapter 5) indicating a definitive differentiation toward the erythroid lineage. Therefore, differentiation toward the erythroid lineage has not been compromised using three-steps at varying cytokine concentrations.

Table 6.2 Surface antigen expression for CD45, CD71 and GPA. Numbers reflect the average expression +/- 1SD (n = 4 except day 16 data: n = 2)

	CD45	**CD71**	**GPA**
Day 4	12.9 ± 10.0%	90.7 ± 4.2%	25.2 ± 25.9%
Day 6	19.3 ± 12.8%	93.8 ± 4.0%	59.7 ± 7.4%
Day 8	6.8 ± 7.0%	97.7 ± 1.3%	82.6 ± 10.0%
Day 10	4.8 ± 3.2%	98.4 ± 0.8%	94.2 ± 2.6%
Day 12	4.4 ± 2.7%	97.0 ± 1.5%	91.8 ± 8.7%
Day 16	1.8 ± 0.7%	92.9 ± 6.0%	90.3 ± 11.0%

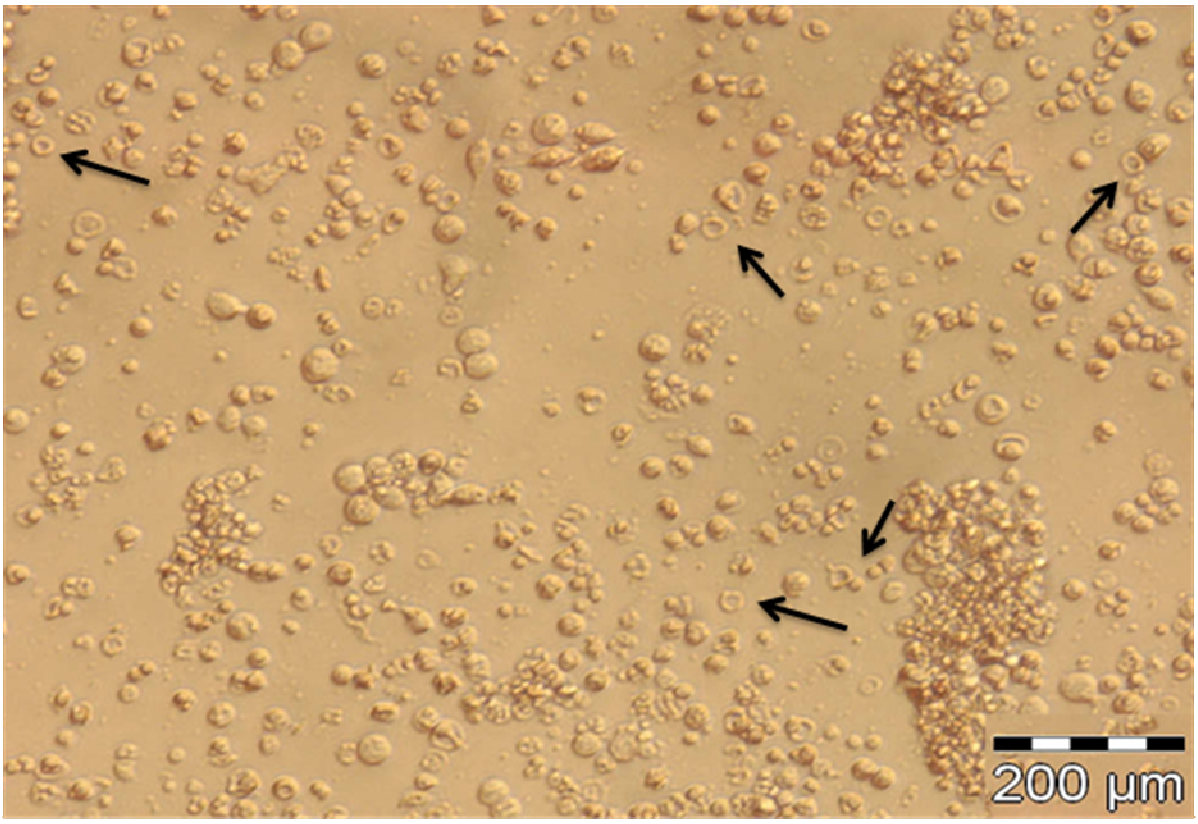

Figure 6.9 Photograph of cord blood cells cultured in 24-well plate on day 16. Arrows indicate some of the cells which resemble a red cell morphology showing a biconcave shape.

6.5 DISCUSSION

Sequential characterisation of *in vitro* erythropoiesis using DOE produced three distinct response surface profiles for each phase of the culture. Phase I (day 0-6) was strongly dependent on concentrations of IGF-II and EPO while phases II (day 6-10) and III (day 10-16) were dependent on SCF and EPO. Though most of the models were significant, repeatability of model results were not easily obtainable particularly for phase III studies – only one out of three experiments produced a significant model. Optimisation of cytokine concentrations for each phase produced a three-step cytokine cocktail. When the three-step cocktail was compared to the single-step, the average growth potential did not show statistically significant differences but the maximum and minimum total cell expansion from the three-step study were higher than that in the single-step study. The rate of erythroid differentiation in the three-step cytokine culture was also not compromised. In the following sections, a discussion relating to the challenges faced in using DOE as an approach for sequential characterisation and the improvements that can be made from what has been learnt in this study is presented. Advantages and disadvantages of the multi-step versus the single-step approach are compared. The implications and practicality of this multi-step approach for bioprocess definition are also evaluated.

6.5.1 Challenges in sequential characterisation

6.5.1.1 Sample variability

One of the major challenges faced in this study is reproducibility of DOE generated models for the sequential characterisation of *in vitro* erythropoiesis of cord blood stem cells.

Several problems were encountered and one of the major obstacles is attributed to significant cord-to-cord variability. Units received from the cord bank were all of research and development grade, which does not go through stringent quality control procedures. As a consequence, the quality of cord blood units received for this study was highly inconsistent and most of the units were of much poorer quality in comparison to those received for the single-step study (Chapter 5). Differences in the quality of cord blood samples generated significant variability in growth performance of cord blood cells between batches which contribute to the differences observed in model responses within each characterisation study. Samples of low quality also showed poorer overall growth performance and less distinct characteristics (less responsive) thus producing larger noise-to-signal ratios (pure error) within each DOE experiment, compromising the fit to the model.

6.5.1.2 Division of time intervals

The division of time intervals to define different phases of the cell culture is perhaps one of the most challenging tasks. The definition of an end-point for each phase is unclear as the *in vitro* kinetics for this process is still unknown. Furthermore, kinetics between cord-to-cord samples can also vary significantly due to differences in the proliferative capacity of each cord unit and quality of the sample. The "end-point" of each phase for each cord sample may therefore differ slightly. The elucidation of process dynamics also seeks finer resolution in process characterisation and demands a greater distinction in culture performance between and within each phase. Cultures with more distinct characteristics make DOE characterisation easier, i.e. more reproducible models with better fit. In this study, significant models were not always achievable in all phases of the culture – cell culture performances were more distinct

in some phases than in others. Characterisation in phases I and III for example were less defined than that in phase II as cellular growth in the latter were significantly slower than in the log phase. Phase III, in particular, has a much weaker overall response to changes in cytokine concentrations as the overall population at this stage is more mature and less proliferative in nature.

6.5.1.3 Concentration ranges

Cytokine concentration ranges define the process window. Concentration ranges in this DOE study were chosen to begin at low values for SCF and EPO, 10 ng/ml and 0.1 IU/ml respectively, instead of beginning at zero concentration. This choice was made due to previous findings (Chapter 5) which determined both SCF and EPO to be critical factors contributing to this process, particularly for cell growth. An absolute zero concentration scenario is to be avoided as cells will not survive without the presence of any growth factors; an absolute zero condition can skew the response surface profiles quite significantly. In the case of IGF-II, which was added as a mid-acting growth factor, the effects of IGF-II are still unknown so the low concentration of IGF-II was selected to be at zero in order to distinguish effects in the presence or absence of this growth factor. Given these considerations, using low concentrations of SCF and EPO as the lower limits of the process reduces the process window as compared to that previously performed in Chapter 5. It will therefore require tighter process outputs (less variability in growth performance) in order to produce models that are reproducible and with better fits.

6.5.2 Improvements in DOE process strategy

6.5.2.1 Process objectives

Conflicting results from this DOE characterisation study poses several queries as to the suitability of the experimental approach taken. One of the conflicting observations made was the lack of effect of SCF at the beginning of the culture and its significance only toward the middle and end of the culture. This is somewhat contradictory to what is known about SCF, as an early-acting growth factor. Similarly, the influence of IGF-II at the beginning to the culture was also somewhat questionable as IGF-II was thought of as a mid-acting growth factor. These observations begin to question suitability of the objectives that were used to define process conditions for each phase of the culture. In this case, the objectives for each phase were identical i.e. to maximise the total cell expansion of red blood cell progenitors. The inclusion of EPO in all of the culture conditions ensured definitive differentiation toward the erythroid lineage. However, this limits the process window particularly in the beginning of the culture where cells were in their most immature state. Should the process objective at the beginning of the process then be slightly different from that used for the later stages? Will this change process dynamics of the culture significantly and impact the final outcome? These questions pose valid concerns that should be studied further to unveil the effects of process dynamics in the final outcome of the culture.

6.5.2.2 Significance of each phase

Characterisation study performed by a division of different phases is a valid approach but has several limitations. As observed from this study, the distinction between different process conditions become less defined at the later stage (phase III) of the process. This is

largely due to the increase in cell population maturing toward the same lineage i.e. less proliferating capacity and is likely to become less responsive toward small changes in cytokine concentrations. Failure to repeatedly produce models with a good fit in phase III studies reflects these challenges. The only factor that consistently played a significant role in cellular growth in the phase III models was EPO concentration which is not surprising as this is consistent with the *in vivo* process.

Observations made in this study suggest that culture definition at the later stages of the process may also not be as crucial as those performed at the initial stages. At the beginning of the culture, where the highest number of $CD34^+$ cells and the greatest proliferating and differentiating capacity of the culture are found, it is crucial to define culture parameters influencing this process most accurately here. Process definition at the early stages of the culture will ultimately influence responses from the later stages and can significantly change the dynamics of the process. Process definition at the early stages of the process is absolutely critical and it is highly recommended that a quantitative characterisation of the initial phases of the cell culture by way of a response surface model is performed. Quantitative characterisation at later stages of the process could then potentially be omitted and a simple optimisation strategy instead of using RSM can be taken.

6.5.2.3 Different DOE approaches

In terms of the DOE designs and experimental approach toward cell culture process characterisation, different design strategies have been undertaken by other researchers and briefly discussed in Chapter 5. In the study performed by Yao et al., use of fractional factorial designs for screening growth factors and serum substitutes suited for cord blood stem cell *ex*

vivo expansion was performed[79]. At the beginning, two fractional factorial designs (a Res III and Res IV) were used to screen nine different growth factors and eight different serum substitutes independently. After identifying the significant factors, a higher resolution factorial design (Res V) was used to determine the first-order linear relationships of each factor to the process of interest. Using these first-order models, they performed an optimisation step via the path of steepest ascent to determine the optimal concentrations of each contributing factor. This approach has several advantages: (1) it is relatively simple and straight-forward and allows screening of a large number of process factors. (2) Optimisation of the process factors using this method does not require a highly defined model and is much quicker way to determine optimal operating conditions. However, this also means that the process relationships achieved in these studies are less defined, since they are only an approximation toward the optimal operating regime. They do not account for process interactions which may or may not be significant in the process of interest, but is certainly a much more straight-forward approach in optimising cytokine concentrations. This approach is highly effective if one can consider process interactions to be negligible in comparison to main process effects, which can very likely be the case in some cell culture processes where main effects control the bulk of the process.

Another approach taken by Cortin and his colleagues, briefly discussed in Chapter 5, was to perform two levels of screening, first at a lower resolution using a PBD, followed by a high resolution (Res V) fractional factorial design, and then process characterisation using a CCD[35]. Although this approach is useful in screening large numbers of factors while requiring only a small number of experiments by way of the PBD, single factors in this design are highly confounded with two-factor interactions which as shown in this study can

produce conflicting results between the repetitions. The deduction of key factors using PBD is therefore not as straight-forward. Characterisation using CCD is a highly useful tool for producing second-order response models, as performed in Chapters 5 and 6 of this thesis, and can reproduce quantitative models for the processes of interest. However, it may be faced challenges due to culture variability and discrepancies in model outcomes particularly in processes that are less responsive to changes.

6.5.2.4 Improved DOE approach

After reviewing different DOE approaches, the recommendations for an improved DOE approach to sequential characterisation of cord blood cell cultures are as follows: Screening experiments are an essential part of the DOE characterisation and optimisation process. Screening can be performed using either the fractional factorial design or PBD depending on the suitability of the parameters and comfort-level of the experimenter regarding each technique. In each phase of the sequential characterisation, a screening experiment should be performed to first identify contributing factors to the process. If the number of factors being studied is no more than 10, the fractional factorial design is recommended. Preferably, a resolution IV design should be used to avoid too many confounding factors in the design matrix.

In the next step, process characterisation particularly at the beginning phases of the culture is critical. Use of an appropriate response surface design such as the CCD is recommended. Selection of concentrations ranges at this stage of the process is also crucial as it will determine the process window. Since a screening experiment prior to this step has been performed and confirmed the significance of each factor, significant factors used in the

characterisation study may begin at low concentration ranges. Optimal cytokine concentrations are determined from the response surface plots. Finally, for phases at the later stages of the process, optimisation of cytokine concentrations via the path of steepest ascent can be taken instead of the RSM approach. This eases variability in the DOE output and could still reproduce process conditions close to the optima. The proposed revised and improved DOE approach is shown in Figure 6.10.

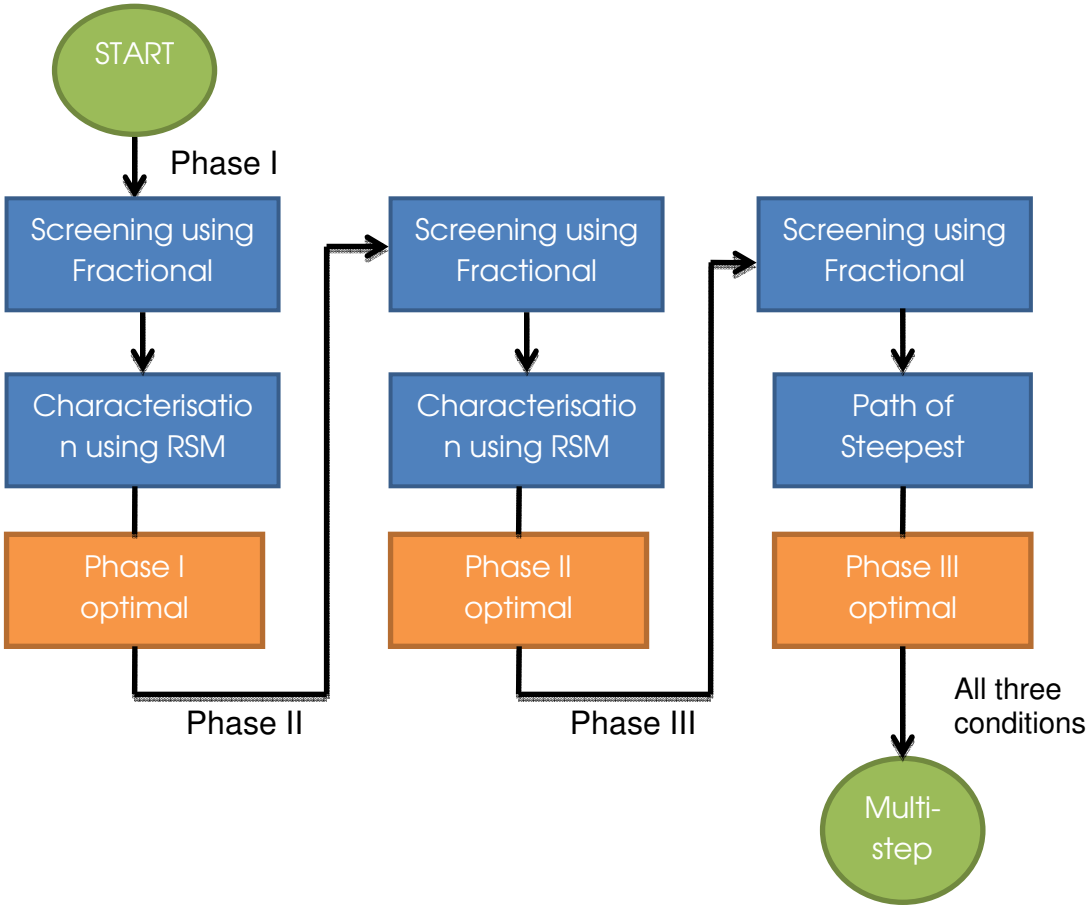

Figure 6.10 Improved DOE approach for sequential characterisation

6.5.3 Multi-step versus single-step

Even though the average total fold expansion in the three-step cytokine culture statistically did not show significant improvements than the single-step cytokine culture due to large process variability, several benefits in the three-step cytokine culture should be highlighted. The multi-step approach, as previously mentioned, was aimed at revealing process dynamics of an *in vitro* process. The multi-step approach is thus more "kinetics"-driven than the single-step approach which is an end-point driven process. The multi-step approach also provides a global analysis rather than a local analysis of the process of interest since it studies variations and changes occurring through the cell culture. It also gives a more accurate account of the process dynamics while the single-step may not be reflective of all stages of the process. Another significant advantage is the flexibility of the multi-step approach to accommodate for variations in process demands. However, the multi-step approach requires a significantly larger amount of time and labour to optimise and is not as simple or straight-forward as the single-step approach. A summary of the advantages and disadvantages of these processes is shown in Table 6.3.

Table 6.3 Summary of advantages and disadvantages of the multi-step versus the single-step

Multi-step approach	**Single-step approach**
"Kinetics"-driven	End-point driven
Global analysis	Local analysis
More accurate account of the process	Not entirely reflective of all process stages
Flexible approach	Simple, straight-forward approach
Tedious and more time-consuming	Significant time-savings and expense

6.6 CONCLUSION

Sequential characterisation using DOE in this study produced successful models that illustrated some of the process dynamics *in vitro*. However, due to large cord-to-cord variability and challenges in process resolution, reproducibility of process models for later stages of the process was particularly more difficult. Process response at later stages in the process was less pronounced than at the early or mid stages. Several adjustments and improvements can be made to better define characteristics of this dynamic process. Some of the important considerations include definition of culture phases, cytokine concentration ranges, process objectives for each phase, and suitability of DOE designs used in each step. Overall, the outcome from the DOE three-step cytokine cocktail produced slightly better results (greater expansion) than that achieved from the single-step cytokine cocktail, even though the average numbers were not statistically different; both the minimum and maximum expansion achieved from the three-step process are better than that achieved in the single-step process. The multi-step approach was also able to show variations in the process responses at the beginning, middle and end of the culture, providing more insight into the process dynamics. Ideally this "kinetics"-driven approach is preferred as it is not only able to better optimise the process based on process requirements closely reflecting to their needs in "real-time" but provide a scientific insight and explanation to the dynamics of *in vitro* bioprocesses.

CHAPTER 7

Spatial profiling using DOE: A temperature study

7.1 INTRODUCTION

The emerging field of tissue engineering and regenerative medicine promises to drastically change clinical practice through cellular therapy. Tissue engineered products such as the bone, skin and blood cells are the future replacement therapy. Production of these engineered cells/tissue for clinical use requires highly reproducible, well-controlled, and optimised stem cell bioprocesses[9,162]. *In vivo*, the body accomplishes organogenesis and homeostasis by maintaining a delicate balance between the differentiation, proliferation, and self-renewal of cells through the real-time, online, and *in situ* sensing of important parameters in the body and the local delivery/removal of nutrients/metabolites, hormones, and growth factors needed[163]. However, most current cell/tissue cultures are information-poor due to the lack of real-time monitoring technologies, and lack the spatial and temporal

resolution required to provide accurate and precise process control. To address limitations encountered in the *in vitro* system, online, real-time, *in situ* monitoring must be implemented to obtain the necessary information required for a tightly-controlled bioprocess operation.

At present, online, real-time process monitoring can be achieved through several methods[81]. One of these methods include the flow injection analysis (FIA) unit which represents a relatively common practice[61,164,165]. In this case, a sample is drawn from the bioreactor and the overall sample concentration is measured externally. Although FIA is successful for bioprocess monitoring, it only provides bulk concentration measurements at specific time intervals. Bulk concentration measurements do not provide spatial information of the culture environment and are often considered a late indicator as it is unable to detect cell populations that are already suffering malnutrition/intoxication due to the dilution effects in bulk concentration measurements. Alternatively, *in situ* electrochemical biosensors can be employed, as proposed in our culture system, to measure culture parameter concentrations locally and in real-time. Furthermore, the use of *in situ* electrochemical biosensors is advantageous in that no sample is lost through the withdrawal from the culture system at any time. In contrast, existing online systems that utilise automated sample withdrawal tend to require large amounts of sample volumes. This impairs the ability to generate many or continuous readings, and results in a bioprocess operation, such as perfusion rate, potentially being dictated by the sampling rate and not by the actual requirements of the system. Conversely, the use of *in situ* biosensors is an invasive technique for cell culture processes and increases the exposure of contamination. Longevity of sensors in serum-containing medium is also another challenge that remains to be addressed.

Measurement of local concentrations is important because it reveals spatial variation of essential culture parameters. Ultimately, this could result in the identification of micro-concentration gradients, which *in vivo* represent the stem cell niches that regulate the proliferation and differentiation processes[153]. Currently, majority of the cell culture systems, including static and perfused, are essentially non-homogeneous[166]. In a traditional two-dimensional (2D) flask/well cultures, cells tend to aggregate together in colonies of varying sizes and randomly disperse themselves in the space available for growth. During cell growth and proliferation, cells metabolise by consuming nutrients, such as glucose and glutamine, while secreting waste products, such as lactate and ammonia. Production and consumption rates of nutrients and metabolites vary depending on cell type, colony size, and stage of cell maturation. Since the cell culture environment is non-homogeneous, local concentration gradients are created which directly affects cell populations locally. Specifically, cells experiencing high consumption/production rates of nutrients/metabolites/cytokines will inevitably be subjected to strain, which would affect their normal physiological status. Bioprocessing has sought to address these challenges by attempting to provide a homogeneous culture environment and employing perfusion to offer better supply of nutrients and removal of metabolites[166]. However, *in vivo*, concentration gradients exist and the body maintains homeostasis through *in situ* monitoring, circulation, and local transport. In contrast, *in vitro,* the spatial distribution of nutrients/metabolites is not monitored resulting in the sub-optimal control of feeding/removal of nutrients/metabolites into the culture system.

To effectively obtain the spatial profiles of culture parameters using *in situ* biosensors, it is crucial to determine the appropriate number and position of biosensors required, especially in the absence of detailed *a priori* knowledge of the culture environment.

Herein, I propose a novel strategy based on DOE as an approach towards statistical sampling to determine the location and number of sensors required to obtain information-rich data that will result in the generation of spatial (and temporal) profiles for important culture parameters. Specifically, in this study, the 2D space of a traditional well-plate culture system was mapped using the face-centred CCD which determined the optimal placement and number of sensors required for spatial profiling.

7.2 AIM AND HYPOTHESIS

The aim of this study is to test the feasibility and validity of using a DOE approach as a statistical method to determine spatial variations in a cell culture/bioreactor system. Due to the flexibility and robustness of DOE methods, the hypothesis is that DOE can be tailored to study spatial variations of an analyte of interest and produce spatial maps showing process variations. The uniqueness and advantage in this approach is in its ability to provide information-rich data using the minimum number of sampling required.

7.3 APPRAOCH TO STUDY

In order to test the feasibility of the DOE approach, a simple and straight-forward experimental setup was employed. This preliminary test did not utilise the culture of cells but has been designed to simulate cell growth in clusters/colonies with the production/consumption of metabolites/nutrients. In particular, miniaturised and highly

sensitive temperature sensors were used, which would correspond to any sensor of interest. Controlled heating elements were used as point sources to generate temperature variations within the culture system. The controlled heating elements, fixed at a certain temperature, were analogous to a constant production of metabolites by the cell clusters/colonies; mass transfer equations were corresponded to heat transfer equations. A DOE approach was used to statistically sample the space in order to obtain representative information, thus establishing the number and location of sensors required. The DOE results were compared with other experiments performed using a random and arbitrary number and position of sensors. Finally, DOE results were validated through comparison with experimental data using additional sensors placed at random positions. The DOE approach resulted in the elucidation of spatial and temporal profiles of temperature, which can be extended to any culture parameter with the use of appropriate sensors (assuming that their sensitivity is adequate). Utilising such information could result in achieving better control of cell culture bioprocesses.

7.4 RESULTS

7.4.1 DOE generated spatial and temporal profiles

Spatial and temporal progression of temperature profiles obtained for the three different experimental setups are displayed in Figure 7.1. Specifically, Figure 7.1a shows the single heating element experiment in a static culture where clearly, after 3 min, the location

of the single heat source can be identified. In particular, at this time-point, the temperature spatial profile indicates that the temperature of the liquid increased around the position of the heating element to 21°C covering approximately less than a third of the area of the culture chamber – the remaining two thirds have a temperature of 19-20°C. As time progresses, heat is continually added and by around 9 min, half of the chamber, close to the heating element, reached a temperature of 22°C whereas the other half had a lower temperature of 21°C. The R^2 value for the temperature profiles in the single heating element experiment is greater than 0.90, indicating an excellent fit of the model (Table 7.1). Furthermore, the low p-value ($p < 0.05$) confirms that the model predictions are significant.

Table 7.1 R^2 and p-values of fitted models from all three experiments

Expt. No.	**Single heating element**		**Dual heating element**		**Perfused system**	
Time	R^2	p-value	R^2	p-value	R^2	p-value
3 min	0.968	0.001	0.859	0.034	0.747	0.129
4.5 min	0.972	0.001	0.854	0.037	0.807	0.071
6 min	0.912	0.011	0.894	0.018	0.763	0.112
9 min	0.928	0.005	0.862	0.033	0.814	0.066

Figure 7.1b shows results from the dual heating element setup in a static culture. In this case, the locations of the two heating sources also begin to be identifiable after 3 min of heating. The overall rate of heating within the chamber is also higher as compared to the case in the single heating element which resulted in an overall higher temperature by the end of 9

min; the majority of the culture chamber had a temperature of 23°C. Although the R^2 value in the dual heating element setup in a static system is lower than the single heating element setup (Table 7.1), it still confirms a reasonably good fit of the model, and the p-value being less than 0.05 confirming that the model predictions are significant.

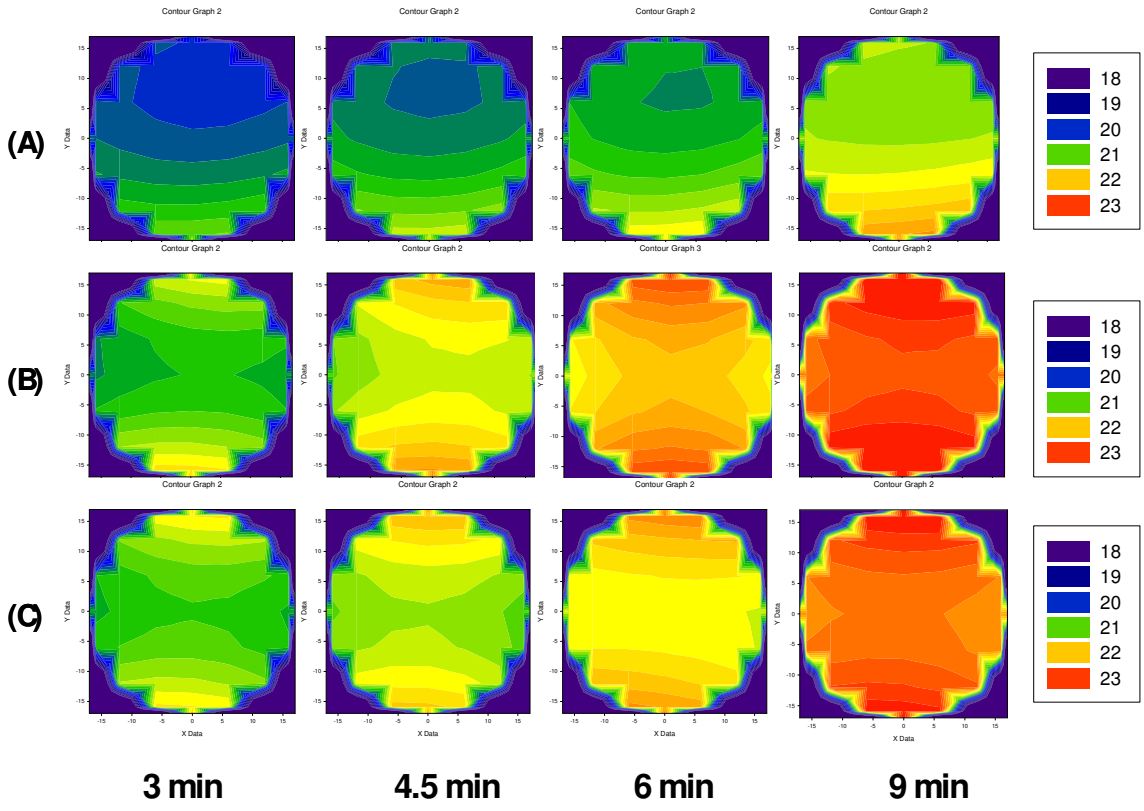

Figure 7.1 Spatial and temporal temperature profiles. (a) Single heating element experiment (static). (b) Dual heating element experiment (static). (c) Dual heating element experiment (perfused). Temperature ranges are displayed in degree C.

Results from the final experiment with dual heating elements in a perfused system are shown in Figure 7.1c. As anticipated, the dual heating sources resulted in an overall higher rate of heating compared to the single heating element thus an overall increase in chamber temperature. However, due to the continuous perfusion of cold water into the chamber, the overall temperature increase is not as high as that reached in the second scenario, dual heating elements in a static culture. The extent of the homogeneity in the temperature spatial distribution is lower and a clear area of slightly lower temperature is identifiable along the path of fluid flow. The R^2 values in this perfused experiment is lower than the static counterpart (Table 7.1) and did not provide a good fit for the model, which was confirmed by the high p-values ($p > 0.05$).

In contrast, random designs used for monitoring temperature variations could not generate spatial profiles as performed by DOE. In the five-sensor random design, the temporal progression of point temperature profiles were generated for each sensor in a single heating element setup under static conditions, as shown in Figure 7.2a. These results obtained from the random placement of sensors show the progression of temperature over time at each sensor position, but could not provide detailed spatial profiles for the whole culture chamber. Therefore, the only meaningful observation concluded to describe the relationship between the temperatures at various locations is that the temperature around the sensors closer to the heating element (positions A and B) was higher than that of the sensors away from the heating element (positions C and D). Similar results were obtained for the second random design which utilised seven randomly placed sensors (Figure 7.2b). The lack of a systematic DOE approach does not allow the generation of spatial profiles from the randomly placed sensor locations. The only quantitative relationship that can be deduced from such designs is

to fit a line/curve through the five points aligning vertically (data not shown), which is not extremely informative as it does not result in a spatial profile that covers the entire space of the bioreactor. Consequently, increasing the number of sensors randomly does not provide for information-rich data that is generated via DOE methods. DOE provides not only spatio-temporal profiles but also achieves that with the minimum required number of sensors and determines their location.

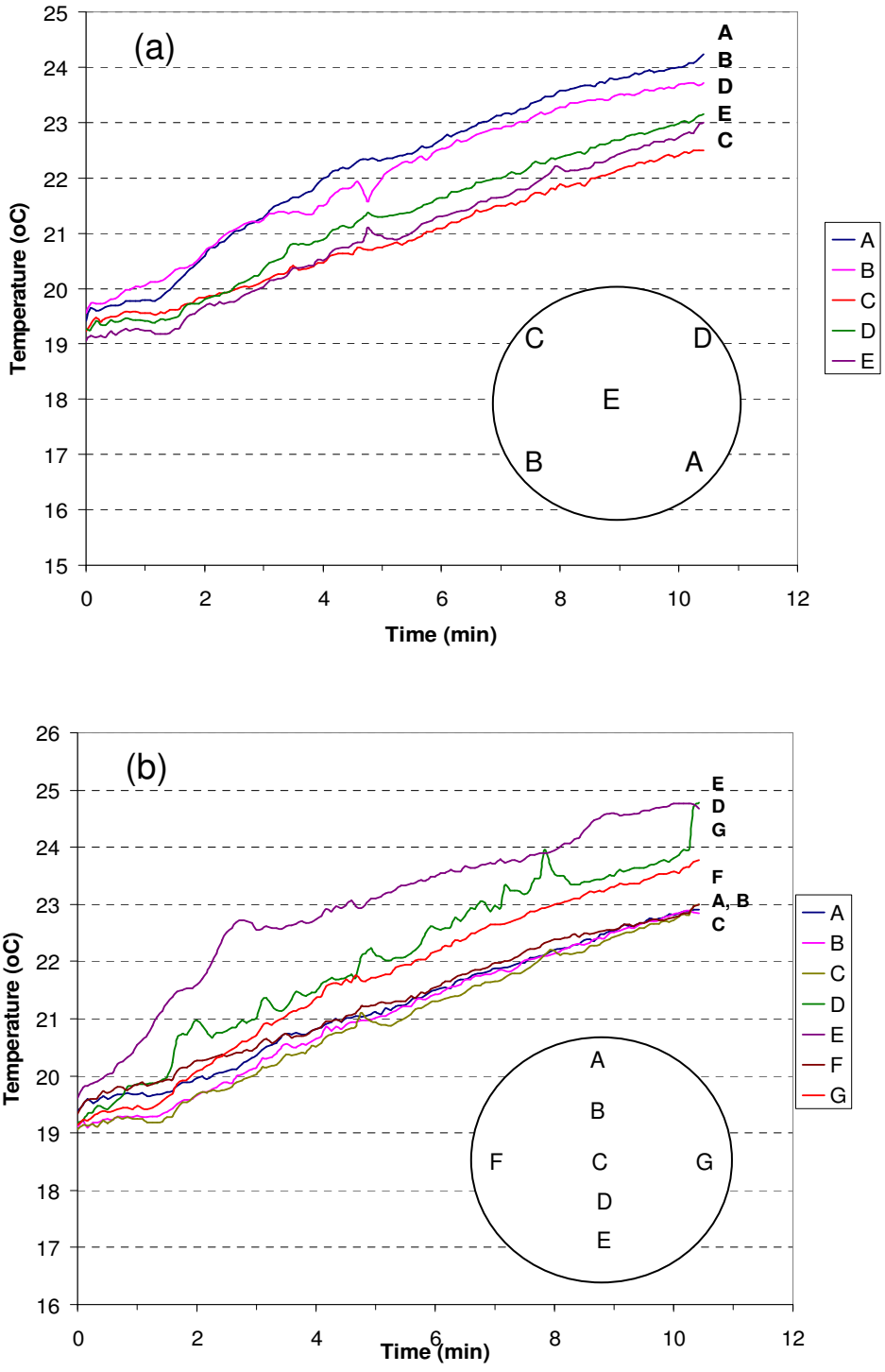

Figure 7.2 Temperature profiles of randomly placed sensors. (a) For five randomly placed sensors (b) For seven randomly placed sensors

7.4.2 Successful validation of DOE models

In order to validate the accuracy of our DOE approach for spatial elucidation, values from the model predictions were compared with experimental results obtained from three randomly placed sensors in a separate experiment. Specifically, the actual temperature measurements from sensors at positions 10, 11 and 12 (Figure 4.2f) were compared to the predicted values from the DOE model for the single heating element scenario taken at various time points (3, 4.5, 6, and 9 min). This comparison is shown in Figure 7.3 where prediction values were set at a 95% confidence interval and the black dots represent the actual temperature measurements. These results confirmed that predictions from the DOE simulation are in agreement with actual experimental values at a 95% confidence interval, apart for one point in this experiment, position 10 taken at 3 min which was 0.4^{o}C off the predicted range (Figure 7.3). This study confirms validity of the temperature models and a DOE approach toward spatial elucidation.

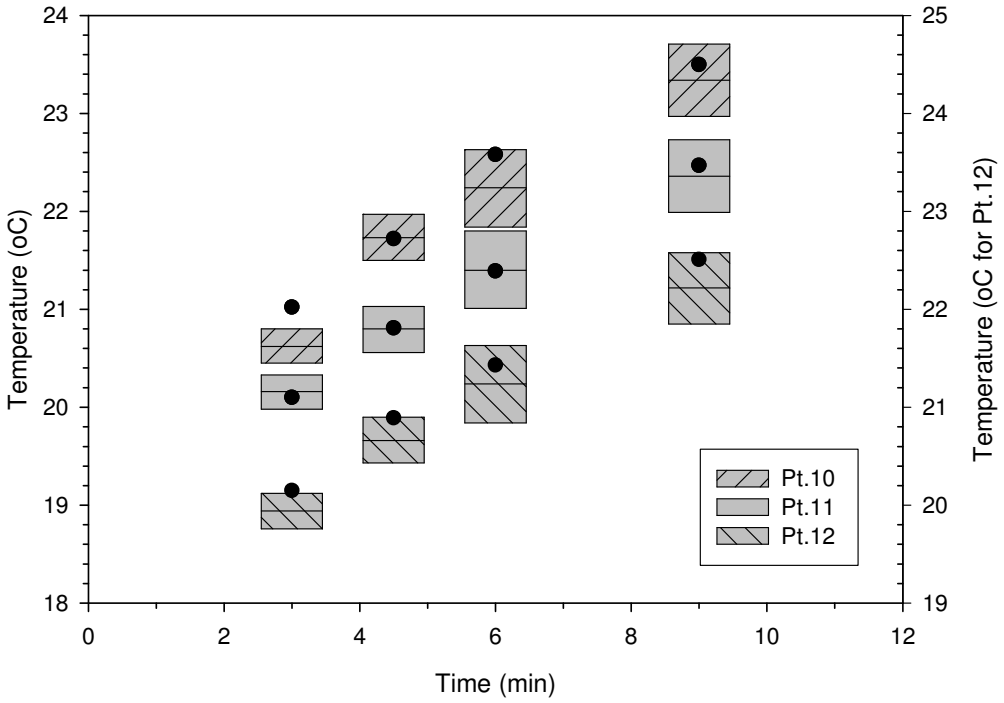

Figure 7.3 Validation results comparing prediction values to experimental values

7.5 DISCUSSION

The production of cells/tissue engineered for clinical applications renders the need for real-time, online, *in situ* monitoring of important culture parameters that will enable tight control, reproducibility, and optimisation of these complex cell culture bioprocesses. In addition, data obtained from the various monitoring platforms need to be harnessed to their full potential to provide "information-rich" profiles that represent the spatial and temporal progression of the bioprocess in operation. Currently, the only approach in determining the

position of sensors within bioreactor culture systems is entirely limited to computational fluid dynamics (CFD) analysis of the fluid flow within the bioreactors. This analysis results in the distinction between turbulent and non-turbulent locations and is extremely mathematical. Within the body and in the vast majority of tissue engineering culture systems, fluid flow is laminar; hence there are no areas of turbulent mass transport[162,163]. Furthermore, fluid dynamics studies do not provide any guidance for the optimal number or positioning of the sensors, and, in certain cases, the simulation results will not converge due to the geometry of the system. CFD has been used extensively in bioprocessing to incorporate flow, mass transport, and reaction kinetics in order to provide valuable information on nutrient/metabolite concentration profiles as well as cellular growth in bioreactor systems[167]. However, CFD simulation results are purely based on theoretical assumptions and approximations, and still need to be experimentally validated. In contrast, this novel DOE approach represents the use of statistical sampling to determine the optimal number and location of *in situ* sensors required to generate spatio-temporal profiles of important culture parameters, without requiring *a priori* knowledge of the culture system and its operation apart from its geometry.

Using DOE, data obtained from the different sensor locations were analysed to provide an information-rich interpretation, thus generating spatial temperature profiles in the culture chamber. In contrast, the random designs provided only point temperature profiles at each sensor location and further information cannot be extracted to obtain spatial profiles. Consequently, the full picture of the concentration gradients can only be provided by DOE designs. The fit of the DOE models on both the single and dual heating element configurations under static conditions was, overall, superb. In contrast, in the perfused

condition, a lack of fit was observed. This lack of fit was attributed to the perfusion rate of 0.01 ml/min, which equates to 14.4 ml/day corresponding to approximately two-volume change per day. This flow rate is considered a high flow rate for standard bioreactor operation. The high perfusion rate acts to homogenise variations within the culture chamber. Therefore, it is anticipated that perfusion with lower flow rates will have a minimal affect on the fit of DOE models.

Model validation was confirmed by comparing actual measured values of three randomly selected sensor locations to the predicted values as determined by the DOE model. Specifically, the experimental data were within the 95% confidence intervals of the predicted values from the DOE model, thus affirming the validity and predictability of the DOE approach for spatial elucidation. However, since the current DOE design used herein to demonstrate this novel methodology fits only to 2^{nd} order polynomial equations, more complex profiles cannot be revealed; other more sophisticated designs will have to be utilised for highly complex non-linear profiles.

7.6 CONCLUSION

Sensor positioning based on DOE designs produced information-rich data which generated spatial (and temporal) profiles for the temperature variation for the whole culture chamber. This easy to implement and powerful technique can be applied to other geometries and would offer knowledge of the local concentration gradients of important culture parameters allowing for the real-time, local, and 'intelligent' bioprocess control. The application of this approach to the monitoring, analysis, control, and optimisation of stem cell

and tissue bioprocesses for clinical applications can be significant. Information-rich data, which are statistically significant, allow for the future development of "intelligent" bioprocess strategies that can respond in real-time to the needs (locally) of the cell culture. This ability closely mimics the situation *in vivo* and points to a novel modality in bioprocessing where information-rich data can be easily obtained. Coupling of the DOE methodologies for the screening, quantification, and optimisation of culture parameters to the DOE-based monitoring and information analysis presents a powerful, yet easy to implement, experimental tool. Adaptation of this strategy to other geometries, including 3D space, should not present significant problems. Inherently, the limitation is due to sensor sensitivity or parameter fluctuation and not due to the analysis.

CHAPTER 8

Process monitoring of ammonia, pH and oxygen

8.1 INTRODUCTION

Advances in biotechnology and cell culture technology have led to an increasing need for process monitoring and optimal bioprocess control. Achievements in bioprocess engineering over the past two decades, both in terms of monitoring tools and control methods, have delivered both scientific and industrial advantages. From the industries' standpoint, improvements in bioprocess operation equate to an increase in product yield, high cell culture viability, excellent process reproducibility and economical process operation[168-170]. From a scientific point of view, reproducibility of bioprocess conditions, as represented by Locher et al., is also imperative to reliable research as it distinguishes scientific (biological, chemical and physical) phenomena from artefacts in the bioprocess operation[168]. Process monitoring has not only enabled both scientists and engineers to distinguish and understand scientific observations but also obtain quantitative representations such as models

of culture bioprocesses[105]. Progress in the area of process monitoring is essential to control drifts in bioreactor operation, drastic changes in physicochemical parameters such as pH and dissolved oxygen should be avoided as it can significantly impact the growth, production kinetics, and product quality in the bioprocess[171]. So far, these advances have greatly benefited the operation of many biotechnological processes such as fermentation and mammalian cell cultures for the production of biological products such as monoclonal antibodies. In the same manner, stem cell culture bioprocesses require advanced and intelligent process monitoring tools and control systems to ensure the safety, reproducibility and quality of stem cell engineered products.

As described in Chapter 7, online real-time monitoring of cell culture bioprocesses is of utmost significance for delivering cell/tissue engineered products as cellular therapies. Use of *in situ* electrochemical sensors and biosensors allows placement/positioning of sensors locally, which could potentially help to identify local concentrations in the cell culture environment[172]. It has been proposed and demonstrated in Chapter 7 the feasibility of using DOE to determine the minimum number and strategic placement of sensors required to achieve spatial profiling of culture parameters of interest. This chapter will illustrate the overall performance of the real-time online *in situ* monitoring platform in obtaining ammonia, pH, and oxygen concentration profiles in a serum-containing cell culture. In addition, an attempt to obtain spatial maps and temporal profiles of each culture parameter using the DOE approach is demonstrated.

One of the major challenges in utilising *in situ* biosensors is their longevity, performance, and biocompatibility for continuous monitoring in cell cultures. Protein build-up due to the presence of serum in the culture media, around the surfaces of the sensor

membrane interferes with sensor reading and depreciates sensor sensitivity. This causes deviations in sensor performance from when it was originally calibrated, at the beginning of the culture, and decreases the longevity of the sensor. Biofouling of sensor electrodes is an irreversible process; it is therefore necessary to optimise the biocompatibility of sensor membranes to extend the performance and longevity of these sensors in a cell culture environment. Possible solutions include modification of the sensor surface membrane or coating of the surface with an appropriate biocompatible material such as PEG or poly(hydroxylethylmethacrylate) (polyHEMA)[145]. Surface modifications can be achieved by introducing functional groups such as carboxyl, amine and hydroxyl. Other methods for improving sensor biocompatibility include the alteration of existing surfaces by immobilisation of active agents such as anticoagulants or platelet adhesion inhibitors. Ammonia, pH, and oxygen sensors used in this system were coated with a biocompatible material suitable for the specific sensor application. In this chapter, the biocompatibility and performance of each sensor type for culture monitoring is presented.

8.2 AIM AND HYPOTHESIS

The aim of this project is to develop an online real-time *in situ* monitoring platform that is capable of simultaneous multi-analyte process monitoring for stem cell culture bioprocesses. With the aid of this unique system, it is hypothesised that bioprocess information critical for monitoring the process can be achieved in real-time and culture conditions can be adjusted according to the needs to the culture. This mode of operation will ultimately result in an overall better bioprocess operation and better outcome/cell-product.

8.3 APPROACH TO STUDY

Sensors for various analytes such as ammonia, pH, oxygen, glucose and lactate were simultaneously developed. Each sensor type will first be tested individually and using the DOE approach described in Chapter 7, temporal and spatial profiles of each process analyte during a cell culture will be pursued. Sensors will also be tested for biocompatibility against 3T3 fibroblast cells. Operational and functional stability of both the monitoring platform and biosensors designed for each analyte will be concurrently evaluated. Unfortunately, glucose and lactate sensors designed for this project were not stable enough for monitoring in cell cultures and is therefore not reported in this thesis.

8.4 RESULTS

8.4.1 Sensor biocompatibility

Ammonia, pH, and oxygen sensors were all tested for biocompatibility by measuring its toxicity against mouse 3T3 fibroblast cells. Figure 8.1 shows the normalised fold expansion of cells grown in bioreactors containing nine sensors in comparison to the control bioreactor which contained no sensors for three independent experiments. In the first study, it was discovered that the ammonia sensors were toxic to cells as no/very few cells were found in the bioreactor containing nine ammonia sensors for all three experiments after six days in culture (Figure 8.1). After a thorough investigation, two materials were identified that could be leaching from the membrane and be toxic to the cells. The first one is the ionophore called

nonactin which makes up 1-2% of the membrane; the other compound is the plasticiser, DOS, a synthetic organic compound making up 60% of the membrane. There is a greater likelihood that DOS leaching will result in higher toxicity levels in the cell culture due to its higher composition used in the membrane.

Sensors of pH which were coated in a Nafion layer did not show any toxic effects on cells in culture: all three experiments showed excellent cellular growth in cultures containing nine pH sensors as compared to the control culture (Figure 8.1). Biocompatibility of pH sensors is therefore assured. Unfortunately for the oxygen sensors, toxicity results were inconsistent; two out of three experiments showed oxygen sensors were in fact toxic to cells (Figure 8.1). Growth performance of cells in bioreactors containing oxygen sensors were also not as efficient as observed those with the pH sensors. These results were surprising since the design of oxygen sensors was very similar to that of pH sensors with the exception of the material used in oxygen sensor membranes, which was PDMS. However, PDMS is known to be biocompatible and has shown no toxic effects on cells in culture, so there is no reason to suspect that the PDMS membrane is the cause of the problem.

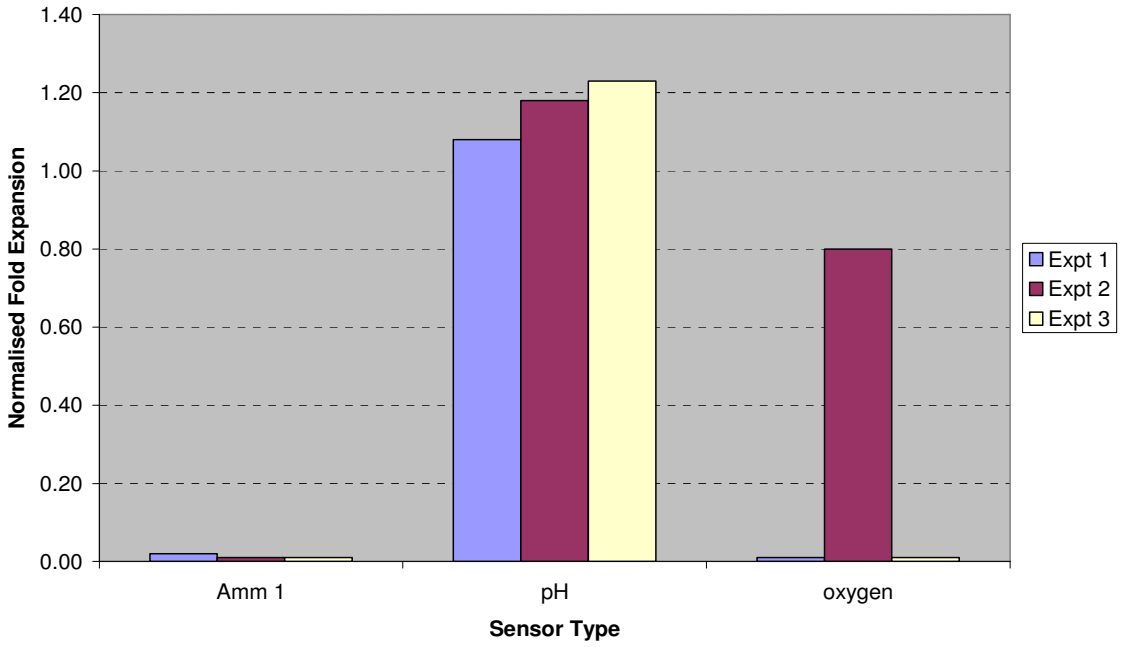

Figure 8.1 Sensor toxicity to cells measured by total cell expansion after six days in culture (n = 3). Values were normalised to the control bioreactor, a cell culture containing no sensors. Biocompatibility of pH sensors is assured while that of oxygen and ammonia sensors requires further improvement due to negative/inconsistent results.

8.4.2 Performance of ammonia sensors in cell culture

Cell culture experiments using ammonia sensors indicated good stability and sensitivity of the sensors over a week's period in serum containing culture. Ammonia concentrations for the static culture showed an increasing trend over the first three days but had no further increase after this period (Figure 8.2a). Increasing ammonia concentrations corresponded to increasing cell density and cellular growth which were observed during the first two days in culture. However, since these sensors were toxic to the cells, as discovered in the toxicity studies, cells also began to die. Subsequently, all further cellular activities including cell death had terminated and the ammonia concentrations from the real-time

monitoring data reached a plateau. Not surprisingly, very few live cells were found at the end of the culture. The lack of biocompatibility of ammonia sensors was affirmed in the toxicity study described in section 8.4.1.

Spatial and temporal profiles of ammonia concentrations inside the bioreactor were attempted via the DOE method. Results that were modelled were taken from the data shown in Figure 8.2a, one sensor (el53) had completely malfunctioned and was eliminated from the DOE analysis. Using the remaining eight data points, data was fitted into a model using the MLR method. Spatial maps of ammonia concentrations through a series of time points in the culture (12hrs, 1 day, 2 days and 4 days) are shown in Figure 8.2b, each has an R^2 value of greater than 0.850 but still showed a lack of fit. The lack of fit to the model is a result of multiple outliers or points with significant variances and missing data-points as reflected in this case. Here, it was also impossible to verify the relevance of the ammonia spatial maps to cellular growth within the bioreactor, since most of the cells had died at the end of the culture.

(A)

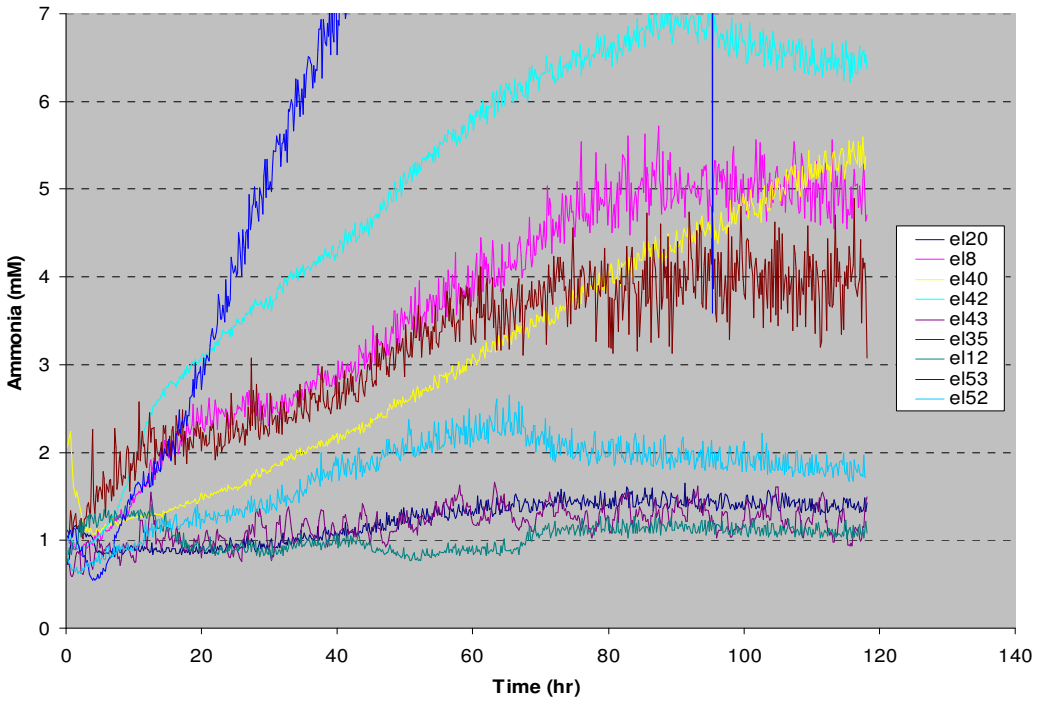

(B)

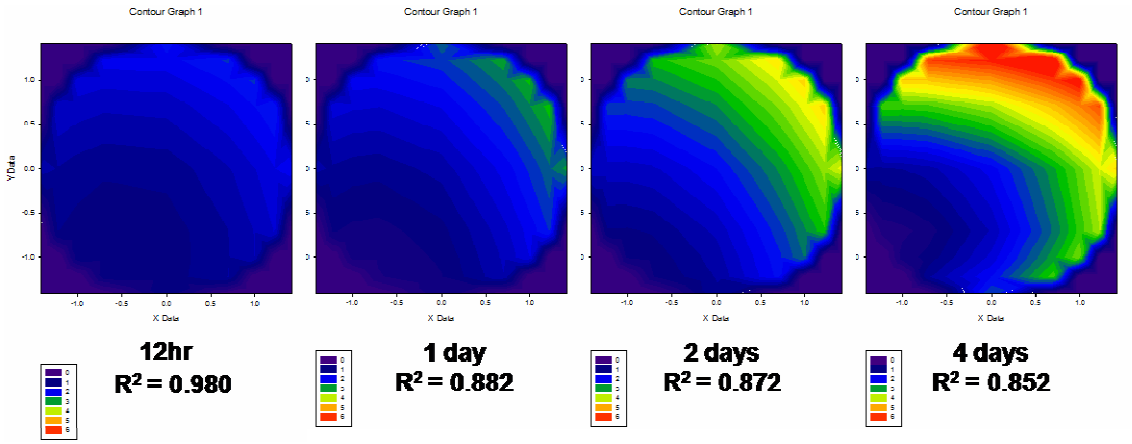

Figure 8.2 Real-time ammonia data and spatial maps for static culture of mouse 3T3 fibroblast cells. (a) Sensors el40 and el53 have malfunctioned. Three sensors (el8, el42 and el35) showed high noise levels toward the end of the culture period. Remaining four sensors showed stable performance throughout the culture period. A 44% success rate in sensor performance was achieved in this experiment. (b) Spatial maps generated in DOE using the MLR method; all models have an R^2 value of greater than 0.850 but showed a lack of fit to the model.

In terms of sensor reliability/failure rate, ammonia sensors were evaluated based on the following criteria: (1) sensors that failed completely and did not give any sensible reading throughout the cell culture (2) noisy sensors which gave a variability of greater than 0.75 mM (3) functional sensors that performed stably throughout the cell culture. From a survey of five independent experiments performed with ammonia sensors, an average success rate of 66% was achieved throughout the cell culture period and a complete failure rate (sensor malfunction not including noisy sensors) of 17% was observed (Figure 8.4). The success rate of functional ammonia sensors is considered rather low with only two thirds of the sensors produced being functional by the time it is assembled in the cell culture bioreactor.

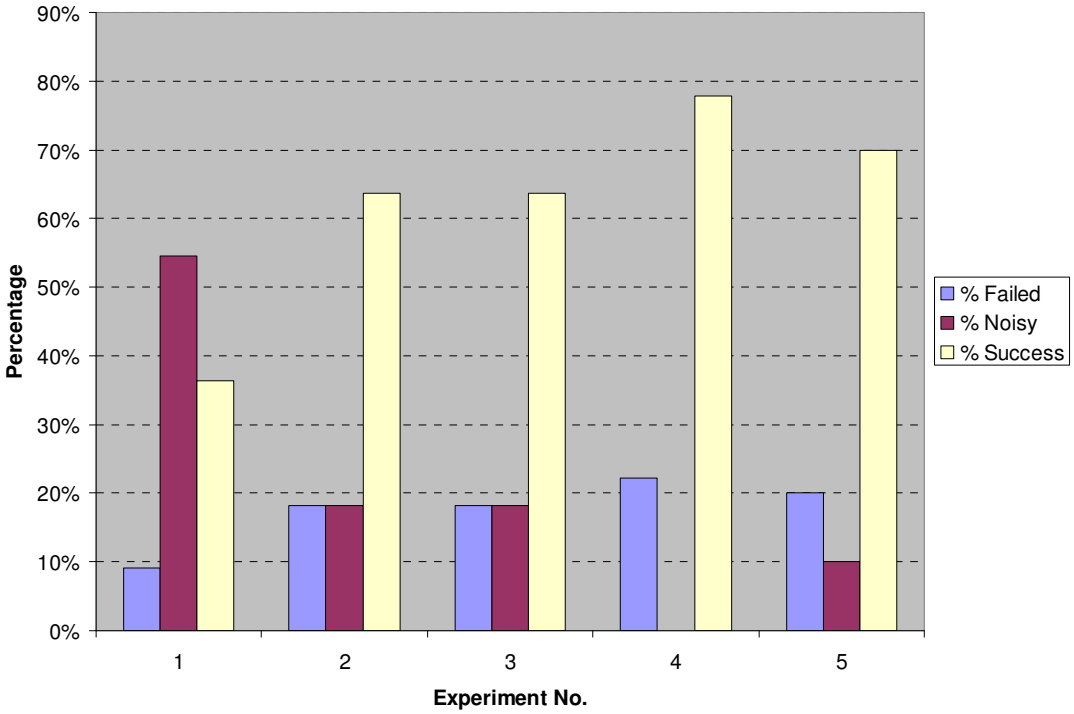

Figure 8.3 Reliability/failure data of ammonia sensors. A 66% success rate was achieved from five independent experiments, 17% of the sensors failed completely while 20% had noisy signals with the first experiment showing the worst performance.

In terms of overall sensor performance, the potentiometric characteristics of the PEG-doped ISEs resembled those of a conventional membrane composition. The typical dynamic response of the PEG-doped electrode to step changes in ammonia concentrations in culture media is provided in Appendix B (Figure B.1). In PBS, the ammonia sensors displayed an almost Nernstian behaviour (52.2 +/- 4.4 mV/electrode) towards ammonium ions but in culture media, it displayed a sub-Nernstian inclination (32.4 +/- 2.2 mV/electrode) due to an increase in background signal caused by the presence of high K^+ and Na^+ species[145]. Ammonia sensors that behaved well showed long-term functional stability and sustained its sensitivity throughout the culture period. In terms of operational stability in cell culture, potentials of the ammonia sensors showed excellent stability, with a 2-3 mV drift over a 24 hr period. The operational stability of ammonia sensors were tested in culture media for up to eight days (Figure B.2) and showed only a slight reduction in sensor sensitivity of up to 4 mV after eight days. From day 0 to day 7, there was only a reduction of 2 mV which occurred in the beginning, after the first day (Figure B.2). A comparison of the calibration curves at the beginning and end of the culture showed that sensors retained 90-95% of their initial sensitivity. Finally, measurements obtained in the data acquisition board designed for this project were comparable to a commercial acquisition system (Figure B.3). No significant differences were observed in sensor readings taken from the two boards.

8.4.3 Instability of pH sensors in cell culture

Cell culture monitoring using pH sensors were unsuccessful as the trends observed in pH behaviour over the culture period did not correspond to that for a typical cell culture. Cell culture pH in a static system generally decreases over time due to the increase in cellular

activities thus increasing waste and metabolite concentrations which acidifies culture media. Independent pH measurements were taken using a pH meter and showed a decrease in the overall pH of the culture media but instead, results from pH sensor readings showed an increasing trend (Figure 8.4a). Sensors deteriorated even further by the end of day 5, with readings rapidly increasing above pH 8.0. These sensors have clearly malfunctioned at this point. Trends in pH variation in the control bioreactors (PBS and media only) also showed an increasing trend, particularly for sensors 12 and 30, sensors placed in culture media (Figure 8.4b). Sensors 4A and 31 showed a much more stable performance in comparison but it still displayed an increasing trend in pH values. No attempt on spatial profiling was made on this set of data since all the pH readings were irrational; spatial maps of pH variation obtained from this dataset would be meaningless.

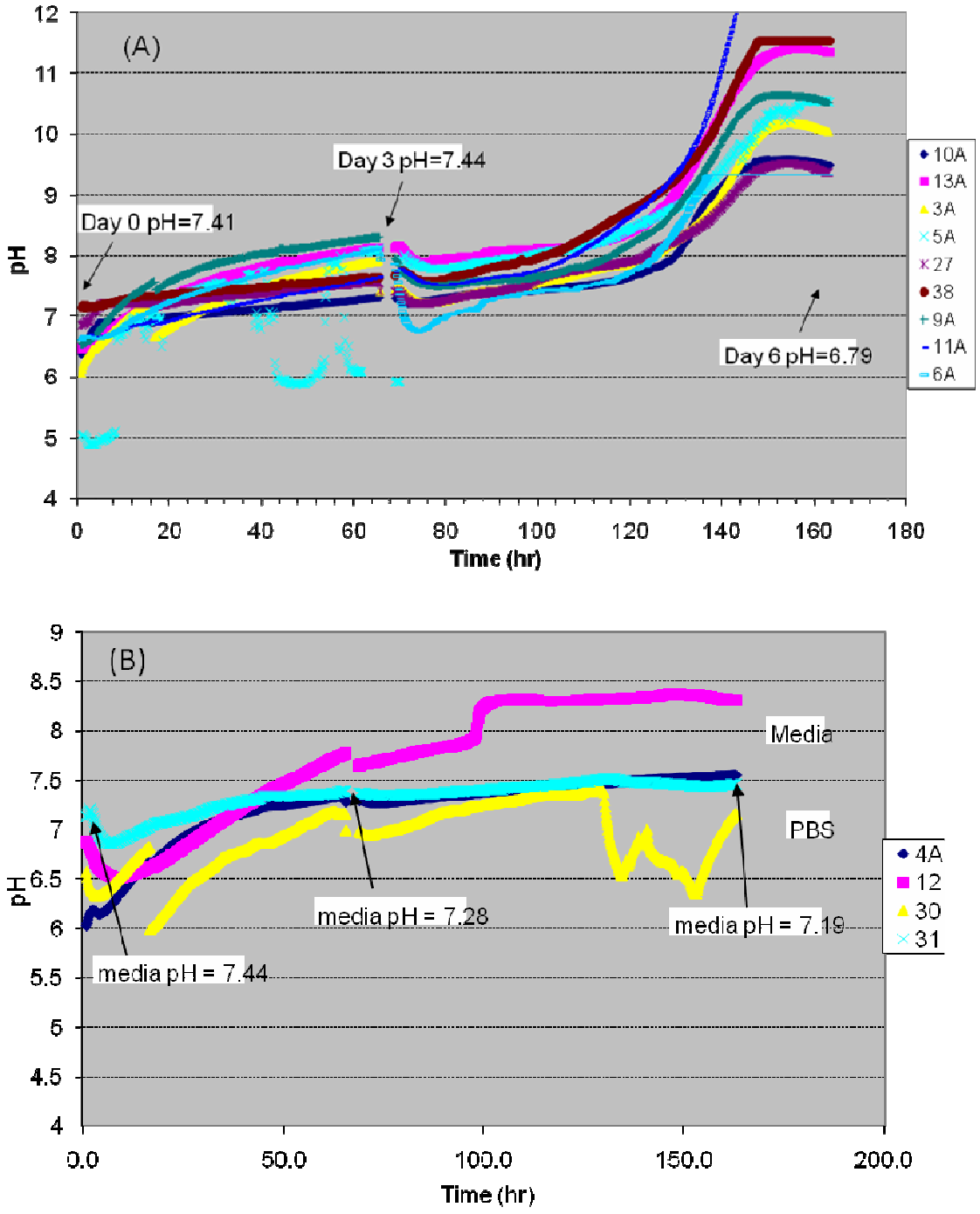

Figure 8.4 Real-time monitoring of pH in static culture for Shh light 3T3 fibroblast cells. (a) Cell culture with nine sensors placed in DOE locations. Trends in pH did not correspond to cell behaviour or observations from culture. (b) Sensors in control bioreactors (4A and 12 were in media while 30 and 31 were in PBS)

One observation made regarding pH sensor performance and stability for long-term cell culture monitoring is the shift in calibration curves of all pH sensors used in the experiment. Upon recalibration after six days in culture, a significant shift in the offset of the sensor calibration curves and a lost in sensor sensitivity was observed (Table 8.1). Sensitivity of pH sensors was reduced to 85.9 +/- 7.2% from its initial values (Table 8.1). This lost in sensitivity is small considering the length of time it has been exposed to a serum-containing culture (six days). However, the shift in the offset value was large and has drastically moved the calibration curve along the y-axis, shifting all the pH readings from when it was originally calibrated. The causes for the shift in the offset are still unclear but they are likely related to instability of the membrane. The shift in the offset is likely to occur over the course of time during the cell culture. However, it was difficult to determine how much this offset has drifted each day during the cell culture so only an estimation of this drift per day can be made. For these reasons, it is very likely that the estimation of the calibration curves used for pH conversion was not very accurate which resulted in inaccurate pH readings throughout the culture study.

Table 8.1 Stability of pH sensors (n = 13). Slopes and offset values of pH calibration curves before and after cell culture. An average lost in sensitivity of 13.3% was observed. Significant shift in the offset values occurred for most all sensors (data provided by Anna Radomska).

Sensor No.	Slope before (mV/decade)	Slope after (mV/decade)	Lost in sensor Sensitivity (%)	Offset value (before)	Offset value (after)
6a	68.83	57.83	16.0	181	8
30	63.17	58.30	7.7	188	85
4a	61.88	41.67	32.7	130	52
3a	58.67	54.67	6.8	206	14
9a	66.67	58.33	12.5	164	34
13a	68.81	55.17	2.0	175	-6
27	54.50	52.83	3.1	46	22
10a	62.34	50.83	18.5	100	-11
31	53.33	52.67	1.2	228	156
12	62.70	54.67	12.8	186	-19
5a	66.67	56.83	14.8	172	34
38	63.81	57.83	9.4	120	9
11a	69.16	57.30	1.7	224	-20

In terms of sensor sensitivity, the calibration curves for three individual pH sensors in media solution are shown in Appendix B (Figure B.4) and an average sensor sensitivity of 61.5 +/- 2.5 mV/pH is achieved in the IrOx electrodes over the range of 3.5 to 9.9 pH values. Readings of pH also did not have issues relating to high noise levels as those encountered with the ammonia sensors; real-time readings were much more stable and less sensitive to external disturbances or interference. Sensor readings from the uniquely designed data acquisition system were almost identical to the readings obtained from a commercial data acquisition system (Table B.1), confirming the compatibility of the data acquisition system to pH sensors and its performance to be equivalent to a commercial system.

8.4.4 Performance of oxygen sensor in cell culture

Oxygen sensors performed well and stably for up to three days in serum-containing cell culture (Figure 8.5). On the third day, sensors were removed and cells, examined under the microscope, looked healthy and increased in cell density. Oxygen sensors were soaked in ultrapure deionised water for about 30 min to remove protein layer that may have adhered onto the surface of the membrane before being placed back into the bioreactor, a media change was also performed during this time. Unfortunately, four out of nine sensor readings subsequent to the third day were extraordinarily high. These values (sensors 12A, 14A, 6A and 9A) were irrational as they indicated readings of greater than the 21% oxygen saturation. Overall, sensor readings were much more stable during the first three days as compared to the last three days (Figure 8.5). However, it is unclear as to why some of the sensors have subsequently malfunctioned as the recalibration performed at the end of the experiment did not indicate these behaviours. All sensor readings from the last three days were generally higher than readings taken from the first three days.

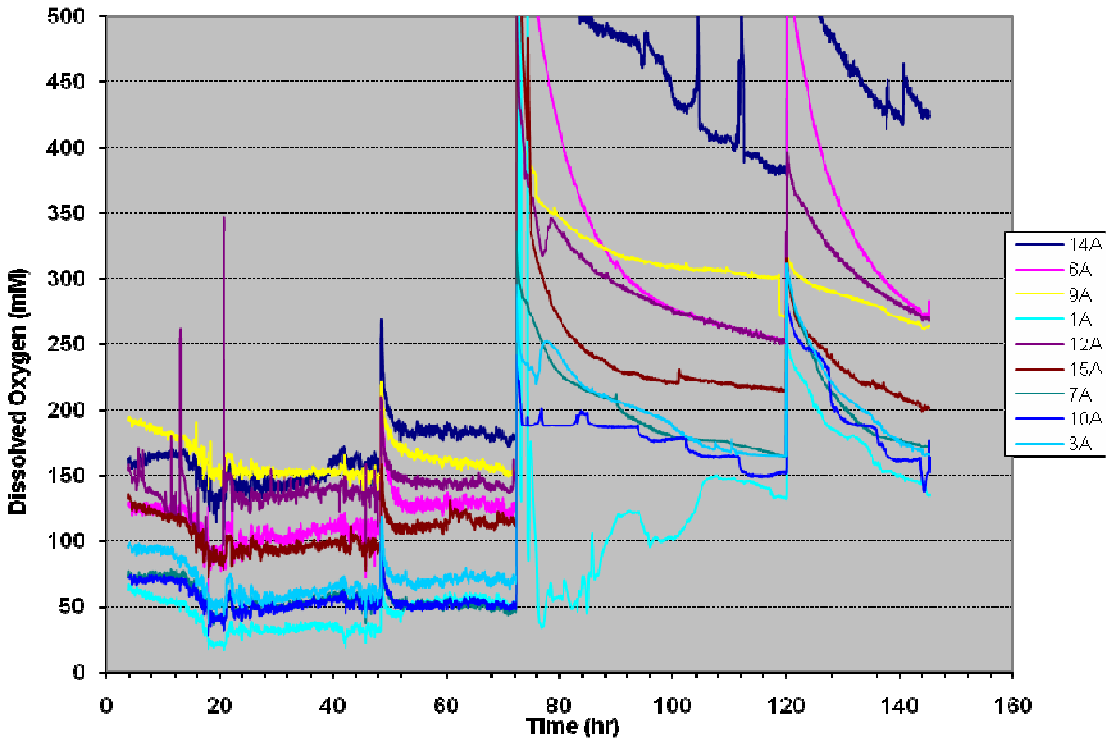

Figure 8.5 Oxygen real-time data for Shh-light fibroblast static culture. Oxygen readings were stable and within operating range during the first three days only, subsequent to that, sensor readings were mostly out of range and appeared to be less stable than its performance during the first three days.

Recalibration performed at the end of the culture showed only an average loss of 9.3% in the sensitivity of sensor performance. Spatial maps for oxygen were created using DOE; the goodness of fit to the models were low (< 0.750) and showed a significant lack of fit suggesting that the models were not appropriate (Figure 8.6). A closer look at the individual data points showed one significant outlier within the data skewing the spatial maps toward a low oxygen regime in that particular area; this resulted in a slight mismatch in the spatial maps of oxygen to the cell map (where cells are located within the bioreactor – see Figure 4.7 for cell seeding map). The cause of the unexpectedly low oxygen reading from

this particular sensor is still unknown and it is unclear if it has been a contribution of physiological conditions or a malfunction in sensor or an interference causing an inaccurate reading. Areas where cells were located are expected to have lower oxygen concentrations, which in this case have been consistent for the four sensors locations at the "pie area" where cells were located (Figure 4.7). As a consequence of the contribution of both outliers, the overall spatial profile in oxygen concentration obtained from this study did not correspond to the cellular spatial map, where cells were confined to a specific area in the bioreactor.

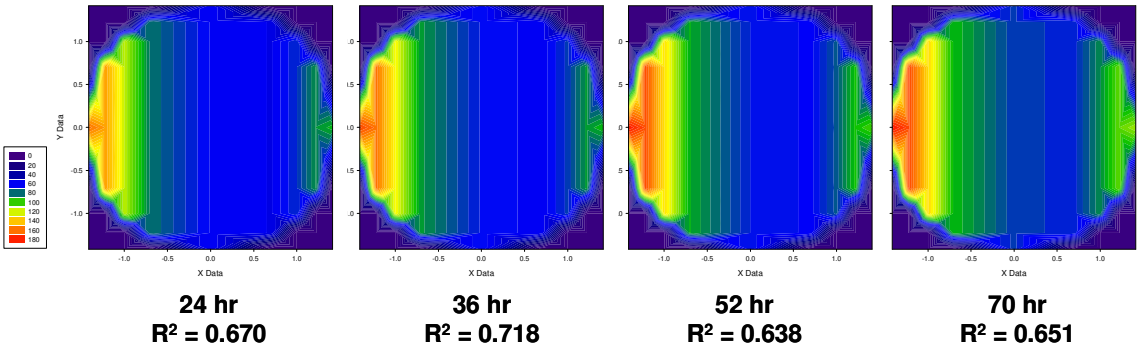

Figure 8.6 Spatial maps for oxygen. Goodness of fit was poor and also showed a lack of fit. A significant outlier was identified which may also have skewed the profiles, causing a mismatch with the cell map shown in Figure 8.7.

Sensor calibration for oxygen was performed at two concentrations, 0 μM and 278 μM which were equivalent to 0% and 21% oxygen saturation at room temperature respectively. The calibration curves for three independent sensors are displayed in Figure B.5 in Appendix B. The recalibration data showing the loss in sensitivity of oxygen sensors after six days in culture is provided in Table B.2. The average lost in sensor sensitivity is 11.0% with a maximum at 35.5% after six days. The comparison of sensor readings between the two

boards (our system versus a commercial system) is shown in Table B.3. Readings taken from the two systems showed insignificant differences: readings were less than 5.0% mean difference. This data confirms the performance of oxygen sensors with our uniquely designed data acquisition system to be comparable to the performance in a commercial system.

8.4.5 Operational stability of data acquisition system

The data acquisition system and GUI uniquely designed for simultaneous monitoring of multiple process analytes have been tested with ammonia, pH, and oxygen sensors in this study. When compared to a commercial system, the data acquisition system provided readings that were very close to those obtained from the commercial system for all three sensors (Appendix B). In terms of continuous process monitoring, initially, the system was tested for up to seven days for cell culture monitoring using a USB interface. Sporadically, there were problems with the USB interface communication which halted all data collection in the middle of a run. The alternate interface built into this system was the PCI bus and is currently switched into this connection. Since moving to the PCI connection, it had no further issues with data collection or interface communication. The system was able to collect, manage and store all real-time data from multiple process analytes efficiently and continuously for up to seven days of a process operation. This system was also tested independently for up to two months of continuous monitoring in the bioengineering laboratory performed by a colleague (X. Yue) in the project. Though the PCI is a much more stable and reliable communication interface, the hardware components were bulky and can be of slight inconvenience. The USB interface is therefore preferred due to its small and slick design, and convenience in use. A new USB card is currently being tested to replace the

existing/problematic card as it is more likely that the lost in USB communication was due to a hardware failure than a system failure. The new USB card will be installed into the system for future testing.

8.5 DISCUSSION

Bioprocess monitoring and control are essential components in ensuring the product quality, reproducibility, and productivity of a bioprocess of interest. The proposed online real-time *in situ* monitoring platform capable of simultaneous monitoring of multiple process analytes can bring significant contributions in cell culture bioprocessing practises. So far, the system has been tested with ammonia, pH and oxygen sensors. Functional and operational stability of the monitoring platform is assured; the main hurdles are faced with sensor performances with each respective sensor. Initial design and testing of each sensor performed in BSA solution showed excellent sensor performance i.e. sensitivity and stability over long periods. However, when tested in cell culture, several problems arose. In the following sections, a discussion regarding the sensor performances is presented.

8.5.1 Requirements for *in situ* sensors

Use of *in situ* sensors is intended to capture any process variation within a cell culture bioreactor. However, there are several challenges in the use of *in situ* sensors for long-term cell culture process monitoring. The four main challenges that need to be addressed in the design of *in situ* biosensors include (a) biocompatibility of the sensors i.e. sensors must not

be toxic to cells and sterilisable, (b) sensor stability and sensitivity in cell culture environment, and (c) longevity of sensors for long-term monitoring of cell cultures. Longevity of *in situ* sensors in continuous cell culture process monitoring is still rather limited. A recent study done by Rodrigues et al. showed the performance of glucose and oxygen amperometric sensors in a continuous culture for up to 2.5 hr[99]. The glucose and oxygen microsensors were integrated in a PDMS cell culture chamber and positioned at the inlet and outlet of the chamber for continuous real-time process monitoring of HepG2 cells in culture. Sensors that were designed for this application showed good response sensitivity and stability in cell culture media but were only able to show their performance for up to 2.5 hr[99]. Longevity of electrochemical and biosensors in a cell culture environment is still one of the major obstacles that needs to be overcome particularly for glucose sensors which are known to have a short lifetime in cell culture. In the following sections, the overall performance of the ammonia, pH, and oxygen sensors in relation to the sensor requirements as stated above and recommendations for further development and improvements will be discussed. Table 8.2 provides a summary of the current status and achievements made for each sensor.

Table 8.2 Achievements and current status of ammonia, pH, and oxygen sensors. Requirements not achieved are highlighted in red.

Sensor	***Biocompatible***	***Sensitivity in BSA***	***Sensitivity in media***	***Stability in culture***	***Longevity in culture***
Ammonia	No	Nernstian	Sub-nernstian	Some noisy sensors	7 days
pH	Yes	Nernstian	Nernstian	No	No
Oxygen	Not clear	Good	Good	Yes	3 days

8.5.1.1 Sensor membrane composition

Biocompatibility of sensor membranes is crucial to ensure its application in long-term monitoring of cell culture bioprocesses. Membrane layers that have been selected for the design of various sensors included PEG for the ammonia sensors, Nafion for the pH sensors, and PDMS for the oxygen sensors.

PEG is a hydrophilic polymer and is commonly used as it can prevent the adsorption of protein on the membrane layer. PEG layer for the ammonia sensors have been doped with DOS in order to provide membrane stability. Unfortunately, the high concentration of DOS used in the membrane layer (60%) appears to be toxic to the cells, causing cell death in long-term static cultures. Concentrations of DOS in the PEG layer could potentially be reduced; however this may affect the performance (sensor stability) for long-term cell culture monitoring. Studies to improve ammonia membrane composition in the effort to reduce the use of toxic components while maintaining stability of the membrane are currently being carried out.

Nafion is a sulfonated tetrafluorethylene copolymer which is commonly used in the production of sensors due to its favourable physical properties such as its conduciveness to cations, resistivity to chemical attacks, and excellent biocompatibility – showing stability in both *in vitro* and *in vivo* applications[173,174]. Many electrochemical and biosensors using Nafion layers showed good biocompatibility. Similarly, in this study, there were no biocompatibility issues with the pH sensors which were coated in Nafion layer.

Finally, PDMS is a widely used silicon-based organic polymer known to be chemically inert, non-toxic and biocompatible. Due to its good mechanical, optical and biological properties, PDMS membranes and materials have been widely used as a bio-

interface for many different types of biosensing devices and for various cell culture applications[175,176]. The oxygen sensors which were coated in PDMS layers surprisingly showed inconsistent results from the biocompatibility and toxicity studies. It is still unclear why oxygen sensors coated in PDMS would be toxic to cells; however results obtained for oxygen toxicity study were inconsistent. The protocol for making oxygen sensors is currently being re-evaluated to determine the cause of the problem.

8.5.1.2 Ammonia sensors

Although sensor stability and longevity of ammonia sensors were assured for up to seven days in cell culture, the main problem lies in its toxicity to cells. Leakage from membrane components into the cell culture is undesirable and the minimisation of toxic leakage is necessary. In a previous experiment performed by another colleague using only two ammonia sensors in a perfused cell culture system, no toxicity effects were observed; cellular growth was achieved with good cell viability at the end of a seven-day culture. However, in this study where nine sensors were placed in a static cell culture with only a media change performed on the third day of the culture, the accumulation of toxic leakage from nine sensors (instead of two in the perfused system) and the lack of continuous media displacement showed that leakage from ammonia sensor membranes can eventually become a problem. It is therefore necessary to improve membrane biocompatibility of ammonia sensors to ensure its performance in any cell culture environment.

The second problem faced with the ammonia sensors is the lack of functional reliability resulting in high failure rate and high noise levels observed in sensor readings. Currently, two thirds of the sensors being produced achieved functional and operational

stability after being assembled in the culture bioreactor. The poor performance in sensor reliability is due to the fragility of sensor packaging itself and the lack of consistency in the manufacturing procedure. An improvement in the assembly of sensor components is currently being looked into and a more careful approach to the making and handling of ammonia sensors will be taken for future studies.

8.5.1.3 pH sensors

The main problem associated with the pH sensors is the shift in the calibration curve mainly relating to the offset value. The cause for this shift in the offset is currently still unknown but a possible explanation that has been suggested is the formation of chloride complexes from iridium (III) to (IV) which led to the loss of the oxide film; causing irreversible changes in the offset calibration values. Coating of sensors using Nafion did not appear to prevent destabilisation of the sensors in the presence of chloride ions. It appears that some modification in the membrane layer/coating has to be made to improve its stability and prevent the formation of soluble complexes. Sensor stability in cell culture environment affects overall longevity of the sensors. If the stability of pH sensors cannot be achieved for up to six days, shorter time lengths can be used which will simply result in more frequent sensor replacement. Other *in situ* pH sensors such as those designed by Krommenhoek et al. were tested for up to 10 hr in fermentation batch culture and the long-term drift rate was determined to be at 1.2 mV/hr[177]. The sensitivity of their sensors was -58 mV/pH unit while the sensitivity of pH sensors designed for this study was around -61.5 mV/pH unit, both are close to the ideal Nernstian behaviour.

8.5.1.4 Oxygen sensors

Of all the three sensors, oxygen sensors showed the most promising results by achieving functional stability for up to three full days in continuous cell culture and obtaining spatial maps that somewhat corresponded to where cells were positioned. The achievement of functional stability for up to three days is of great significance as current *in situ* oxygen sensors have only been tested for up to 15 hr in a continuous fermentation culture by Krommenhoek et al.[177] and up to 2.5 hr in cell culture media by Rodriguez et al[99,177] . The electrochemical sensor from Krommenhoek et al. achieved a sensitivity of 0.96 nA/mg O_2/L[177] while the oxygen sensors designed in this study achieved a sensitivity of 0.17 nA/μM O_2, which is equivalent to 5.35 nA/mg O_2/L. Higher sensor sensitivity is achieved in this study. Unfortunately, biocompatibility of the oxygen sensors remains questionable as the results showed inconsistent findings. Membrane packaging of oxygen sensors are currently being improved and biocompatibility tests will be repeated before further experiments are pursued.

8.5.2 Analyte spatial profiling using DOE

Limitations in obtaining the spatial profiles for each process analyte of interest currently lie in the lack of sensitivity and functional stability of the sensors and not by limitations of the DOE method. Weaknesses in the performance of the sensors are reflected by variability in the readings of the sensors and in some cases, the lack of functional stability over the course of time. Significant noise levels due to the lack of sensor stability or environmental interferences does not provide a good basis for obtaining models in the spatial profiles with good fits. The DOE software, such as the one used in these experiments

(MODDE7 from Umetrics), can however accommodate the presence of "bad" process data or missing values in the DOE matrix. In the default setting, when all process responses are available, the MLR method is used to obtain a model fit. When a missing data is present, the partial least squares (PLS) method is used instead. In the PLS mode, up to two "bad" process data can be accommodated and still achieve a reasonable fit to the process model. However, if the process data for most points in the DOE are scattered randomly, this will be reflected in a poor fit or lack of fit in the model. Based on the results currently observed from the ammonia and oxygen sensors, the overall functional stability of each sensor type needs to be improved as significant process variability in the data points were observed thus generating models with poor fit or even a lack of fit in some cases.

8.6 CONCLUSION

The successful integration and functional operation of ammonia, pH, and oxygen sensors with the uniquely designed multi-channel, multi-analyte data acquisition system was achieved in this study. Operational stability of the hardware and software components for the online real-time monitoring platform has been established for continuous cell culture monitoring for up to seven days. Oxygen sensors were also stable for up to three days in continuous cell culture. Real-time process information obtained for ammonia and oxygen generated spatial and temporal maps that have not yet been performed elsewhere. These information-rich DOE models can elucidate spatial variations that exist within a bioreactor and will allow us to improve process homogeneity. Currently, the elucidation of process variations using the DOE method is impaired by sensor sensitivity and stability which

resulted in poor model fits. Even though there are still several problems associated with each sensor type, the achievements made in this study has brought us yet another step closer to the realisation of an intelligent online real-time monitoring system capable of simultaneous process monitoring and ultimately process control for stem cell culture bioprocesses. The success of this intelligent system will help to overcome many of the bioprocess limitations currently faced in stem cell cultures, and accelerate the translation and scale-up of stem cell cultures from a research environment to a manufacturing production.

CHAPTER 9

Overall Conclusions and Future Work

9.1 OVERALL CONCLUSIONS

The main goal in this thesis is to develop statistical design strategies and an online real-time *in situ* monitoring system for the characterisation, optimisation, and control of haematopoietic stem cell culture bioprocesses. Overall conclusions as a result of the efforts toward this goal are summarised in the following sections.

9.1.1 Single-step process characterisation

In this study, successful expansion and accelerated differentiation of cord blood stem cells toward the erythroid lineage was achieved via a simple DOE experimental strategy. The investigation not only demonstrated the efficiency and effectiveness in using DOE for the

characterisation and optimisation of complex cell culture bioprocesses such as those in HSCs, but also produced quantitative models that can be used to describe the process of interest. Optimisation based on the DOE models provided optimal process conditions which produced results far more superior to comparable studies achieved without using the DOE method. However, the optimisation of this process as a single-step cytokine culture is end-point driven and does not reveal *in vitro* process dynamics.

9.1.2 Multi-step process characterisation

Sequential characterisation in order to reveal *in vitro* process dynamics was much more challenging than defining a single-step cytokine culture using DOE. Challenges in sequential characterisation include definition of culture phases, process objectives, concentration ranges, and selection of DOE designs. In this study, three independent process models were successfully generated using the proposed DOE approach. These models reflect differences in process requirements and provide some insights into the process dynamics. A slight improvement in growth performance was also achieved in the three-step cytokine culture versus the single-step without any compromise in erythroid maturation. However, optimisation of the three-step culture required significantly more time and effort than the single-step culture. Benefits in using the multi-step approach must be weighed against the single-step according to process goals. The conclusion from this study still presents the multi-step DOE approach as a powerful tool for revealing process intricacies and is important for achieving a better understanding of *in vitro* cell culture bioprocesses.

9.1.3 Spatial profiling

As a statistical method, DOE was successfully applied to the sampling of analytes in a process area of interest and generated information-rich data by way of spatial and temporal profiles for the parameter of interest, in this case, temperature. Sampling using DOE also provided a way to minimise the use of sensors while still maximising the amount of information extracted from process data. The success in this approach allowed knowledge of local concentration gradients that will ultimately lead to real-time, local and "intelligent" bioprocess control. In an ideal system, such bioprocess operation and control is one that will resemble processes occurring in our body (*in vivo*).

9.1.4 Cell culture process monitoring

In this study, successful integration and functional operation of a uniquely designed online real-time *in situ* monitoring platform was achieved for the monitoring of pH, oxygen and ammonia. Compatibility of each sensor type with the data acquisition system was demonstrated and readings obtained from this system were comparable to those obtained from a commercial system. Oxygen sensors achieved sensor longevity of up to three days in continuous culture and only require slight modifications to improve the biocompatibility of the sensors. Ammonia sensors also appeared to be stable for up to seven days in culture but have severe toxicity on cells and may require significant modifications. The pH sensors were most biocompatible but lost significant sensitivity in cell culture. Although results from sensor performances were somewhat disappointing, this study is a key step toward stem cell culture bioprocessing efforts that brings us closer to the realisation of a real-time monitoring system that is economical, convenient, and practical for stem cell culture bioprocesses.

9.2 FUTURE WORK

Experimental studies performed for DOE characterisation and optimisation of HSC cultures have demonstrated the efficiency and effectiveness of DOE methods in studying complex culture bioprocesses. As a single-step, process optimisation using DOE was straight-forward, but as a multi-step that is kinetics-driven challenges in process optimisation arose. Utilisation of DOE for spatial elucidation of process analytes showed promising applications for cell culture process monitoring. The successful integration and operational performance of the unique online real-time monitoring platform designed for stem cell culture bioprocesses has also been demonstrated. However, functional stability of sensors in cell culture was not established and the generation of spatial profiles from sensor process data was difficult. The following sections will discuss possible research directions toward achieving better DOE characterisation strategies for revealing process dynamics and future developments needed in the real-time monitoring platform for stem cell culture bioprocesses.

9.2.1 DOE strategies for revealing process dynamics

Sequential characterisation of cell culture bioprocesses can be improved by performing factor screening at each stage of the culture to identify main influences on the process of interest. This screening step is necessary as the effects of certain factors, as supported in Chapter 6 and in other studies, may be transitional. A resolution IV fractional factorial design is still recommended as it is very useful in identifying individual effects independently. Subsequent to the screening process, factors influencing the culture can be characterised using the CCD design. Process screening and characterisation should be

performed sequentially as demonstrated in the new workflow proposed in Figure 6.10. Process ranges selected for each factor in this case can begin at low concentrations since the screening step pre-determines the significance of each factor. For the later stages of the process, optimisation using the path of steepest ascent can be taken to optimise process conditions that are required for this stage of the process.

Definition of culture phases is one of the key considerations in the multi-step process optimisation. In reality, it is almost impossible to determine the ideal/optimal number of phases required for each cell culture process of interest as this "number" may vary from process to process or even sample to sample. As a starting point, definition of culture phases based on growth kinetics is a good consideration. A comparison to the *in vitro* process and an attempt to mimic that may also be worthwhile considerations. Ultimately, the decision to determine the number of phases in a culture will also be dependent on the feasibility and practicality of the approach since more phases will mean more characterisation experiments, labour, and expenses required.

The process objective for each phase of the culture is an important consideration. In this study, the objectives in each phase were identical which may not have been the ideal approach but it also depends on the overall goal of the experiment. However, it is important to realise that the objective in each phase may significantly affect the results in subsequent phases. A careful consideration of the objective must therefore be taken. Definition of the process objective in each phase also allows flexibility in the control of the cell culture outcome.

9.2.2 Future developments for the monitoring platform

Functional stability and sensor sensitivity for each type of sensors (ammonia, pH and oxygen) must be improved in order to achieve more stable and reliable process readings during a continuous cell culture. This will significantly improve models of the spatial maps obtained via the DOE method and provide a better account of local concentration gradients. In addition, biocompatibility of ammonia and oxygen sensors has to be assured, and any modification made to membrane composition should not compromise sensor sensitivity. Multiple analyte process monitoring using all three sensors simultaneously will then be tested for this system to demonstrate operational functionality of the system for multi-analyte monitoring. The development of glucose and lactate sensors is also being pursued to deliver monitoring of nutrients and metabolites in a cell culture.

Future sensor developments that will provide significant advantages in process applications should include miniaturisation and the design of multiple analytes bounded into a single sensor unit. Miniaturisation of the sensor unit will allow more precise readings obtained at the specific sensor locations and minimise the invasiveness of each probe unit. Bundling of sensor units will also minimise invasiveness and provide greater convenience in the use of multiple sensors.

Wireless communication for the data acquisition system is highly desirable as it will minimise the use of connectors and wires running through the incubators. The ability to achieve wireless communication in sensor readings will greatly enhance the uniqueness and convenience in the use of this online real-time monitoring system. A control algorithm that is suitable for stem cell culture bioprocesses must also be designed and tested to achieve optimal bioprocessing practises.

References

1. Pallister CJ. Haematology. London: Replika Press Pvt. Ltd.; 2005.

2. Breems DA, Lowenberg B. Acute myeloid leukemia and the position of autologous stem cell transplantation. Seminars in Hematology. 2007;44:259-266.

3. Pant S, Copelan EA. Hematopoietic stem cell transplantation in multiple myeloma. Biology of Blood and Marrow Transplantation. 2007;13:877-885.

4. Noel G, Bruniquel D, Birebent B, et al. Patients suffering from acute graft-versus-host disease after bone-marrow transplantation have functional $CD4^{+}CD25^{hi}Foxp3^{+}$ regulatory T cells. Clinical Immunology. 2008;129:241-248.

5. Toubai T, Sun Y, Reddy P. GVHD pathophysiology: is acute different from chronic? Best Practice & Research Clinical Haematology. 2008;21:101-117.

6. Bradley MB, Cairo MS. Cord blood immunology and stem cell transplantation. Human Immunology. 2005;66:431-446.

7. McNiece I, Briddell R. *Ex vivo* expansion of hematopoietic progenitor cells and mature cells. Experimental Hematology. 2001;29.

8. McNiece I, Jones R, Bearman SI, et al. *Ex vivo* expanded peripheral blood progenitors cells provide rapid neutrophil recovery after high-dose chemotherapy in patients with breast cancer. Blood. 2000;96:3001-3007.

9. Mason C, Hoare M. Regenerative medicine bioprocessing: Building a conceptual framework based on early studies. Tissue Engineering. 2007;13:301-311.

10. Edwards P, Enver T, Hughes S, et al. Histology: The lives and deaths of cells in tissues. In: Alberts B, Johnson A, Lewis J, Raff M, Roberts K, Walter P, eds. Molecular biology of the cell (ed 4th). New York: Garland Publishing; 2002.

11. Abboud CN, Lichtman MA. Structure of the marrow and the hematopoietic microenvironment. In: Beutler E, Lichtman MA, Coller BS, Kipps TJ, Seligsohn U, eds. Williams Hematology (ed 6th): McGraw-Hill; 2001.

12. Quesenberry PJ, Colvin G. Hematopoietic stem cells, progenitor cells and cytokines. In: Beutler E, Lichtman MA, Coller BS, Kipps TJ, Seligsohn U, eds. Williams Hematology (ed 6th): McGraw-Hill; 2001.

13. Ryan DH. Examination of the blood. In: Beutler E, Lichtman MA, Coller BS, Kipps TJ, Seligsohn U, eds. Williams Hematology (ed 6th): McGraw-Hill; 2001.

14. Kaufman RM, Anderson KC. Hematologic complications and blood bank support. In: Kufe DW, Pollock RE, Weichselbaum RR, et al., eds. Cancer Medicine. Hamilton, Canada: BC Decker Inc.; 2003.

15. Kurzrock R. Hematopoietic growth factors. In: Kufe DW, Pollock RE, Weichselbaum RR, et al., eds. Cancer medicine. Hamilton: BC Decker, Inc.; 2003.

16. Ishikawa F, Livingston AG, Minamiguchi H, Wingard JR, Ogawa M. Human cord blood long-term engrafting cells are $CD34^{+}$ $CD38^{-}$. Leukemia. 2003;17:960-964.

17. Bhatia M, Wang JCY, Kapp U, Bonnet D, Dick JE. Purification of primitive human hematopoietic cells capable of repopulating immune-deficient mice. Proceedings of the National Academy of Sciences USA. 1997;94.

18. Wang J, Kimura T, Asada R, et al. SCID-repopulating cell activity of human cord blood-derived $CD34^{-}$ cells assured by intra-bone marrow injection. Blood. 2003;101:2924-2931.

19. Kiyoyuki O, Chikako S, Mikiki T, et al. Identification and hematopoietic potential of CD45- clonal cells with very immature phenotype (CD45-CD34-CD38-Lin-) in patients with myelodysplastic syndromes. Stem Cells. 2005;23:619-630.

20. CorCell. 2005. Diseases treated with current stem cell applications [Online]. Available: http://www.corcell.com/expectant/diseases_treated.html [13 June 2005]

21. Barker JN, Wagner JE. Umbilical cord blood transplantation: current practice and future innovations. Critical Reviews in Oncology/Hematology. 2003;48:35-43.

22. Arcese W, Picardi A, Cerretti R, et al. The therapeutic use of cord blood. Cell Preservation Technology. 2006;4:161-168.

23. Cohen Y, Nagler A. Umbilical cord blood transplantation - how, when and for whom? Blood Reviews. 2004;18:167-179.

24. Watt SM, Contreras M. Stem cell medicine: Umbilical cord blood and its stem cell potential. Seminars in Fetal & Neonatal Medicine. 2005;10:209-220.

25. Cord blood stem cell transplantation [Online]. Available: http://www.leukemia-lymphoma.org/ [18 July 2008]

26. The history of cord blood banking [Online]. Available: http://www.cordbloodawareness.org/history_cord_blood_banking.htm [23 Sept 2008]

27. Ende N, Lu S, Alcid MG, Chen R, Mack R. Pooled umbilical cord blood as a possible universal donor for marrow reconstitution and use in nuclear accidents. Life Sciences. 2001;69:1531-1539.

28. Conrad PD, Emerson SG. *Ex vivo* expansion of hematopoietic cells from umbilical cord blood for clinical transplantation. Journal of Leukocyte Biology. 1998;64:147-155.

29. Douay L, Andreu G. *Ex vivo* production of human red blood cells from hematopoietic stem cells: what is the future in transfusion? Transfusion Medicine Reviews. 2007;21:91-100.

30. Gilmore GL, DePasquale DK, Lister J, Shadduck RK. *Ex vivo* expansion of human umbilical cord blood and peripheral blood $CD34^+$ hematopoietic stem cells. Experimental Hematology. 2000;28:1297-1305.

31. Collins PC, Papoutsakis TE, Miller WM. *Ex vivo* culture systems for hematopoietic cells. Current Opinion in Biotechnology. 1996;7:223-230.

32. Heike T, Nakahata T. *Ex vivo* expansion of hematopoietic stem cells by cytokines. Biochimica et Biophysica Acta. 2002;1592:313-321.

33. Kobari L, Pflumio F, Giarratana M-C, et al. *In vitro* and *in vivo* evidence for the long-term multi-lineage (myeloid, B, NK and T) reconstitution capacity of *ex vivo* expansion human $CD34^+$ cord blood cells. Experimental Hematology. 2000;28:1470-1480.

34. Paquette RL, Dergham ST, Karpf E, et al. Culture conditions affect the ability of *ex vivo* expanded peripheral blood progenitor cells to accelerate hematopoietic recovery. Experimental Hematology. 2002;30:374-380.

35. Cortin V, Garnier A, Pineault N, Lemieux R, Boyer L, Proulx C. Efficient *in vitro* megakaryocyte maturation using cytokine cocktails optimized by statistical experimental design. Experimental Hematology. 2005;33:1182-1191.

36. Pick M, Eldor A, Grisaru D, Zander AR, Shenhav M, Deutsch VR. *Ex vivo* expansion of megakaryocyte progenitors from cryopreserved umbilical cord blood: A potential source of megakaryocytes for transplantation. Experimental Hematology. 2002;30:1079-1087.

37. Frias AM, Porada CD, Crapnell KB, Cabral JMS, Zanjani ED, Almeida-Porada G. Generation of functional natural killer and dendritic cells in a human stromal-based sreum-free culture system designed for cord blood epxnasion. Experimental Hematology. 2008;36:61-68.

38. Smits K, De Smedt M, Naessens E, et al. Tumor necrosis factor promotes T-cell at the expense of B-cell lymphoid development from cultured human $CD34^+$ cord blood cells. Experimental Hematology. 2007;35:1272-1278.

39. Shimakura Y, Kawada H, Ando K, et al. Murine stromal cell line HESS-5 maintains reconstituting ability of *ex vivo*-generated hematopoietic stem cells from human bone marrow and cytokine-mobilized peripheral blood. Stem Cells. 2000;18:183-189.

40. Goncalves R, Lobato da Silva C, Ferreira BS, et al. Kinetic analysis of the *ex vivo* expansion of human hematopoietic stem/progenitor cells. Biotechnology Letters. 2006;28:335-340.

41. Liu Y, Liu T, Fan X, Ma X, Cui Z. *Ex vivo* expansion of hematopoietic stem cells derived from umbilical cord blood in rotating wall vessel. Journal of Biotechnology. 2006;124:592-601.

42. Plett PA, Frankovitz S, Jetmore A, Abonour R, Orschell-Traycoff CM. Proliferation and functional characterization of human $CD34^+$ bone marrow cells cultured in simulated microgravity. Experimental Hematology. 2000;28:98.

43. Cabrita GJM, Ferreira BS, da Silva CL, Goncalves R, Almeida-Porada G, Cabral JMS. Hematopoietic stem cells: from the bone to the bioreactor. Trends in Biotechnology. 2003;21:233-240.

44. Feng Q, Chai C, Jiang X-S, Leong KW, Mao H-Q. Expansion of engrafting human hematopoietic stem/progenitor cells in three-dimensional scaffolds with surface-immobilized fibronectin. Journal of Biomedical Materials Research Part A. 2006;78A:781-791.

45. Ma K, Chan CK, Liao S, Hwang WYK, Feng Q, Ramakrishna S. Electrospun nanofiber scaffolds for rapid and rich capture of bone marrow-derived hematopoietic stem cells. Biomaterials. 2008;29:2096-2103.

46. Chua K-N, Chai C, Lee P-C, Ramakrishna S, Leong KW, Mao H-Q. Functional nanofiber scaffolds with different spacers modulate adhesion and expansion of cryopreserved umbilical cord blood hematopoietic stem/progenitor cells. Experimental Hematology. 2007;35:771-781.

47. Sasaki T, Takagi M, Soma T, Yoshida T. Analysis of hematopoietic microenvironment containing spatial development of stromal cells in nonwoven fabrics. Journal of Bioscience and Bioengineering. 2003;96:76-78.

48. Sasaki T, Takagi M, Soma T, Yoshida T. 3D culture of murine hematopoietic cells with spatial development of stromal cells in nonwoven fabrics. Cytotherapy. 2001;4:285-291.

49. Bagley J, Rosenzweig M, Marks DF, Pykett MJ. Extended culture of multipotent hematopoietic progenitors without cytokine augmentation in a novel three-dimensional device. Experimental Hematology. 1999;27:496-504.

50. Yoshida T, Takagi M. Cell processing engineering for *ex vivo* expansion of hematopoieitc cells: a review. Biochemical Engineering Journal. 2004;20:99-106.

51. Cho CH, Eliason JF, Matthew HWT. Application of porous glycosaminoglycan-based scaffolds for expansion of human cord blood stem cell in perfusion culture. Journal of Biomedical Materials Research A. 2008;86A:98-107.

52. Yang H, Miller WM, Papoutsakis ET. Higher pH promotes megakaryocytic maturation and apoptosis. Stem Cells. 2002;20:320-328.

53. McAdams TA, Miller WM, Papoutsakis TE. pH is a potent modulator of erythroid differentiation. British Journal of Haematology. 1998;103:317-325.

54. Hevehan DL, Papoutsakis TE, Miller WM. Physiologically significant effects of pH and oxygen on granulopoiesis. Experimental Hematology. 2000;28:267-275.

55. Mostafa SS, Papoutsakis TE, Miller WM. Oxygen tension modulates the expression of cytokine receptors, transcription factors, and lineage-specific markers in culture human megakaryocytes. Experimental Hematology. 2001;29:873-883.

56. Hevehan DL, Papoutsakis TE, Miller WM. Physiologically significant effects of pH and oxygen on granulopoiesis. Experimental Hematology. 2000;28:267-275.

57. Proulx C, Dupuis N, St-Amour I, Boyer L, Lemieux R. Increased megakaryopoiesis in cultures in CD34-enriched cord blood cells maintained at 39°C. Biotechnology and Bioengineering. 2004;88:675-680.

58. Ozturk SS, Thrift JC, Blackie JD, Naveh D. Real-time monitoring and control of glucose and lactate concentrations in a mammalian cell perfusion reactor. Biotechnology and Bioengineering. 1996;53:372-378.

59. Dremel BAA, Li S-Y, Schmid RD. On-line determination of glucose and lactate concentrations in animal cell culture based on fiber optic detection of oxygen in flow-injection analysis. Biosensor & Bioelectronics. 1992;7:133-139.

60. Huang YL, Li S-Y, Dremel BAA, Bilitewski U, Schmid RD. On-line determination of glucose concentration throughout animal cell cultures based on chemilluminescent detection of hydrogen peroxide coupled with flow-injection analysis. Journal of Biotechnology. 1991;18:161-172.

61. Male KB, Gartu PO, Kamen AA, Luong JHT. On-line monitoring of glucose in mammalian cell culture using flow injection analysis (FIA) mediated biosensor. Biotechnology and Bioengineering. 1997;55:497-504.

62. Jung B, Lee S, Yang IH, Good T, Cote GL. Automated on-line non-invasive optical glucose monitoring in a cell culture system. Applied Spectroscopy. 2002;56:51-57.

63. Cruz HJ, Freitas CM, Alves PM, Moreira JL, Carrondo MJT. Effects of ammonia and lactate on growth, metabolism, and productivity of BHK cells. Enzyme and Microbial Technology. 2000;27:43-52.

64. Fernandes AM, Fernandes TG, Diogo MM, Lobato da Silva C, Henrique D, Cabral JMS. Mouse embryonic stem cell expansion in a microcarrier-based stirred culture system. Journal of Biotechnology. 2007;132:227-236.

65. Lazzari L, Lucchi S, Rebulla P, et al. Long-term expansion and maintenance of cord blood haematopoietic stem cells using thrombopoietin, Flt3-ligand, interleukin (IL)-6 and IL-11 in a serum-free and stroma-free culture system. British Journal of Hematology. 2001;112:397-404.

66. Alcorn MJ, Holyoake TL. Ex vivo expansion of haematopoietic progenitor cells. Blood Reviews. 1996;10:167-176.

67. Banu N, Deng B, Lyman SD, Avraham H. Modulation of haematopoietic progenitor development by Flt3-ligand. Cytokine. 1998;11:679-688.

68. Piacibello W, Garetto L, Aglietta M. *Ex vivo* expansion of megakaryocytes. Transfusion Science. 1999;22:107-110.

69. Flores-Guzman P, Guiterrez-Rodriguez M, Mayani H. *In vitro* proliferation, expansion and differentiation of a $CD34^+$ cell-enriched hematopoietic cell population from human umbilical cord blood in response to recombinant cytokines. Archives of Medical Research. 2002;33:107-114.

70. Sakatoku H, Inoue S. *In Vitro* proliferation and differentiation of erythroid progenitors of cord blood. Stem Cells. 1997;15:268-274.

71. Shearer WT, Rosenwasser LJ, Bochner BS, Martinez-Moczygemba M, Huston DP. Biology of common beta receptor-signaling cytokines: IL-3, IL-5 and GM-CSF. Journal of Allergy and Clinical Immunology. 2003;112:653-665.

72. Audet J, Miller CL, Eaves CJ, James MP. Common and distinct features of cytokine effects on hematopoietic stem and progenitor cells revealed by dose-response surface analysis. Biotechnology and Bioengineering. 2002;80:393-404.

73. Zandstra PW, Petzer AL, Eaves CJ, Piret JM. Cellular determinants affecting the rate of cytokine depletion in cultures of human hematopoietic cells. Biotechnology and Bioengineering. 1997;54:58-66.

74. Laluppa JA, Papoutsakis TE, Miller WM. Evaluation of cytokines for expansion of the megakaryocyte and granulocyte lineages. Stem Cells. 1997;15:198-206.

75. Lewis JL, Marley SB, Blackett NM, Szydlo R, Goldman JM, Gordon MY. Interleukin 3, but not stem cell factor increases self-renewal by human erythroid burst-forming cells *in vitro*. Cytokine. 1998;10:49-54.

76. Zandstra PW, Conneally E, Petzer AL, Piret JM, Eaves CJ. Cytokine manipulation of primitive human hematopoietic cell self-renewal. Proceedings of the National Academy of Sciences. 1997;94:4698-4703.

77. Montgomery DC. Introduction. Design and analysis of experiments (ed 5th): John Wiley & Sons, Inc.; 2001.

78. Montgomery DC. Introduction to factorial designs. Design and analysis of experiments (ed 5th): John Wiley & Sons, Inc.; 2001.

79. Yao C-L, Chu I-M, Hsieh T-B, Hwang S-M. A systematic strategy to optimize *ex vivo* expansion medium for human hematopoietic stem cells derived from umbilical cord blood mononuclear cells. Experimental Hematology. 2004;32:720-727.

80. Yao C-L, Liu C-H, Chu I-M, Hsieh T-B, Hwang S-M. Factorial designs combined with the steepest ascent method to optimize serum-free media for *ex vivo* expansion of human hematopoietic stem cells. Enzyme and Microbial Technology. 2003;33:343-352.

81. Lim M, Ye H, Panoskaltsis N, et al. Intelligent bioprocessing of hematopoietic cell cultures using monitoring and design of experiments. Biotechnology Advances. 2007;25:353-368.

82. Myers RH, Montgomery DC. Response Surface Methodology: Process and product optimization using designed experiments (ed 2nd): John Wiley and Sons, Inc.; 2002.

83. Montgomery DC. Design and Analysis of Experiments (ed 5th). Arizona: John Wiley and Sons, Inc.; 2001.

84. Montgomery DC. Response surface methods and other approaches to process optimization. In: Montgomery DC, ed. Design and analysis of experiments (ed 5th): John Wiley and Sons, Inc.; 2001.

85. Mohr GJ, Wolfbeis OS. Optical sensors for a wide pH range based on azo dyes immbolized on a novel support. Analytica Chimica Acta. 1994;292:41-48.

86. Weigl BH, Holobar A, Trettnak W, et al. Optical triple sensor for measuring pH, oxygen, and carbon dioxide. Journal of Biotechnology. 1994;32:127-138.

87. Gao FG, Jeevarajan AS, Anderson MM. Long-term continuous monitoring of dissolved oxygen in cell culture medium for perfused bioreactors using optical oxygen sensors. Biotechnology and Bioengineering. 2004;66:425-433.

88. Jeevarajan AS, Vani S, Taylor TD, Anderson MM. Continuous pH monitoring in a perfused bioreactor system using an optical pH sensor. Biotechnology and Bioengineering. 2002;78:467-472.

89. Ferguson JA, Healey BG, Bronk KS, Barnard SM, Walt DR. Simulatenous monitoring of pH, CO2 and O2 using an optical imaging fiber. Analytica Chimica Acta. 1997;340:123-131.

90. Williams SNO, Callies RM, Brindle KM. Mapping of oxygen tension and cell distribution in a hollow-fiber bioreactor using magnetic resonance imaging. Biotechnology and Bioengineering. 1997;56:56-61.

91. K. A. McGovern JSS, J. P. Wehrle, C. E. Ng, J. D. Glickson,. Gel-entrapment of perfluorocarbons: A fluorine-19 NMR spectroscopic method for monitoring oxygen concentration in cell perfusion systems. Magnetic Resonance in Medicine. 1993;29:196-204.

92. Bernard Gallez CB, Bénédicte F. Jordan,. Assessment of tumor oxygenation by electron paramagnetic resonance: principles and applications. NMR in Biomedicine. 2004;17:240-262.

93. Baker BC. Precision Temperature-sensing with RTD circuits: Microchip Technology Inc.; 2003:1-8.

94. Watlow. Temperature sensors. The Watlow Educational Series: Watlow Electric Manufacturing Company; 1995:1-36.

95. Larson TM, Gawlitzek M, Evans H, Albers U, Cacia J. Chemometric evaluation of on-line high-pressure liquid chromatography in mammalian cell cultures: analysis of amino acids and glucose. Biotechnology and Bioengineering. 2002;77:553-563.

96. Brooks SL, Higgins IJ, Newman JD, Turner APF. Biosensors for process control. Enzyme and Microbial Technology. 1991;13:946-955.

97. Luong JHT, Male KB, Glennon JD. Biosensor technology: Technology push versus market pull. Biotechnology Advances. 2008;26:492-500.

98. Liu X, Shi L, Niu W, Li H, Xu G. Amperometric glucose biosensor based on single-walled carbon nanohorns. Biosensors and Bioelectronics. 2008;23:1887-1890.

99. Rodriguez NP, Sakai Y, Fujii T. Cell-based microfluidic biochip for electrochemical real-time monitoring of glucose and oxygen. Sensors and Actuators B: Chemical. 2008;132:608-613.

100. Male KB, Gartu PO, Kamen AA, Luong JHT. A flow-injection (FI) mediated biosensor for on-line monitoring of lactate in mammalian cell culture. Analytica Chimica Acta. 1997;351:159-167.

101. Bracewell DG, Gill A, Hoare M. An in-line flow injection optical biosensor for real-time bioprocess monitoring. Trans Institute of Chemical Engineering. 2002;80:71-77.

102. Yang M, Yang Y, Liu B, Shen G, Yu R. Amperometric glucose biosensor based on chitosan with improved selectivity and stability. Sensors and Actuators B. 2004;101:269-276.

103. Wu B-Y, Hou S-H, Yin F, et al. Amperometric glucose biosensor based on layer-by-layer assembly of multilayer films composed of chitosan, gold nanoparticles and glucose oxidase modified Pt electrode. Biosensors and Bioelectronics. 2006;22:2854-2860

104. Xue H, Shen Z, Li C. Improved selectivity and stability of glucose biosensor based on *in situ* electropolymerized polyaniline-polyacrylonitrile composite. Biosensor & Bioelectronics. 2005;20:2330-2334.

105. Arnold AS, Crowley J, Woods N, Harvey LM, McNell B. *In situ* near infrared spectrscopy to monitor key analytes in mammalian cell cultivation. Biotechnology and Bioengineering. 2003;84:13-19.

106. McShane MJ, Cote GL. Near-Infrared spectroscopy for determination of glucose, lactate, and ammonia in cell culture media. Applied Spectroscopy. 1998;52:1073-1078.

107. Rhiel MH, Cohen MB, Arnold MA, Murhammer DW. On-line monitoring of human prostate cancer cells in a perfusion rotating wall vessel by near-infrared spectroscopy. Biotechnology and Bioengineering. 2004;86:852-860.

108. Rhiel MH, Ducommun P, Bolzonelle I, Marison I, Stocker UV. Real-time in situ monitoring of freely suspended and immobilized cell cultures based on mid-IR spectroscopic measurements. Biotechnology and Bioengineering. 2002;77:174-185.

109. Lewis CB, McNichols RJ, Gowda A, Cote GL. Investigation of near-infrared spectroscopy for periodic determination of glucose in cell culture medial *in situ*. Applied Spectroscopy. 2000;54:1453-1457.

110. Martinelle K, Doverskog M, Jacobsson U, Chapman BR, Kuchel PW, Haggstrom L. Elevated glutamate dehydrogenase flux in glucose-deprived hybridoma and myeloma cells: Evidence from $^{1}H/^{15}N$ NMR. Biotechnology and Bioengineering. 1998;60:508-517.

111. Bonarius HPJ, Ozemre A, Timmerarends B, et al. Metabolic-flux analysis of continuously cultured hybridoma cells using $^{13}CO_2$ mass spectrometry in combination with ^{13}C-lactate nuclear magnetic resonance and metabolite balancing. Biotechnology and Bioengineering. 2001;74:528-538.

112. Foluso A, Jan FMP. ^{31}P NMR characterization of cellular metabolism during dexamethasone induced apoptosis in human leukemic cell lines. Journal of Cellular Physiology. 1994;158:180-186.

113. Sastry PSRK. Metabolic rate determines haematopoietic stem cell self-renewal. Medical Hypotheses. 2004;63:476-480.

114. Baker KN, Rendall MH, Patel A, et al. Rapid monitoring of recombinant protein products: a comparison of current technologies. Trends in Biotechnology. 2002;20:149-156.

115. Ray CA, Bowsher RR, Smith WC, et al. Development, validation, and implementation of a multiplex immunoassay for the simultaneous determination of five cytokines in human serum. Journal of Pharmaceutical and Biomedical Analysis. 2005;36:1037-1044.

116. Hixson CS, Binder SR. Approaches to autoimmune antibody profiling using protein arrays. IVD Technology. 2005:41-48.

117. Pala P, Hussell T, Openshaw PJM. Flow cytometric measurement of intracellular cytokine. Journal of Immunological Methods. 2000;243:107-124.

118. Arora SK. Analysis of intracellular cytokines using flow cytometry. Methods in Cell Science. 2002;24:37-40.

119. Maino VC, Picker L. Identification of functional subsets by flow cytometry: Intracellular detection of cytokine expression. Cytometry. 1998;34:207-215.

120. Nagy G, Pallinger E, Antal-Szalmas P, et al. Measurement of intracelluar interferon-gamma and interleukin-4 in whole blood T lymphocytes from patients with systemic lupus erythematosus. Immunology Letters. 2000;74:207-210.

121. Zelnickova P, Faldyna M, Stepanova H, Ondracek J, Kovaru F. Intracellular cytokine detection by flow cytometry in pigs: Fixation, permeabilization and cell surface staining. Journal of Immunological Methods. 2007;327:18-29.

122. Canziani GA, Zhang W, Cines D, et al. Exploring biomolecular recognition using optical biosensor. Methods. 1999;19:253-269.

123. Malmqvist M. Surface plasmon resonance for detection and measurement of antibody-antigen affinity and kinetics. Current Opinion in Immunology. 1993;5:282-286.

124. Revoltella RP, Robbio LL, Vikinge T, Pardi E, Levantini E, Beffy P. Human GM-CSF interaction with the alpha-chain of its receptor studied using surface plasmon resonance. Biosensors & Bioelectronics. 1999;14:555-567.

125. Scibek JJ, Evergreen E, Zahn S, Canziani GA, Van Ryk D, Chaiken IM. Biosensor analysis of dynamics of interleukin 5 receptor subunit beta-c interaction with IL5:IL5R-alpha complexes. Analytical Biochemistry. 2002;307:258-265.

126. Delegau A, Freitag R, Middendorf C, et al. Immuno- and flow cytometric analytical methods for biotechnological research and process monitoring. Journal of Biomechanics. 1992;25:115-144.

127. Shapiro HM. Practical Flow Cytometry (ed 4th). Hoboken, New Jersey: John Wiley & Sons, Inc.; 2003.

128. Guez JS, Cassar JP, Wartelle F, Dhulster P, Suhr H. Real time *in situ* microscopy for animal cell-concentration monitoring during high density culture in bioreactor. Journal of biotechnology. 2004;111:335-343.

129. Joeris K, Frerichs J-G, Konstantinov K, Scheper T. *In situ* microscopy: Online process monitoring of mammalian cell cultures. Cytotechnology. 2002;38:129-134.

130. Cartnell S, Huynh K, Lin A, Nagaraja S, Guldberg R. Quantitative microcomputed tomography analysis of minerialization within three-dimensional scaffolds *in vitro*. Journal of Biomedical Materials Research Part A. 2004;69A:97-104.

131. Meinel L, Karageorgiou V, Hormann S, et al. Engineering bone-like tissue *in vitro* using human bone marrow stem cells and silk scaffolds. Journal of Biomedical Materials Research A. 2004;71:25-34.

132. Zupke C, Foy B. Nuclear magnetic resonance analysis of cell metabolism. Current Opinion in Biotechnology. 1995;6:192-197.

133. Notingher I, Bisson I, Polak JM, Hench LL. *In situ* spectroscopic study of nuclei acids in differentiating embryonic stem cells. Vibrational Spectroscopy. 2004;35:199-203.

134. Haemonetics. 2008. The world blood supply [Online]. Available: http://www.haemonetics.com/site/content/bloodsupply/bloodsupply.asp [27 Sept 2008]

135. Collins P, Nielsen L, Patel S, Papoutsakis E, Miller W. Characterization of hematopoietic cell expansion, oxygen uptake, and glycolysis in a controlled, stirred-tank bioreactor system. Biotechnology Progress. 1998;14:466-472.

136. Bullock T, Wen B, Marley S, Gordon M. Potential of CD34 in the regulation of symmetrical and asymmetrical divisions by hematopoietic progenitor cells. Stem Cells. 2007;25:844-851.

137. Chadwick N, Nostro MC, Baron M, Mottram R, Brady G, Buckle A-M. Notch signaling induces apoptosis in primary human CD34(+) hematopoietic progenitor cells. Stem Cells. 2007;25:203-210.

138. Mason C, Dunnill P. Translation regenerative medicine research: essential to discover and outcome. Regenerative Medicine. 2007;2:227-229.

139. Mantalaris A, Keng P, Bourne P, Chang AYC, Wu DJH. Engineering a human bone marrow model: A case study on *ex vivo* erythropoiesis. Biotechnological Progress. 1998;14:126-133.

140. Munugalavadla V, Kapur R. Role of c-kit and erythropoietin in erythropoiesis. Critical Reviews in Oncology/Hematology. 2005;54:63-75.

141. Dimitriou H, Vorgia P, Stiakaki E, et al. *In vitro* proliferative and differentiating characteristics of $CD133^+$ and $CD34^+$ cord blood cells in the presence of TPO or EPO. Leukemia Research. 2003;27:1143-1151.

142. Merchav S, Silvian-Drachsler I, Tatarsky I, Lake M, Skottner A. Comparative studies of the erythroid-potentiating effects of biosynthetic human insulin-like growth factors I and II. Journal of Clinical Endocrinology and Metabolism. 1992;74:447-452.

143. Miharada K-I, Hiroyama T, Sudo K, Nagasawa T, Nakamura Y. Refinement of cytokine use in the *in vitro* expansion of erythroid cells. Human Cell. 2006;19:30-37.

144. Neildez-Nguyen TMA, Wajcman H, Marden MC, et al. Human erythroid cells produced *ex vivo* at large scale differentiate into red blood cells *in vivo*. Nature Biotechnology. 2002;20:467-472.

145. Radomska A, Singhal S, Hua Y, et al. Biocompatible ion selective electrode for monitoring metabolic activity during the growth and cultivation of human cells. Biosensors and Bioelectronics. 2008;24:435-441.

146. Yue X, Drakakis EM, Lim M, et al. A real-time, multi-channel monitoring system for stem cell culture process. IEEE transactions on Biomedical Circuits and Systems. 2008;in press.

147. Wagner LW, Wallace E. Why should clinicians be concerned about blood conservation? Blood Transfusions. 2005:118-126.

148. Clinical practice guidelines: Appropriate use of red blood cells [Online]. Available: http://www.nhmrc.health.gov.au [18 Nov 2008]

149. Detmer K, Walker AN. Bone morphogenetic proteins act synergistically with haematopoietic cytokines in the differentiation of haematopoietic progenitors. Cytokine. 2002;17:36-42.

150. Loken M, Shah VO, Dattilio KL, Civin CI. Flow cytometric analysis of human bone marrow: I. Normal erythroid development. Blood. 1987;69:255-263.

151. Wojchowski DM, Menon MP, Sathyanarayana P, et al. Erythropoietin-dependent erythropoiesis: New insights and questions. Blood Cells, Molecules and Diseases. 2006;36:232-238.

152. Schaefer A, Magocsi M, Marquard H. Signalling mechanism in erythropoiesis: The enigmatic role of calcium. Cell Signal. 1997;7:483-495.

153. Lichtman MA, Beutler E, Kipps TJ, Seligsohn U, Kaushansky K, Prchal J. Williams Hematology (ed 7th): McGraw-Hill; 2005.

154. Mason-Garcia M, Beckman BS, Brookins JW, et al. Development of a new radioimmunoassay for erythropoietin using recombinant erythropoietin. Kidney International. 1990;38:969-975.

155. Panzenbock B, Bartunek P, Mapara MY, Zenke M. Growth and differentiation of human stem cell factor/erythropoietin-dependent erythroid progenitor cells *in vitro*. Blood. 1998;92:3658-3668.

156. Giarratana M-C, Kobari L, Lapillonne H, et al. *Ex vivo* generation of fully mature human red blood cells from hematopoietic stem cells. Nature Biotechnology. 2005;23:69-74.

157. Miharada K, Hiroyama T, Sudo K, Nagasawa T, Nakamura Y. Efficient enucleation of erythroblasts differentiated *in vitro* from hematopoietic stem and progenitor cells. Nature Biotechnology. 2006;24:1255-1256.

158. Lu S-J, Feng Q, Park JS, et al. Biological properties and enucleation of red blood cells from human embryonic stem cells. Blood. 2008;in press.

159. Beutler E. Production and destruction of erythrocytes. In: Beutler E, Lichtman MA, Coller BS, Kipps TJ, Seligsohn U, eds. Williams Hematology. New York: McGraw-Hill; 2001:355-368.

160. Jung YJ, Cha J-E, Kim HJ, et al. Erythropoietin-independent and -dependent stages during *in vitro* erythropoiesis. Acta Haematologica. 2007;118:222-225.

161. Wang W, Horner DN, Chen WLK, Zandstra PW, Audet J. Synergy between erythropoietin and stem cell factor during erythropoiesis can be quantitatively described without co-signally effects. Biotechnology and Bioengineering. 2008;99:1261-1272.

162. Zandstra PW, Nagy A. Stem cell bioengineering. Annual Review of Biomedical Engineering. 2001;3:275-305.

163. Guyton AC. Textbook of Medical Physiology: W.B. Saunders Company; 1986.

164. Male KB, Luong JHT, Tom R, Mercille S. Novel FIA amperometric biosensor system for the determination of glutamine in cell culture systems. Enzyme Microbiology & Technology. 1993;15:26-32.

165. Bracewell DG, Gill A, Hoare M. An in-line flow injection optical biosensor for real-time bioprocess monitoring. Trans IChemE. 2002;80:71-77.

166. Safinia L, Panoskaltsis N, Mantalaris A. Bone marrow tissue engineering bioreactors. In: Al-Rubeai M, Chaudhuri K, eds. Bioreactors in Tissue Engineering: Principles, design and operation: Kluwer Academic Publishers; 2005.

167. Ma CYJ, Kumar R, Xu XY, Mantalaris A. A combined fluid dynamics, mass transport and cell growth model for a three-dimensional perfused bioreactor for tissue engineering of haematopoietic cells. Biochemical Engineering Journal. 2007;35:1-11.

168. Locher G, Sonnleitner B, Fiechter A. Automatic bioprocess control. 3. Impacts on process perception. Journal of Biotechnology. 1991;19:173-192.

169. Merbel NCvd, Lingeman H, Brinkman UAT. Sampling and analytical strategies in on-line bioprocess monitoring and control. Journal of Chromatography A. 1996;725:13-27.
170. Stockar Uv, Valentinotti S, Marison I, Cannizzaro C, Herwig C. Know-how and know-why in biochemical engineering. Biotechnology Advances. 2003;21:417-430.
171. Hanson MA, Ge X, Kostov Y, Brorson KA, Moreira AR, Rao G. Comparison of optical pH and dissolved oxygen sensors with traditional electrochemical probes during mammalian cell culture. Biotechnology and Bioengineering. 2007;97:833-841.
172. Lim M, Ye H, Drakakis EM, et al. Towards information-rich bioprocessing: Generation of spatio-temporal profiles through the use of design of experiments to determine optimal number and location of sensors - an example of thermal profiles. Biochemical Engineering Journal. 2008;40:1-7.
173. Gerritsen M, Kros A, Sprakel V, Lutterman JA, Nolte RJM, Jansen JA. Biocompatibility evaluation of sol-gel coatings for subcutaneously implantatble glucose sensors. Biomaterials. 2000;21:71-78.
174. Moussy F, Harrison D, Rajotte R. A miniaturized Nafion-based glucose sensor: in vitro and in vivo evaluation in dogs. International Journal of Artifical Organs. 1994;17:88-94.
175. Ma Y, Chan Y, Trau D, Huang P, Chen E. Micromolding of PDMS scaffolds and microwells for tissue culture and cell patterning: A new method of microfabrication by the self-assembled micropatterns of diblock copolymer micelles. Polymer. 2006;47:5124-5130.
176. Thangawang AL, Ruoff RS, Swartz MA, Glucksberg MR. An ultra-thin PDMS membrane as a bio/micro-nano interface: fabrication and characterization. Biomedical Microdevices. 2007;9:587-595.
177. Krommenhoek EE, Leeuwen Mv, Gardeniers H, et al. Lab-scale fermentation tests for microchip with integrated electrochemical sensors for pH, temperature, dissolved oxygen and viabile biomass concentration. Biotechnology and Bioengineering. 2008;99:884-892.

APPENDIX A

ANOVA analysis for DOE characterisation studies

ANOVA for characterisation studies from Chapters 5 and 6 are presented in Appedix A. Tables A.1 and A.2 are for Chapter 5. Tables A.3 to A.8 are for Chapter 6.

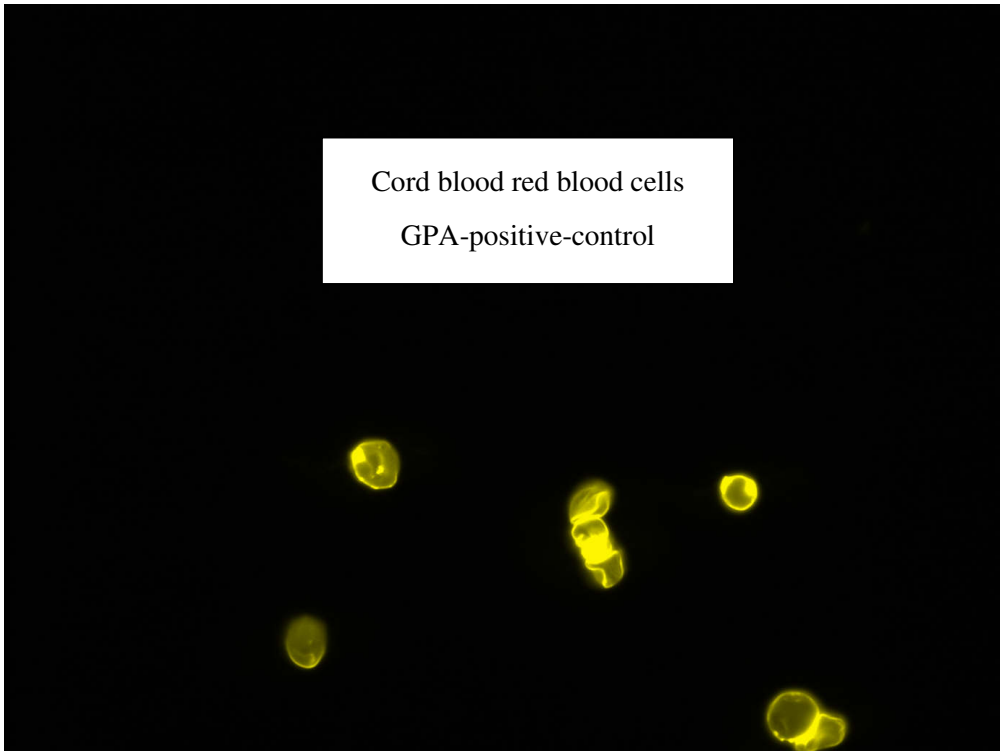

Figure A.1 GPA-PE positive control using red blood cells obtained from the cord

Table A.1 ANOVA for fold expansion of cord blood cultured cells in DOE optimised cocktail

Response: Fold Transform: Base 10 log Constant: 8.5
ANOVA for Response Surface Quadratic Model

Backward Elimination Regression with Alpha to Exit = 0.050

Removed	Coefficient Estimate	t for H_0 Coeff=0	Prob > |t|	R-Squared	MSE
B^2	-0.22	-1.78	0.1256	0.9650	0.040

Source	Sum of Squares	DF	Mean Square	F Value	Prob > F
Model significant	7.78	4	1.94	48.31	< 0.0001
A	*1.28*	*1*	*1.28*	*31.86*	*0.0008*
B	*0.83*	*1*	*0.83*	*20.68*	*0.0026*
A^2	*4.40*	*1*	*4.40*	*109.31*	*< 0.0001*
AB	*0.67*	*1*	*0.67*	*16.56*	*0.0048*
Residual	0.28	7	0.040		
Lack of Fit	*0.22*	*3*	*0.073*	*4.77*	*0.0827*
Pure Error	*0.062*	*4*	*0.015*		
Cor Total	8.06	11			

Std. Dev.	0.20	R-Squared	0.9650
Mean	2.16	Adj R-Squared	0.9451
C.V.	9.29	Pred R-Squared	0.8356
PRESS	1.32	Adeq Precision	16.259

Coefficient Factor	Estimate	DF	Standard Error	95% CI Low	95% CI High
Intercept	2.73	1	0.083	2.54	2.93
A-SCF	0.46	1	0.082	0.27	0.66
B-EPO	0.41	1	0.091	0.20	0.63
A^2	-1.22	1	0.12	-1.50	-0.95
AB	0.41	1	0.10	0.17	0.65

Final Equation in Terms of Actual Factors:

$$\text{Log}_{10}(\text{Fold} + 8.50) = 1.04438 + 0.049933 * \text{SCF} + 2.26926\text{E-}003 * \text{EPO} - 4.88514\text{E-}004 * \text{SCF}^2 + 2.72105\text{E-}003 * \text{SCF} * \text{EPO}$$

Table A.2 ANOVA for red cell maturation of cord blood cultured cells in DOE optimised cocktail

Response: %RBC Transform: Power Lambda: 1 Constant: 0.666
ANOVA for Response Surface Quadratic Model

Analysis of variance table [Partial sum of squares]

Source	Sum of Squares	DF	Mean Square	F Value	Prob > F	
Model	5091.88	3	1697.29	127.42	< 0.0001	significant
A	*79.50*	*1*	*79.50*	*5.97*	*0.0404*	
B	*3605.40*	*1*	*3605.40*	*270.67*	*< 0.0001*	
B^2	*2144.75*	*1*	*2144.75*	*161.01*	*< 0.0001*	
Residual	106.56	8	13.32			
Lack of Fit	*91.08*	*4*	*22.77*	*5.88*	*0.0572*	
Pure Error	*15.49*	*4*	*3.87*			
Cor Total	5198.44	11				

Std. Dev.	3.65	R-Squared	0.9795
Mean	54.89	Adj R-Squared	0.9718
C.V.	6.65	Pred R-Squared	0.8920
PRESS	561.59	Adeq Precision	29.486

Factor	Coefficient Estimate	DF	Standard Error	95% CI Low	95% CI High
Intercept	64.04	1	1.38	60.86	67.22
A-SCF	3.64	1	1.49	0.20	7.08
B-EPO	27.41	1	1.67	23.57	31.25
B^2	-27.44	1	2.16	-32.43	-22.46

Final Equation in Terms of Actual Factors:

$$(\%RBC + 0.67)^1 = +5.54600 + 0.072800 * SCF + 27.43206 * EPO - 3.04942 * EPO^2$$

Table A.3 ANOVA for response surface model of phase I characterisation study (Experiment 1)

Response: Cell expansion

ANOVA for Response Surface Quadratic Model

Source	Sum of Squares	Mean DF	Square	F Value	Prob > F	
Model	765.62	4	191.41	13.06	0.0001	significant
B	*33.86*	*1*	*33.86*	*2.31*	*0.1509*	
C	*417.32*	*1*	*417.32*	*28.47*	*0.0001*	
C^2	*133.95*	*1*	*133.95*	*9.14*	*0.0091*	
BC	*180.50*	*1*	*180.50*	*12.31*	*0.0035*	
Residual	205.25	14	14.66			
Lack of Fit	*152.08*	*10*	*15.21*	*1.14*	*0.4874*	*not significant*
Pure Error	*53.17*	*4*	*13.29*			
Cor Total	970.87	18				

Std. Dev.	3.83	R-Squared	0.7886
Mean	41.38	Adj R-Squared	0.7282
C.V.	9.25	Pred R-Squared	0.5526
PRESS	434.36	Adeq Precision	11.414

Factor		Coefficient Estimate	DF		Standard Error	95% CI Low	95% CI High
Intercept		44.18	1		1.28	41.44	46.92
B-IGFII		1.84	1		1.21	-0.76	4.44
C-EPO	6.46	1	1.21	3.86	9.06		
C^2	-5.32	1	1.76	-9.09	-1.54		
BC	-4.75	1	1.35	-7.65	-1.85		

Final Equation in Terms of Coded Factors:

2E fold	=
+44.18	
+1.84	* B
+6.46	* C
-5.32	* C^2
-4.75	* B * C

Table A.4 ANOVA for response surface model of phase I characterisation study (Experiment 2)

Response: Cell expansion

ANOVA for Response Surface Quadratic Model

Source	Sum of Squares	DF	Mean Square	F Value	Prob > F	
Model	2700.38	4	675.09	10.76	0.0003	significant
B	*795.66*	*1*	*795.66*	*12.69*	*0.0031*	
C	*1054.73*	*1*	*1054.73*	*16.82*	*0.0011*	
C^2	*433.82*	*1*	*433.82*	*6.92*	*0.0198*	
BC	*416.16*	*1*	*416.16*	*6.64*	*0.0220*	
Residual	878.07	14	62.72			
Lack of Fit	*369.33*	*10*	*36.93*	*0.29*	*0.9487*	*not significant*
Pure Error	*508.73*	*4*	*127.18*			
Cor Total	3578.44	18				

Std. Dev.	7.92	R-Squared	0.7546
Mean	66.06	Adj R-Squared	0.6845
C.V.	11.99	Pred R-Squared	0.5682
PRESS	1545.23	Adeq Precision	11.050

Factor	Coefficient Estimate	DF	Standard Error	95% CI Low	95% CI High
Intercept	71.10	1	2.64	65.44	76.76
B-IGFII	8.92	1	2.50	3.55	14.29
C-EPO	10.27	1	2.50	4.90	15.64
C^2	-9.57	1	3.64	-17.37	-1.77
BC	-7.21	1	2.80	-13.22	-1.21

Final Equation in Terms of Coded Factors:

$$
\begin{aligned}
2L &= \\
&+71.10 \\
&+8.92 * B \\
&+10.27 * C \\
&-9.57 * C^2 \\
&-7.21 * B * C
\end{aligned}
$$

Table A.5 ANOVA for response surface model of phase II characterisation study (Experiment 1)

Response: Cell expansion
ANOVA for Response Surface Quadratic Model

Source	Sum of Squares	DF	Mean Square	F Value	Prob > F	
Model	1993.74	3	664.58	7.41	0.0028	significant
A	*469.22*	*1*	*469.22*	*5.23*	*0.0371*	
C	*974.17*	*1*	*974.17*	*10.87*	*0.0049*	
C^2	*550.35*	*1*	*550.35*	*6.14*	*0.0256*	
Residual	1344.90	15	89.66			
Lack of Fit	*962.38*	*11*	*87.49*	*0.91*	*0.5930*	*not significant*
Pure Error	*382.53*	*4*	*95.63*			
Cor Total	3338.65	18				

Std. Dev.	9.47	R-Squared	0.5972
Mean	56.42	Adj R-Squared	0.5166
C.V.	16.78	Pred R-Squared	0.3812
PRESS	2065.97	Adeq Precision	7.906

Factor	Coefficient Estimate	DF	Standard Error	95% CI Low	95% CI High
Intercept	62.09	1	3.16	55.36	68.82
A-SCF	6.85	1	2.99	0.47	13.23
C-EPO	9.87	1	2.99	3.49	16.25
C^2	-10.78	1	4.35	-20.05	-1.51

Final Equation in Terms of Coded Factors:

$$2F = +62.09 + 6.85 * A + 9.87 * C - 10.78 * C^2$$

Table A.6 ANOVA for response surface model of phase II characterisation study (Experiment 2)

Response: Cell expansion

ANOVA for Response Surface Quadratic Model

Source	Sum of Squares	DF	Mean Square	F Value	Prob > F	
Model	13080.17	3	4360.06	34.90	< 0.0001	significant
A	*2344.57*	*1*	*2344.57*	*18.77*	*0.0006*	
C	*7022.50*	*1*	*7022.50*	*56.21*	*< 0.0001*	
C^2	*3713.09*	*1*	*3713.09*	*29.72*	*< 0.0001*	
Residual	1874.08	15	124.94			
Lack of Fit	*1270.25*	*11*	*115.48*	*0.76*	*0.6735*	*not significant*
Pure Error	*603.83*	*4*	*150.96*			
Cor Total	14954.25	18				

Std. Dev.	11.18	R-Squared	0.8747
Mean	121.16	Adj R-Squared	0.8496
C.V.	9.23	Pred R-Squared	0.8055
PRESS	2908.62	Adeq Precision	16.597

Factor	Coefficient Estimate	DF	Standard Error	95% CI Low	95% CI High
Intercept	135.90	1	3.73	127.96	143.84
A-SCF	15.31	1	3.53	7.78	22.85
C-EPO	26.50	1	3.53	18.97	34.03
C^2	-28.00	1	5.14	-38.94	-17.05

Final Equation in Terms of Coded Factors:

$$2G = +135.90 + 15.31 * A + 26.50 * C - 28.00 * C^2$$

Table A.7 ANOVA for response surface model of phase III characterisation study (Experiment 1)

Response: Cell expansion

ANOVA for Response Surface Quadratic Model

Source	Sum of Squares	DF	Mean Square	F Value	Prob > F	
Model	125.73	4	31.43	23.42	< 0.0001	significant
A	*15.23*	*1*	*15.23*	*11.35*	*0.0042*	
C	*42.44*	*1*	*42.44*	*31.62*	*< 0.0001*	
A^2	*13.81*	*1*	*13.81*	*10.29*	*0.0059*	
C^2	*13.42*	*1*	*13.42*	*10.00*	*0.0065*	
Residual	20.13	15	1.34			
Lack of Fit	*13.17*	*10*	*1.32*	*0.95*	*0.5623*	*not significant*
Pure Error	*6.96*	*5*	*1.39*			
Cor Total	145.86	19				

Std. Dev.	1.16	R-Squared	0.8620
Mean	8.83	Adj R-Squared	0.8252
C.V.	13.12	Pred R-Squared	0.7303
PRESS	39.34	Adeq Precision	12.830

Factor	Estimate	Coefficient DF	Standard Error	95% CI Low	95% CI High
Intercept	10.89	1	0.39	10.06	11.72
A-SCF	1.23	1	0.37	0.45	2.01
C-EPO	2.06	1	0.37	1.28	2.84
A^2	-2.08	1	0.65	-3.46	-0.70
C^2	-2.05	1	0.65	-3.43	-0.67

Final Equation in Terms of Coded Factors:

$$2K = +10.89 + 1.23 * A + 2.06 * C - 2.08 * A^2 - 2.05 * C^2$$

Table A.8 ANOVA for response surface model of phase III characterisation study (Experiment 2)

Response: Cell expansion

ANOVA for Response Surface Quadratic Model

Source	Sum of Squares	DF	Mean Square	F Value	Prob > F	
Model	14.91	3	4.97	5.97	0.0063	significant
A	*0.12*	*1*	*0.12*	*0.14*	*0.7119*	
C	*8.85*	*1*	*8.85*	*10.63*	*0.0049*	
A^2	*5.94*	*1*	*5.94*	*7.13*	*0.0168*	
Residual	13.32	16	0.83			
Lack of Fit	*11.64*	*11*	*1.06*	*3.15*	*0.1076*	*not significant*
Pure Error	*1.68*	*5*	*0.34*			
Cor Total	28.24	19				

Std. Dev.	0.91	R-Squared	0.5281
Mean	4.27	Adj R-Squared	0.4396
C.V.	21.39	Pred R-Squared	0.3598
PRESS	18.08	Adeq Precision	7.548

Factor	Coefficient Estimate	DF	Standard Error	95% CI Low	95% CI High
Intercept	3.72	1	0.29	3.11	4.33
A-SCF	-0.11	1	0.29	-0.72	0.50
C-EPO	0.94	1	0.29	0.33	1.55
A^2	1.09	1	0.41	0.22	1.95

Final Equation in Terms of Coded Factors:

2N	=
+3.72	
-0.11	* A
+0.94	* C
+1.09	* A^2

APPENDIX B

Sensor calibration curves and performance data

Appendix B provides all sensor calibration curves and operational stability performance of ammonia, pH and oxygen sensors. This work was done by Anna Radomska at the Institute of Biomedical Engineering, collaborators in this project. All graphs were produced and kindly provided by her.

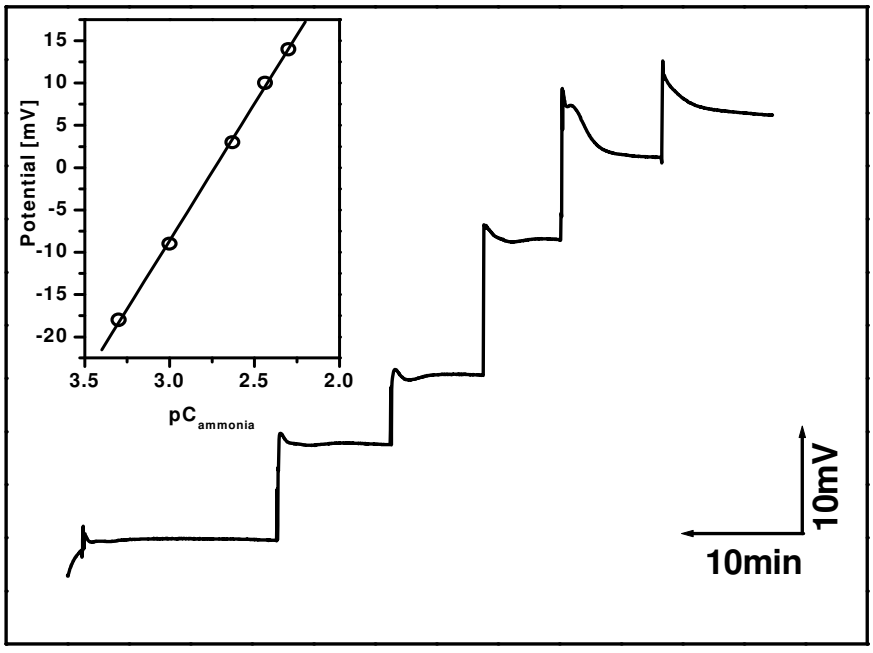

Figure B.1 Dynamic response of PEG-modified electrode toward ammonium ions in step changes of 0.5 mM ammonia concentrations.

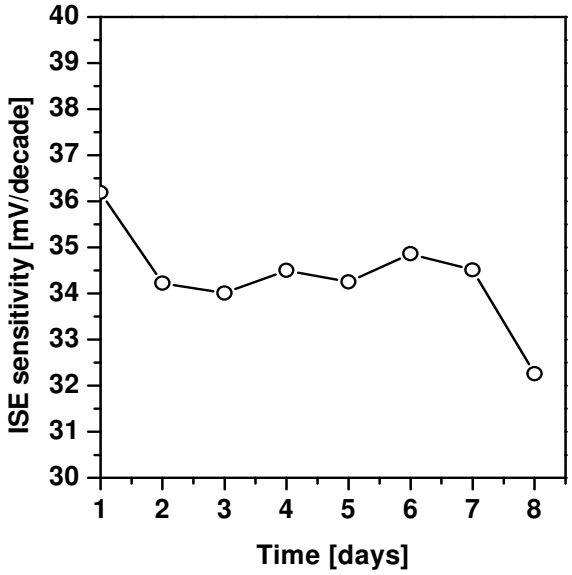

Figure B.2 Operational stability of ammonia sensors in culture media over eight day period. A comparison of the ISE sensitivity after every 24 hours is used.

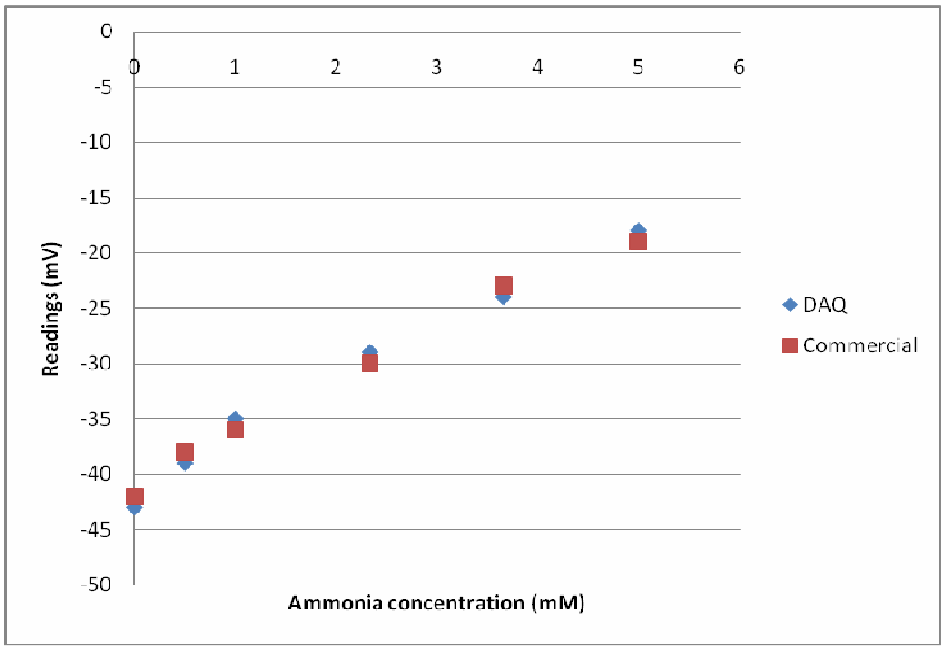

Figure B.3 Comparison of ammonia readings performed on our system (DAQ) versus a commercial system (Commercial).

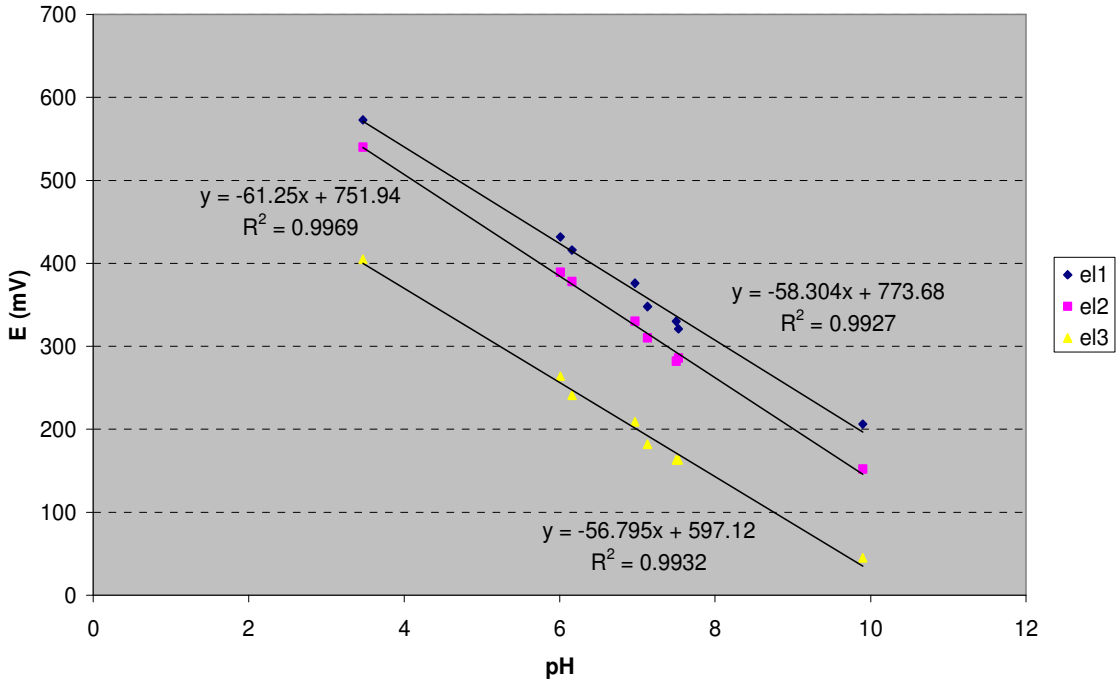

Figure B.4 Calibration curves for three independent pH sensors. The average slope in response is 58.8 mV/pH.

Table B.1 Comparison of pH readings taken from our system (DAQ) versus a commercial system.

Sensor No.	DAQ	Commercial board
El 38	46	46
El 6A	122	124
El 13A	109	109

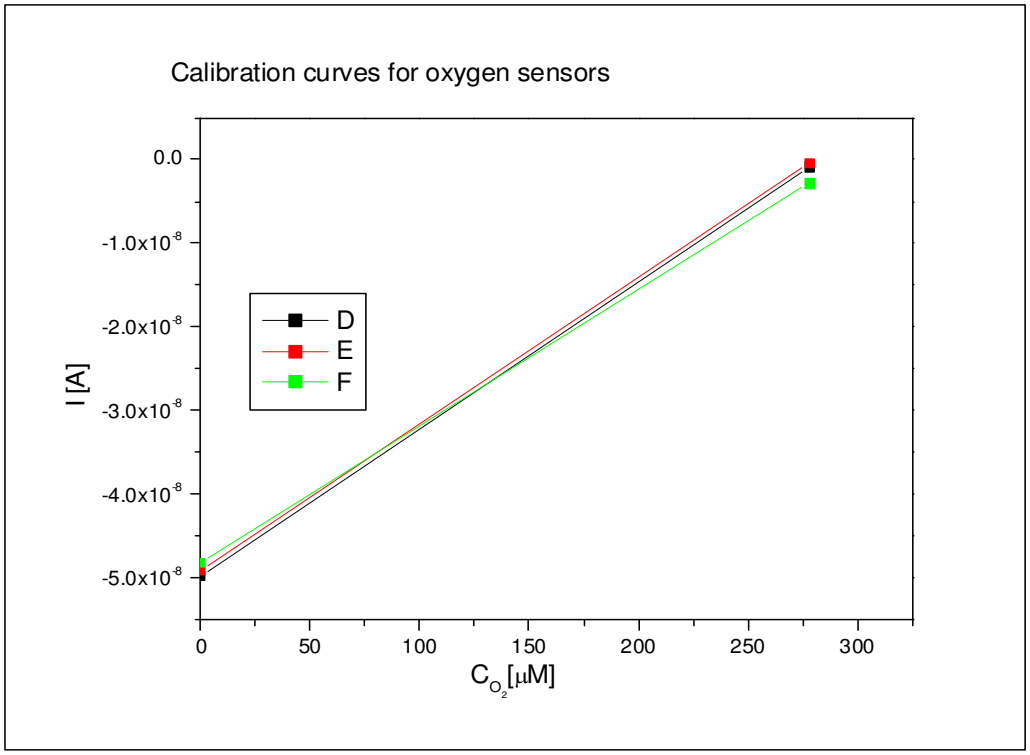

Figure B.5 Oxygen sensor calibration curves for three independent sensors. Average sensor slope is 1.71×10^{-10} A/μM

Table B.2 Recalibration data and lost of sensitivity in oxygen sensors after six days in culture.

Sensor	Slope (before)	Slope (after)	Lost in sensitivity
12a	-6.47	-6.21	4.02%
7a	-5.33	-5.21	2.25%
4a	-3.04	-3.06	-0.82%
9a	-6.30	-4.06	35.48%
15a	-4.43	-2.97	33.10%
3a	-5.77	-5.57	3.45%
6a	-5.66	-4.54	19.79%
2a	-5.662	-5.01	11.57%
1a	-4.99	-4.98	0.24%
8a	-4.84	-4.80	0.89%

Table B.3 Comparison of oxygen sensor readings taken from our system versus a commercial system.

Sensor	DAQ	Commercial
El2A	-5.655	-5.665
El12A	-6.021	-6.210